UNIVERSIDAD DE CANTABRIA

ESCUELA DE DOCTORADO

Programa de Doctorado en Ingeniería Industrial: Tecnologías de Diseño y Producción Industrial

MEMORIA DE TESIS PARA OBTENER EL TÍTULO DE DOCTOR POR LA UNIVERSIDAD DE CANTABRIA

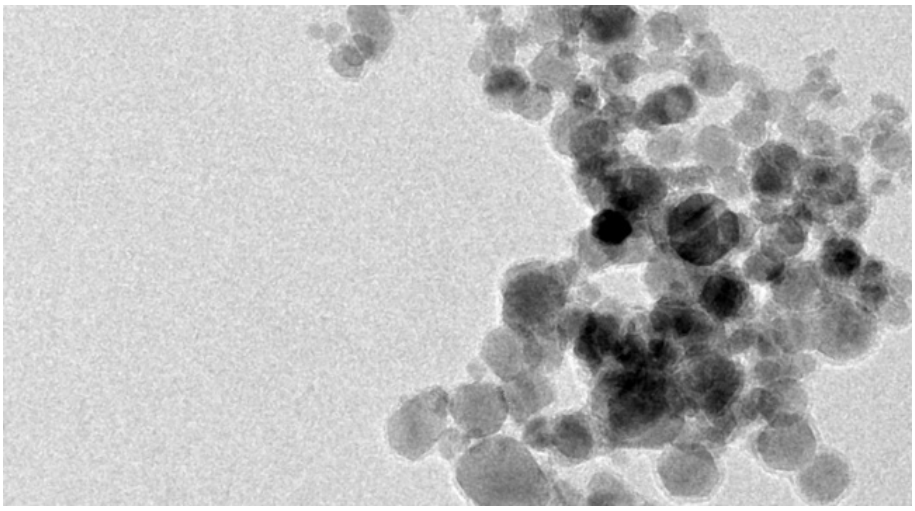

EVOLUCIÓN DE LAS PROPIEDADES TÉRMICAS Y DIELÉCTRICAS DE UN ACEITE VEGETAL DE TRANSFORMADOR MEJORADO CON NANOPARTÍCULAS

(Evolution of the thermal and dielectric properties of a transformer vegetal oil enhanced with nanoparticles)

Cristian Olmo Salas

Directores de la tesis:

Fernando Delgado San Román
Félix Ortiz Fernández

Santander, 2020

UNIVERSITY OF CANTABRIA

SCHOOL OF INDUSTRIAL ENGINEERING AND TELECOMMUNICATIONS

Department of Electric and Energy Engineering

DOCTORAL THESIS FOR THE DEGREE OF PhD IN THE UNIVERSITY OF CANTABRIA

PhD PROGRAM IN INDUSTRIAL ENGINEERING: DESIGN AND INDUSTRIAL PRODUCTION TECHNOLOGIES

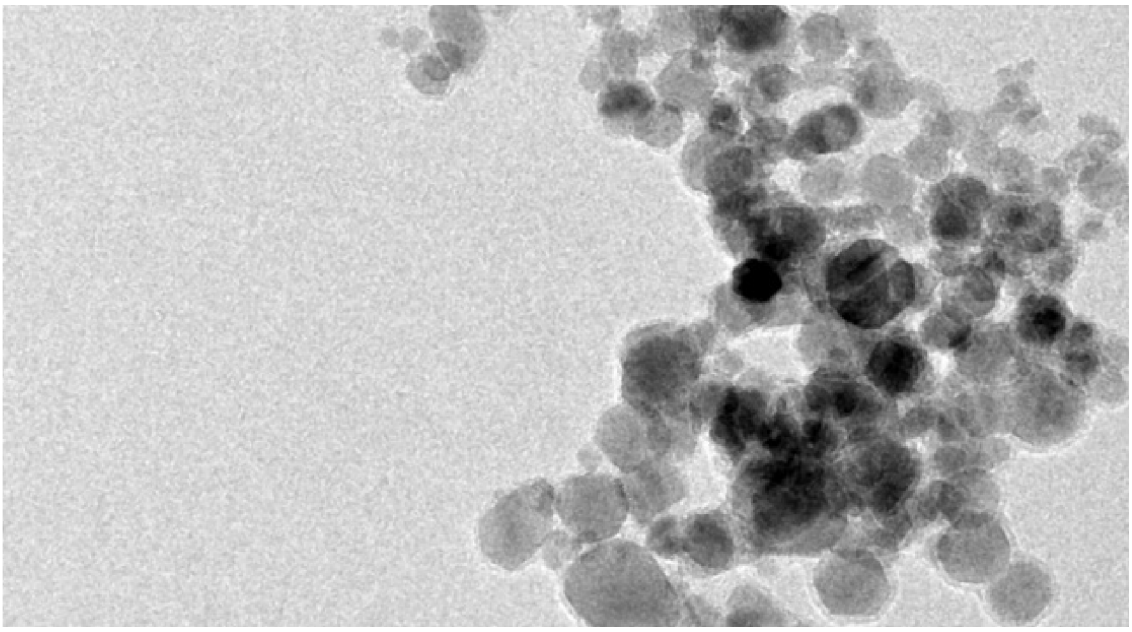

EVOLUTION OF THE THERMAL AND DIELECTRIC PROPERTIES OF A TRANSFORMER VEGETAL OIL ENHANCED WITH NANOPARTICLES

(Evolución de las propiedades térmicas y dieléctricas de un aceite vegetal de transformador mejorado con nanopartículas)

Cristian Olmo Salas

Thesis directors:

Fernando Delgado San Román
Félix Ortiz Fernández

Santander, 2020

“Hay libros cortos que, para entenderlos como se merecen, se necesita una vida muy larga”

Francisco de Quevedo

AGRADECIMIENTOS

El desarrollo de esta tesis bebe no solo del trabajo del que aquí escribe, y merece ser reconocido y agradecido.

En primer lugar, quisiera agradecer a los que han sido mis directores de tesis, Fernando Delgado y Félix Ortiz, y a Alfredo Ortiz, por todo el apoyo y la orientación recibida durante la realización de este trabajo. También quisiera agradecer al grupo GITEP y al Departamento de Ingeniería Eléctrica y Energética de la Universidad de Cantabria por integrarme en su seno y proporcionarme los medios necesarios para el trabajo desarrollado, y especialmente a sus miembros Inmaculada Fernández, Carlos Renedo, Agustín Santisteban y Cristina Méndez, a cuya ayuda tantas veces he recurrido.

También quisiera agradecer al Instituto Schering de la Universidad Leibniz de Hannover y a la compañía Sea Marconi Technologies de Turín, por permitirme pasar tres meses en sus instalaciones, ampliando así mi formación, y por toda la ayuda y el buen trato recibido por su parte.

Por último, quisiera agradecer a mi familia y amigos todo su apoyo y comprensión, sin las que la finalización de esta tesis hubiera sido imposible.

A todos ellos, muchas gracias.

ABSTRACT

This research assesses the performance of several nanofluids as cooling and dielectric fluid for electrical transformers, focusing on their main properties.

In the first place, an extensive review of the previous works in this field was done. It is focused on all the aspects that condition the performance of a nanofluid, as the characteristics of its components or the preparation method, and the resulting properties. The applicability of the nanofluids has been also studied. This information has been used as reference and starting point of this work. To be more precise, it has focussed on some of the weaknesses noticed in this research field such as it is the scarce information available about the application of dielectric nanofluids in existing devices, even at laboratory scale. Even more those oils expected to substitute the traditional mineral oils at transformers in the mid-term have been analysed: the biodegradable natural esters.

Four different nanofluids have been prepared, with four different nanoparticles (Fe_2O_3, TiO_2, ZnO and CuO) and a dielectric natural ester as a base, using several concentrations, all of them below 2.0 kg/m^3. The preparation method, and the concentrations have been selected according to the knowledge available in the reviewed references. These prepared nanofluids and the base fluid have been characterized from the thermal-dielectric standpoint. According to the standards, they have been determined and compared those properties on which the performance of the fluid depends: breakdown voltage, resistivity, loss factor, density, thermal conductivity and viscosity.

The suitability of each combination nanoparticle-base fluid has been analysed, determining the optimal concentration and identifying those nanofluids most suitable for their testing in an actual electric device. In this sense, considering their dielectric properties, only the Fe_2O_3 and TiO_2 nanofluids shows a better behaviour than the base fluid (in a way according to the literature) while the results with ZnO and CuO nanoparticles are not clear. Respecting the thermal conductivity, none of the

combinations studied present higher capacities than the base fluid. The affectation of other properties such as the viscosity or the loss factor is similar to that found in other works. Based on these results, the optimal concentration from the dielectric point of view are 0.2 kg/m^3 of Fe_2O_3 and 0.5 kg/m^3 of TiO_2. To use them in the following steps, and Despite their erratic behaviour, 0.7 kg/m^3 and 0.2 kg/m^3 concentrations are chosen for the ZnO and CuO nanofluids, respectively, as the improvement of the dielectric properties is more pronounced with them.

The selected nanofluids and the base fluid have been tested as cooling fluids in an experimental setup. This platform consists in a transformer, immersed in a tank with oil, that feed a resistive circuit (set of rheostats). Inside the tank, the heat transfer is mainly carried out by natural convection. Five sensors are located inside the tank (winding, core, and at the bottom and the top of the tank) and outside, in the laboratory, to measure the temperatures. These probes are controlled, and their temperatures registered, by a microcontroller. By adjusting the resistive circuit, three different load regimes have been set during the tests of the four nanofluids, and the evolution of the temperatures of the transformer has been studied. The results show how while the Fe_2O_3 nanofluid is able to cool the transformer in a more efficient way, this is not the case with the other nanoparticles, whose performance is, in general, worse than the one showed by the base fluid.

While the improvement in the dielectric properties can be explained by the well-known capacity of some nanoparticles to capture electrons and to delay the propagation of streamers and discharges, the improvement of the cooling capacity that appears in the Fe_2O_3 nanofluid cannot be explained by a similar theory regarding an enhancement of the thermal conductivity. The magnetic nature of these nanoparticles, together with the absence of this improvement with the other nanoparticles (not magnetic) seem to support the existence of thermal-magnetic buoyancy forces that improve the convection at the tank, due to the interaction magnetic field-nanoparticles.

RESUMEN

La presente investigación aborda el estudio de la actuación de los nanofluidos dieléctricos como líquidos refrigerantes en transformadores eléctricos, poniendo el foco en sus principales propiedades.

En primer lugar, se ha realizado una profunda revisión de los trabajos ya realizados en este campo. Se ha puesto principalmente atención en aquellos aspectos que condicionan la actuación de un nanofluido, como son las características de los componentes que lo forman o el método de preparación utilizado, así como en las propiedades resultantes. La aplicabilidad de los nanofluidos ha sido también abordada. Esta información ha sido la referencia y origen de este trabajo, que se centra en algunas de las deficiencias encontradas en el estado del arte de este campo científico, como es la escasez de información disponible sobre la aplicación de nanofluidos dieléctricos en equipos existentes, incluso a escala de laboratorio, especialmente con aquellos aceites llamados a sustituir en el medio plazo a las alternativas tradicionalmente usadas: Los ésteres naturales biodegradables.

Cuatro tipos diferentes de nanofluido han sido preparados, con cuatro diferentes composiciones químicas de nanopartículas (Fe_2O_3, TiO_2, ZnO y CuO) y con un éster dieléctrico natural como fluido base, en concentraciones hasta 2.0 kg/m^3. Estas concentraciones, así como el método de preparación, han sido elegidos de acuerdo con la información disponible en las referencias revisadas. La preparación ha consistido en una combinación de agitación mecánica y sonicación ultrasónica, seguida de un periodo de reposo para la eliminación de burbujas.

Estos nanofluidos, así como el fluido base, tras pasar por el mismo procedimiento de preparación han sido sometidos a su caracterización desde el punto de vista termo-dieléctrico. Aquellas propiedades de las que depende su efectividad en ese sentido han sido analizadas, de acuerdo con la normativa relacionada, y los resultados han sido comparados. La idoneidad de cada combinación de nanopartícula y fluido base ha sido

criticada, y se ha analizado la existencia de concentraciones óptimas desde el punto de vista operativo, identificando los nanofluidos más adecuados para su posterior testeo en un dispositivo eléctrico experimental. Las propiedades involucradas en la caracterización han sido la tensión de ruptura dieléctrica, resistividad y factor de pérdidas dieléctricas, al igual que la densidad, viscosidad y conductividad térmica. El contenido de humedad de las muestras también ha sido analizado para permitir comparar los resultados obtenidos.

Desde el punto de vista dieléctrico, solo los nanofluidos de Fe_2O_3 y TiO_2 presentan una mejora clara de sus propiedades respecto del aceite base, hasta un máximo del 15,1 y del 33,2%, respectivamente. El mejor comportamiento del nanofluido de óxido de titanio respecto al de maghemita es corroborado por la mejor evolución que muestran la resistividad y el factor de pérdidas dieléctricas con su concentración. Por su parte, los resultados obtenidos con nanopartículas de ZnO y CuO no son definitorios. Presentan mejoras incluso superiores a las logradas por el Fe_2O_3, pero no son consistentes con la evolución esperada de este parámetro con la concentración de fase sólida.

En cualquiera de estos casos, la mejora de la capacidad aislante del fluido base mediante la adición de nanopartículas se debe a la capacidad de estas de capturar y ralentizar los electrones surgidos durante la ionización del aceite al estar sometido a elevados campos eléctricos. Al ser capturados se evita su migración rápida hacia el cátodo y la generación de una zona cargada positivamente que potencia el campo exterior y promueve dicha ionización, terminando por generar una descarga completa o streamer. Esta capacidad se ve limitada a elevadas concentraciones debido a la aparición de puentes conductivos de nanopartículas, justificando la existencia de concentraciones óptimas, hasta el punto de que se puede llegar a reducirse la capacidad aislante por debajo de la del fluido base.

Respecto de las propiedades térmicas, ninguna de las combinaciones estudiadas presenta una mejora clara de la conductividad térmica, contradiciendo la tendencia general en este tipo de estudios respecto de esta propiedad. Otras propiedades como

la viscosidad o la densidad se ven afectadas de manera limitada, según lo esperado debido a las bajas concentraciones utilizadas. Estas bajas concentraciones puede ser también la explicación para la ausencia de variación de la conductividad térmica.

De acuerdo con lo expuesto, las concentraciones óptimas se fijaron en base a los resultados de la tensión de ruptura, y resultaron ser de 0,2 kg/m^3 de Fe_2O_3 y 0,5 kg/m^3 de TiO_2. A pesar de su comportamiento errático, y para poder testar igualmente los nanofluidos de ZnO y CuO desde el punto de vista térmico, se eligieron aquellas concentraciones donde se observaron los mayores incrementos de las propiedades dieléctricas, siendo 0,7 kg/m^3 and 0,2 kg/m^3 respectivamente.

Estos nanofluidos y el fluido base fueron puestos a prueba como fluidos refrigerantes en un equipo experimental. Este presenta un transformador, refrigerado de forma natural por el aceite contenido en un tanque en el que está inmerso, y que alimenta un circuito eléctrico resistivo, formado por un conjunto de reóstatos. Las temperaturas en diferentes posiciones del tanque y el transformador, así como en el exterior, son registradas automáticamente gracias a varias sondas controladas por un equipo informático mientras el transformador alimenta el circuito. Mediante el ajuste de los reóstatos, la actuación de los fluidos ha sido testeada a diferentes regímenes de carga, correspondientes con la carga nominal y con sobrecarga y subcarga del 30% respecto a la primera.

Los resultados de temperatura registrados y convertidos en gradiente respecto a la temperatura ambiente muestran que, mientras que con el nanofluido de Fe_2O_3 la refrigeración es mejorada (hasta un 11,2%, en función del régimen de carga), con las otras nanopartículas se produce un empeoramiento con respecto de lo visto con el fluido base, que puede llegar también a los dos dígitos.

Mientras que la mejora de las propiedades dieléctricas se puede explicar en base a la capacidad de las nanopartículas de capturar electrones y demorar la ocurrencia de la ruptura dieléctrica, como ya se ha comentado, la comprobada mejora de la capacidad

refrigerante del ferrofluido no se ve explicada por un aumento de la conductividad térmica. La ausencia de esta mejora con las otras nanopartículas testadas, y el distintivo carácter magnético de las partículas de Fe_2O_3 parecen apoyar la existencia de fuerzas termo-magnéticas que promuevan la convección en el aceite sometido al campo magnético del transformador.

En vista a todo lo anterior se ha concluido:

- Entre las nanopartículas testeadas, solo las de Fe_2O_3 y TiO_2 han demostrado clara y fiablemente mejorar la tensión de ruptura dieléctrica del éster natural utilizado como fluido base, especialmente la segunda de ellas.
- La dependencia de este parámetro en la humedad o la concentración de nanopartículas de Fe_2O_3 y TiO_2 ha demostrado ser como se explica en la bibliografía al respecto.
- Las concentraciones optimas, desde el punto de vista dieléctrico, fueron de 0.2 kg/m^3 de Fe_2O_3 y 0.5 kg/m^3 of TiO_2.
- En el caso de las nanopartículas de CuO y ZnO su influencia en la tensión de ruptura no es clara, a pesar de detectar mejoras. Esto puede deberse a que estas cuentan con una distribución de tamaños menos homogénea.
- El resto de propiedades dieléctricas analizadas (resistividad y factor de pérdidas) parecen corroborar los resultados previos.
- En resumen, las nanopartículas de óxidos metálicos añadidas en bajas concentraciones han demostrado ser capaces de mejorar las propiedades dieléctricas también de los aceites alternativos de transformador.

Respecto de las propiedades termo-físicas se concluye:

- Al contrario que la densidad o la conductividad térmica, solo la viscosidad parece ser afectada por la presencia de nanopartículas a las concentraciones utilizadas. En cualquier caso, este efecto es limitado, cumpliendo aún los nanofluidos el valor límite de viscosidad que fija la normativa para ésteres nuevos.

- Resumiendo, las propiedades térmicas no condicionan la capacidad refrigerante previa del fluido base y no influyen al seleccionar las concentraciones óptimas.

Finalmente, respecto de lo descubierto con la plataforma experimental se concluye:

- Existe una discrepancia entre los resultados experimentales de los diferentes nanofluidos. Dichos resultados tienden a señalar un empeoramiento de la refrigeración con los nanofluidos TiO_2, ZnO y CuO. Sin embargo, lo visto con el nanofluido de Fe_2O_3 es lo opuesto, refrigerando mejor que el fluido base, más cuanto más alta es la temperatura de la muestra, a pesar del ligero aumento de la viscosidad y del mantenimiento de la conductividad térmica.
- Esto, junto con la distintiva naturaleza magnética de las nanopartículas de Fe_2O_3 parece apuntar a la existencia de fuerzas de flotabilidad de origen magneto-térmico que potencian la convección en el tanque.

Partiendo de este trabajo y sus conclusiones, se plantean las líneas de investigación futura:

- Llevar a cabo la validación experimental de la naturaleza magnética de la mejora vista en la refrigeración. Este trabajo deberá ser apoyado con modelos de dinámica computacional de fluidos de la plataforma. Para ello se deberá realizar una caracterización de las propiedades magnéticas de la plataforma, las nanopartículas y los nanofluidos.

- Desarrollar un estudio sobre la estabilidad de los nanofluidos aquí presentados, tratándolos con surfactantes hasta garantizar su aplicabilidad. Diferentes surfactantes, concentraciones y condiciones de tratamiento serán testadas, buscando también mantener las propiedades mejoradas de los nanofluidos. Tras identificar el tratamiento más adecuado, será aplicado como una etapa del procedimiento óptimo de preparación de nanofluidos propuesto, que a su vez debe ser comprobado y ajustado.

- Otra etapa del estudio de aplicabilidad será el sometimiento de los nanofluidos estables a procesos de envejecimiento térmico acelerado, para el estudio de la evolución de sus propiedades con el tiempo bajo condiciones de trabajo.

- Finalmente, se propone testear los nanofluidos estables en circuitos de refrigeración reales, poniendo el foco en qué consecuencias tiene la presencia de nanopartículas no solo en su efectividad desde el punto de vista termo-dieléctrico sino también sobre el propio circuito, vigilando la aparición de desgaste, depósitos,…, y estudiando cómo evitar estos efectos negativos.

TABLE OF CONTENTS

LIST OF FIGURES

LIST OF TABLES

LIST OF ACRONYMS, ABBREVIATIONS AND SYMBOLS

ε: Relative Permittivity

σ: Electric Conductivity

τ: Relaxation Time Constant

AC: Alternating Current

BDV: Breakdown Voltage

C: Capacity*

C: Load Index*

CIGRE: International Council of Large Electronic Systems

CNT: Carbon Nanotubes

D: Diameter

DC: Direct Current

DDF: Dielectric Dissipation Factor

DP: Degree of polymerization

f: Frequency*

f: Viscometer geometric factor*

H: Magnetic Field

HV: High Voltage

I: Current Intensity

IDE: Integrated Development Environment

IEC: International Electrotechnical Commission

L: Length

LV: Low Voltage

M: Magnetization*

M: Viscometer geometric constant*

Md: Torque value

m: Moisture Content

n: Rotor Speed

P: Power

PD: Partial Discharge Magnitude

PDIV: Partial Discharge Inception Voltage

PF: Power Factor

PEA: Pulse Electroacoustics

R: Radius*

R: Electric Resistance*

RMS: Root Mean Square

S: Surface

T: Temperature

TSC: Thermally Stimulated Current

TSO: Transmission System Operator

V: Volume*

V: Voltage*

*Those symbols marked with this sign represent different parameters depending on the text context.

CHAPTER 1:

INTRODUCTION

1. INTRODUCTION

The electric grids will grow in importance in the mid-term due to the generalization of the electric transportation. The road transport represented more than the 25% of the final energy consumption in EU28 by 2015 [1], covered mainly by fossil fuels. Under the fight against pollution, the environmental public policies promote the transition of this demand towards renewable sources by increasing the share of electric vehicles [2], with two main objectives. First, to reduce the pollution at the cities, causative of milliards of deaths every year, and second, to reduce the emission of greenhouse gases, according to the programs against the climate change [2]. The production of electricity has migrated progressively during the last years from technologies based in fossil combustibles to renewable sources, and it is expected be based only on them in a close future [3]. Thus, on view of this general situation an increase of the percentage of energy delivered by the electric grid is expected [4].

In parallel to this, it must be considered that the main renewable energy sources (solar and wind power stations) can disrupt the planned operation of the Transmission System Operators (TSO) of the electric grid. Due to their variable nature, the transportation grids must be prepared for the management of eventual peaks of production, allowing its exploitation [4]. The future needs require grids with higher capacity and reliability.

These challenges would be especially demanding for electric transformers, as nodes in the networks. The grid resilience can be enhanced by the adoption of transformers with extra-loadability. These must be adapted to manage these levels of power in safety by increasing their efficiency. A traditional problem is the weakness of the cellulosic insulation of transformer windings due to hot spots produced by high loads. Several TSOs are starting to use transformers equipped with high-temperature insulating materials (natural esters and thermally upgraded Kraft papers) able to provide a permanent overloading up to 150% of nominal rating [5], [6] of power transformers, could rise from the nanotechnology. Attempting to increase the life expectancy and

efficiency of these machines other techniques are under development to improve their cooling and isolation, such as the application of dielectric oil-based nanofluids.

1.1. NANOTECHNOLOGY AT THE ELECTRICAL SYSTEM

Nanoparticles have unique properties that arise from scale effects. Due to their size, their ratio surface/volume (S/V) is much larger than bulk materials. Consequently, the relative presence of atoms and their availability for surface interactions with surrounding media is higher, providing them with special properties. This is the main principle behind the nanofluids, those fluids that contains a solid fraction of particles suspended, whose size distribution is in the nanometer scale and that present consequently modified properties and capacities.

The use of nanoparticles and nanofluids is currently growing in importance, in medicine, in detection and treatments against cancer or in the administration of medicines [7], [8], in material science, obtaining enhanced properties polymers and materials for several applications [9], [10], in the treatment of industrial wastes, as they are able to capture polluting substances [11], and also in energy and thermal engineering, for energy and heat storage and cooling [12]–[14].

Beyond their potential applications in the generation and storage of energy, nanoparticles may play an important role in energy transmission systems. The improvement of transformer's cooling systems by the application of dielectric nanofluids is also under investigation since it was proposed in the late 90's [15]. Originally proposed by *Segal et al.*, who started research in this area, the main idea is to translate the supposed advantages of nanofluids as a cooling medium (pointed out a few years earlier by Choi et al. [16]) to the cooling systems of high power transformers. This is achieved by the addition and dispersion of low quantities of nanoparticles in traditional transformer mineral oils.

Theoretically, the larger thermal conductivity of nanoparticles in comparison to the fluid may lead to an improvement in cooling and therefore a reduction in hot spots and the mean temperatures of the copper wires. This provides an opportunity for the power enhancement of this equipment, while protecting the components from thermal failure more effectively. Nevertheless, to ensure that the use of nanofluids on transformers is viable, other properties must be considered.

This is why, over the last two decades, different researchers have put their efforts into the study of dielectric nanofluids. They have investigated properties related to thermal transport and cooling, such as thermal conductivity, viscosity, convective coefficient, and specific heat; electric isolation capabilities of the fluid (mainly dielectric strength); and those that define the relationship between the fluid and other components of the system or how the materials evolve over time under different stresses and environments, such as stability, aging resilience, and the degree of polymerization of a dielectric cellulosic immersed in nanofluid.

The results were very often positive and unexpected. This encouraged further investigation, with the aim of obtaining a suitable thermal-dielectric nanofluid.

1.2. PROBLEM STATEMENT

Despite the efforts and time dedicated to this topic, the vast majority of the works and researches have been focused on the simply characterization of the properties, mainly dielectric, of the nanofluids. Different combinations of dielectric oils and nanoparticles of different nature have been prepared and tested, trying to first check their effects on the properties of the base fluid, later to notice how these effects depend on the type, size, shape, concentration or treatments of the particles.

Thus, it has been noticed how the dielectric strength or the thermal conductivity of a dielectric oil can be enhanced by the addition of nanoparticles, mainly metal oxides, or that these improvements are usually conditioned by the nanoparticles concentration

due to the existence of an optimal one, as it is said in the section 2. Nevertheless, there is a lack of experience on their application at actual electrical devices in operation. To ensure their applicability not only the properties of the nanofluids must be known separately, but also it is necessary to know how the different physics involved in the performance of a thermal-dielectric fluid interact.

Additionally, these works have focussed mainly on the most traditional transformer oils, as they are the commercial mineral dielectric oils available. In this sense, the oil industry is now making a great effort for the substitution of these traditional oil by their biodegradable counterparts, based on natural ester derived from crops as soybean, sunflower seeds or rapeseed, because of environmental and economical reasons [17]. This is foreseen to occur in the medium term, and consequently the research for dielectric nanofluids may be based mainly on these alternative fluids from now on.

1.3. THESIS OBJECTIVES

The general objective of this doctoral thesis is to make progress in the knowledge about dielectric nanofluids beyond the mere characterization of their properties, taking an additional step towards the current application of these kind of fluids, specifically those with biodegradable base. More accurately, the specific objectives are:

- To assess the nanoparticles to find those suitable for their addition to a commercial natural ester by the thermal-dielectric characterization of different combinations.
- To determine experimentally the optimal concentrations of the suitable combinations of nanoparticles and base fluid, again in the basis of their properties characterization.
- To test the suitability and the behaviour of the best nanofluid samples according their properties in an actual case: the cooling of an experimental setup with a transformer at different load conditions.

1.4. DOCUMENT STRUCTURE

This thesis document if formed by five sections.

In this first section the structure of the document, as well as a brief description of the thesis objectives and the work carried out according to them, are presented.

The second section is a review of the state of the art in this topic. It shows a review of the researches developed by other authors about the dielectric nanofluids. First, it focuses on the preparation methods found in dielectric-nanofluid research and how these methods condition the properties of the resulting dispersions. The consequences on these properties have been then addressed, especially the essential aspects which the application of dielectric nanofluids relies on. In this sense, the focus has been on the cooling capacities and dielectric properties of nanofluids. Their evolution with time and how their presence affects other transformer components have also been analysed. Finally, some conclusions are drawn.

The third section affords the explanation of the experimental methodology followed during this research for the characterization of the nanofluids, and collects the available information about the components used during their preparation. Likewise, the design and functioning of the experimental setup are explained.

For its part, at the fourth section, the results obtained are presented and discussed. More precisely, in this section it is justified the selection of the optimal nanofluids concentration, according to the characterization results, and their performance as a cooling fluid at the setup is addressed.

Finally, at the fifth section, the conclusions of this work, together with the main contributions and publications derived, are presented. In the same way, the future lines of work beyond this thesis are pointed out.

CHAPTER 2:

STATE OF THE ART

2. STATE OF THE ART

The present section presents a bibliographic revision of the works of other authors about the characterization of dielectric nanofluids for transformers, focusing on those properties in which depend the suitability of these fluids for their application in actual equipment. The section starts with a brief description of the methods used in the preparation of the nanofluids, as well as with a collection of the design parameters considered with the purpose of providing these nanofluids of the best characteristics.

2.1. PREPARATION AND DESIGN OF THE NANOFLUIDS

The final configuration of a nanofluid, whatever its purpose, depends not only on a proper election of its components (base fluid, nanoparticles, surfactants) but also on the conditions during the mixture of them. The characteristics of the base fluid or the solid fraction are as crucial as how they are mixed, as on this depend if these characteristics result according the intended way.

2.1.1. Preparation methods of a nanofluid

As one of the main branches of nanotechnology, with several potential applications in different fields such as medicine and engineering, in Nanofluidics different nanofluid preparation methods have been developed and adapted in function of the final characteristics pursued by the researchers and producers, but also depending on the raw materials and available equipment. A compendium is available describing the wide range of production methods in [18]. This explains that they are classified in three categories: two-step and one-step methods, and all other methods. The first two differ from each other in how nanoparticles are introduced into the base fluid. Two-step methods first produce nanoparticles as dry powders, by top-down or bottom-up methods (Figure 2.1), which are added and dispersed in a second stage; while one-step methods produce the nanoparticles directly within the final fluid. Other methods require the transference of nanoparticles between phases during synthesis; this takes

place when new radicals appear on the surface of the particles, changing the inclination of solids to a determinate fluid. These alternatives are represented in Figure 2.2.

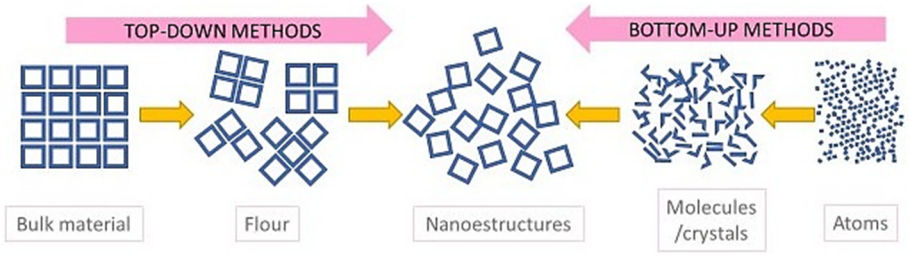

Figure 2.1. Synthesis methods of nanoparticles and nanostructures.

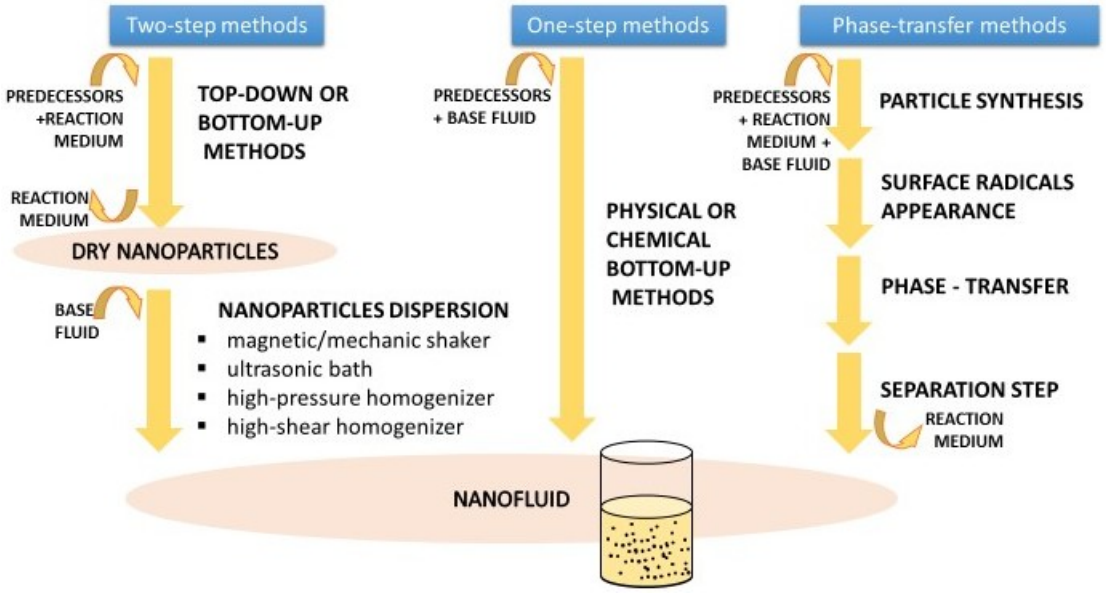

Figure 2.2. Available preparation methodologies for nanofluids.

Every methodology presents its own disadvantages [18]. In two-step methods, as particles must be recovered from the reaction solution and kept as a powder, aggregation processes take place. Dispersion in the base fluid, carried out by magnetic/mechanic shakers, ultrasonic baths, or homogenizers, used to ensure a proper distribution of particles, are useful in breaking up the aggregates created during handling. Despite the dispersion steps, aggregates continue to be created. This may have consequences for the stability of the nanofluids, as aggregates migrate to the bottom of the dispersion faster. Therefore, surface treatments with surfactants to avoid aggregation become necessary. The main problem with one-step methods is that, as the nanoparticles remain in reaction fluid, so do the reaction waste products and residual

reactants; these are able to distort the nanoparticle effects over the base fluid properties [18]. Moreover, there is often little knowledge about the characteristics of these additional particles.

Two-step methods were followed in most of the papers we reviewed. Regardless of their origin, for the preparation of nanofluids, a certain amount of nanoparticles was added, until the desired concentration in the base fluid was achieved. One-step methods were found only in articles using water as base fluid [19], [20]. Thermal-dielectric nanofluids are habitually based on mineral oils, but there are several examples prepared using esters. In this case natural esters prevailed over synthetic alternatives, as shown in Table 2.1. Frequently, dielectric base fluids suffer pre-treatments such as filtration or drying, to eliminate impurities that affect their performance as an isolation medium, as specified in the regulations for transformer oils by the International Council on Large Electronic Systems (CIGRE) or the International Electrotechnical Commission (IEC).

To disperse particles in the base fluid, in these cases, both magnetic/mechanical shakers and ultrasonic baths are used, [21]–[32] frequently for less than 30 minutes, especially with the former, according to Table 2.2. Aggregates are thus broken apart, ensuring the homogeneity of the nanofluids. Therefore, sonication is sometimes used as a final step in the particle preparation, as it occurs with milling [33]. An alternative method of homogenization is available in which a mixture of the base fluid and solid fraction are passed through a high-pressure homogenizer that divides the sample stream into different microchannels [34]. The mixture suffers high velocities, shear forces, crashes, and cavitation, which break the aggregates apart and disperse the particles. Another method uses a high shear homogenizer that breaks aggregates apart by friction, with samples set between its stator and its turning rotor [35].

Table 2.1. Classification of references in function of base fluid used.

Base fluid	Reference
Water	[19], [25], [35]–[48]
Mineral oil	[15], [23], [24], [30]–[34], [40], [41], [49]–[128]
Synthetic ester	[73]
Natural ester	[26]–[29], [126], [127], [129]–[134]
Paraffinic oil	[53], [77]
Wasted oil	[135]
Ethylene Glycol	[38]–[40], [77], [136]
Hydrocarbons	[25], [77], [137]
Organic solvents	[25], [40], [56], [138]

During these phases, especially with ultrasounds, samples are exposed to heating [139] which can harm the bonds between the surfactant and particles. In some articles, variations on the general method of dispersion are used. For example, the dispersion process may be repeated several times to eliminate excess surfactant completely, in an attempt to optimize the coating of particles and to avoid the formation of a double layer of organic acids [112]. In other studies, sonication is implemented with regular stops to prevent the excessive heating of samples under treatment [23], [47], [62], while others include a cooling system [139].

Once the nanofluid is prepared, before its application, it is frequently dried under heat and vacuum, as with nanoparticles, for at least for 12 hours [28]–[30], [49], [50], [128]. This enhances the dielectric strength of the fluid, prevents the formation of new bubbles, gives the fluid time to dissipate existing bubbles [26] [32], [51]–[53], and can even eliminate traces of volatile solvents [33].

Table 2.2. Homogenization times during nanofluids preparation.

Time	Sonication	Stirrer shaking	Nanoparticle	Base fluid
<30 min	[27], [30], [54]–[57], [132], [134]	[58]–[64], [134]	Fe_2O_3 - Fe_3O_4 - TiO_2 - SiO_2 - AlN	Mineral oil - Natural ester
30 min-1 h	[67], [108]	[65]–[67]	BN - Fe_2O_3 - Fullerene - TiO_2	Mineral oil
1-2 h	[42], [60]–[66], [127]		SiO_2 - TiO_2 - Al_2O_3 - Fullerene - Fe_3O_4 – Carbon nanotubes	Mineral oil - Natural ester - Paraffinic oil
	[23], [59], [114]	[23]	TiO_2 - BN - Graphene	Mineral oil
6-12 h	[41]		Cu	Mineral oil
12-24 h		[78]	Fe_3O_4	Mineral oil

2.1.2. Design characteristics of the nanofluids

The disadvantages of nanofluids are mainly due to the size and concentration of the particles used, as their instability, the sedimentation of the solid fraction, resulting in the loss of any improvement in the base fluid properties, and other undesirable consequences such as abrasion of the pipes and an increase in the pumping power requirements due to a penalty on pressure drop. It must be considered that the current mean residence time of a traditional dielectric fluid in a transformer under use is several years [51], [140]. So, the aim is to find nanofluid dispersions that last as long as possible, with reduced maintenance, and economical operation of installations.

The stability of the particle dispersion depends on these parameters, as they predetermine if gravity, buoyancy forces, and the surface interactions with the fluid are

in equilibrium. A greater mean size or lower S/V ratio leads to a reduction in the surface interactions and to greater gravitational forces, promoting sedimentation [18]. Similarly, a higher concentration of particles promotes aggregation, as the probability of successful contacts between particles rises. Moreover, it increases abrasion and the pumping requirements.

Thus, a fluid with fewer and smaller particles may have an optimized number and strength of interactions among the different components, reaching a new equilibrium of forces that keeps the dispersion stable. At the same time, due to the low concentration of particles used, this nanofluid may be less abrasive and would have a viscosity and density close to the base fluid, resulting in a more suitable fluid for use in cooling circuits. All these provisions have been considered during the preparation of dielectric nanofluids.

By definition, nanoparticles have a maximum size of 100 nm in any direction [141], but most of the references we examined were carried out with mean sizes below 20 nm (63 %), or with maximum sizes below 50 nm (78 %), in order to increase S/V. The reviewed papers are classified as a function of the size of the added particles in Table 2.3.

As mentioned earlier, the stability of the particle dispersion depends on the particle size, and this parameter grows with time due to aggregation. This phenomenon occurs when particles collide with each other, and it becomes more frequent as the particle concentration increases. This, together with the consequences of over viscosity, hinders the use of elevated concentrations, even though it is supposed that the beneficial effects of nanoparticles would increase with concentration. So, a compromise solution was pursued. A volume fraction under 1 % is recommended in [93], which is a mass fraction of 5.9 % or 52 g/l for magnetite in mineral oil, and 4.47 % or 39 g/l for titania in mineral oil. Table 2.4 summarizes the concentration ranges of the tested nanofluids, very often only ten to one hundred times the trace concentration, or even less. Approximately 77

% of the reviewed papers presented concentrations under the recommended maximal value.

Table 2.3. Mean and maximum distribution size in dielectric nanofluids.

Size	Reference
Mean size	
< 10 nm	[23], [26], [31], [32], [34], [42], [54], [58], [65], [66], [68]–[76], [128], [133]–[135], [142]
10-20 nm	[23], [33], [42], [49], [51], [52], [54], [60], [61], [66], [77]–[91], [127], [128], [142]
20-30 nm	[24], [27], [55], [62], [65], [92]
30-40 nm	[30], [42], [56], [129]
40-50 nm	[33], [54], [56], [67], [93]–[95], [130]
50-100 nm	[41], [53], [59], [61], [96], [129]
> 100 nm	[56], [97]
Distribution larger size:	
< 10 nm	[34], [98]
10-20 nm	[34], [63], [81], [85], [86], [89], [99]–[106]
20-50 nm	[25], [28], [29], [42], [51], [64], [78], [95], [107], [108]
50-100 nm	[59], [96], [107], [108]
100-250 nm	[71], [133]
250-1000 nm	[129]

Dielectric cooling fluids for transformers are organic chain compounds obtained from petroleum and vegetal sources, as is the case for mineral oils and ester-based fluids respectively. These are mainly non-polar and hydrophobic molecules, so their interactions with nanoparticle surfaces are not electrostatic like those in watery colloids [18]. Beyond size and concentration, the surface characteristics and interactions with the surrounding medium must be considered, along with other aspects, both internal and external, that can affect stability. According to the references, this includes the

shape and behaviour under high temperatures and magnetic fields. Thus, nanoparticles added to dielectric fluids should necessarily gather chemical stability under the expected work conditions and have a tendency to interact with the base fluid.

Table 2.4. Nanoparticle content in dielectric nanofluids in revised literature.

Concentration	Reference
% volume	
< 0.05 %	[29], [34], [61], [63], [107], [131], [133]
0.05-0.1 %	[24], [97], [104], [109], [126]
0.1-0.5 %	[30], [56], [74], [94], [128]
0.5-1 %	[23], [42], [52], [53], [55], [57], [76], [93], [101], [103] [104], [110], [111]
1-5 %	[31], [33], [72], [77], [78], [90], [97], [98], [112], [113], [137]
5-10 %	[41], [143]
20-40 %	[95]
% weight	
<0.01 %	[26], [27], [32], [61], [130]
0.01-0.05 %	[28], [59], [66], [107], [134]
0.05-0.1 %	[60], [63], [65], [67], [71], [109], [114], [115]
0.5-1 %	[27], [132]
1-5 %	[58]
g/l	
<0.1 g/l	[51], [62], [87]–[89]
0.1-1 g/l	[24], [49], [50], [54], [64], [70], [73], [91], [96], [108], [116], [127], [128]
1-10 g/l	[81], [95], [117], [118]
10-50 g/l	[56], [80], [82], [83]

Since the beginning of these investigations, the most common nanoparticles have been metal oxides, which are very stable compounds, specifically magnetite (Fe_2O_3) and other

iron species (38 % of thermal-dielectric nanofluids) and titania (TiO_2) (20 %). Alumina (Al_2O_3) and silica (SiO_2) are also common (approximately 10 % each), with other metallic oxides (10 %), and all other nanoparticles (12 %) occurring less frequently. Some examples can be found using pure metal nanoparticles, which tend naturally to oxidation. Over time, as they become more frequent in other fields of nanotechnology, different nanostructures such as graphene, fullerene, and carbon nanotubes (CNT) have been used with the expectation that their organic composition will make them suitable for dispersions with long-term stability. Table 2.5 gives a breakdown of the different nanoparticles found in the works we reviewed, specifically dedicated to thermal-dielectric analysis.

From the point of view of their properties, mainly based on their respective bulk materials, these nanoparticles fulfil the condition of having thermal conductivities several times greater than the dielectric base fluids, approximately ten times greater for magnemite and more than ten thousand times greater for diamond and carbon nanotubes (Table 2.6) [18], [34], [53], [65], [94], [114].

Table 2.5. Composition of nanoparticles used in references.

Nanoparticle composition	Reference
Magnetite (Fe_3O_4)	[15], [26]–[29], [31], [32], [49], [50], [54], [55], [57] [62], [68]–[70], [72], [73], [75], [76], [78], [79], [90]–[92], [95], [98], [102], [112], [115], [116], [118]–[120], [127]–[129], [132], [137], [143], [144]
Maghemite (Fe_2O_3)	[53], [79], [108], [133], [134]
Hematite & other Fe oxides	[77], [111], [134]
Polymetallic ferrites	[113], [142]
Titania (TiO_2)	[23], [24], [51], [56], [59], [62], [65], [80], [82]–[86], [88], [89], [95], [101], [103]–[108], [110], [131]
SiO_2	[42], [53], [54], [60], [61], [63], [66], [79], [81], [110], [121]
Al_2O_3	[33], [53], [64], [69], [79], [81], [84], [93], [95], [97] [108], [117]
ZnO	[52], [56], [79], [93], [110]
CuO	[97], [108]
ZrO, CeO	[58], [107]
Cu, Al, Ag	[42], [41], [97]
AlN, BN, SiC	[30], [33], [53], [67], [94], [114], [115], [126]
Carbon Nanotubes (CNT)	[34], [42], [109]
Fullerene	[42], [65], [66], [71]
Graphite/Graphene/Diamond	[34], [114]

Nanoparticles can also be classified according to their electric conductivity in conductive, semiconductive, and isolating [87], as Table 2.7 shows [94], [114], [145]. Contrary to general belief, the addition of resistive nanoparticles is not required to achieve dielectric nanofluids.

Table 2.6. Thermal conductivities of nanoparticles and dielectric oil.

Bulk material	SiO_2	CuO	Fe_3O_4	Fe_2O_3	Al_2O_3	TiO_2	ZnO
***k* (W/m·K)**	10.4	76.5	1.39	80	36	8.4	13

Bulk material	AlN	SiC	Diamond	CNT	Fullerene	Mineral Oil
***k* (W/m·K)**	140	35	2200	3000	0.4	0.1

Considering shape, it seems that nanoparticles with an elongated shape, such as nanotubes with high aspect ratio length/diameter (L/D), tend easily to aggregation [33], [42], [44]. The nanoparticles used in the reviewed researches were mainly described as spherical or quasi-spherical, especially the metallic oxides.

Table 2.7. Classification of nanoparticles in function of their electric conductivity.

Conductive	Fe_3O_4
	Fe_2O_3
	ZnO
	Graphene
Semiconductive	TiO_2
	CuO
	ZrO_2
Isolating	SiO_2
	Diamond
	Al_2O_3
	BN
	AlN

Considering other aspects, it is very important to conditionate the nanofluid component selection for the expected application and the associated environmental conditions, trying to fulfil the requirements for the physical integrity of the particles over time, suitable behaviour, and a beneficial relationship with the base fluid. It appears that

coolant-nanofluid dispersion could be improved by controlling the operating temperature. The Brownian movement of particles in fluids is enhanced as the temperature increases, so perdurable interactions between particles become less probable, hindering aggregation, as noticed in [68], [122]. Nevertheless, it is compulsory for these nanoparticles to withstand such conditions. Magnetic nanoparticles can be affected by external magnetic fields; as they line up according to the field direction, their Brownian movement is constrained, and their interactions get stronger [77], [99], [100].

Also depending on the expected application of nanoparticles, further treatments may be necessary, where surfactantion is the most common when nanofluids are involved. This consists of the coating of particles with products that make them more prone to remain in suspension [18].

Substances are selected for this according to the particle and base fluid [23], [90], [113], [146], environmental conditions they must withstand [44], [135], and the effects of the surfactant on the properties of the fluid [30]. Considering the addition of nanoparticles to an oil or ester, most of the examples here reviewed show surface functionalization with organic acids of different hydrocarbon chain lengths, mainly oleic acid (55 % of the papers where the presence/absence of a surfactant is mentioned). Table 2.8 summarizes the products used as nanoparticle surfactants in the reviewed papers. The length of the organic acids regulates the particles susceptible to being functionalized, as shorter molecules are only suitable for dispersing a lower fraction of the particles in suspension [147].

These can be included either as reagents during the synthesis of particles [22], [23]–[25], [27]–[29], [31], [50], [134], [144], [148], added to nanoparticles afterwards [26], [27] [30], [32], [33], [45], [78], [113], [119], [146], [149]–[152], or at both times [25]; they can be in a aqueous solution [23], [25], [55], [112], [113], [133], organic solvent [26], [28]–[30], [32], [33], [134], or oil [25], [78]. When using water as a solvent and organic acids

as the surfactant it may be convenient to add substances to enable the contact with the particles, sodium hydroxide or organic solvents such as acetone, for example [21], [25].

Table 2.8. Surfactants used in thermal-dielectric nanofluids.

Surfactant	Reference	Nanoparticles	Base fluid
None	[15], [60], [71], [81], [88], [94], [99], [100], [114]	Fe_3O_4 - Fullerene - SiO_2 - Al_2O_3 - TiO_2 - AlN - Graphene	Mineral oil
CTAB	[32], [59], [96]	Fe_3O_4 - TiO_2	Mineral oil
SDBS	[64]	Al_2O_3	Mineral oil
Span 80	[53], [65], [69]	Fe_3O_4 - Fe_2O_3 - SiO_2 - Al_2O_3 -SiC - TiO_2	Mineral oil
Oleic acid	[23], [24], [26]–[31], [33], [41], [50], [52], [54], [55], [69], [72], [73], [75], [77], [78], [90], [92], [101], [102] [109], [112], [113], [118], [120], [128]–[130], [133], [134]	Fe_3O_4 - Fe_2O_3 - SiO_2 - Al_2O_3 - Cu - TiO_2 - AlN - CNT	Mineral oil - Natural ester - Synthetic ester
Lauric acid	[41]	Cu	Mineral oil
Stearic acid	[69], [80], [82], [83], [88]	Fe_3O_4 - Al_2O_3 - TiO_2	Mineral oil
Silane	[30], [60], [80], [83], [88]	SiO_2 - TiO_2 - AlN	Mineral oil - Natural ester

Under shacking and with the proper amount of energy, acid molecules are adsorbed by particles through physical or chemical interactions; since the last are stronger, they are better at maintaining the coating [133]. Theoretically, the carboxylic groups in surfactant molecules bond to the nanoparticle surface [146], by keeping organic chains towards the surrounding medium, changing surface polarity [60], [129], [149], and by occupying

the active surface [64]. Due to their length, these chains hinder approaching particles by increasing the osmotic pressure, which is known as steric repulsion and is represented in Figure 2.3. The larger distances between particles means that the strength of the van der Waals forces and polar interactions among them are reduced [64], [96], [130], [142], [144], [153]. Additionally, interactions between these chains and the surrounding oil are enhanced, as organic acids are soluble in it [33], [42], [114], [154]. Therefore, this creates coated particles, with both an improved resistance to aggregation and relationship with surrounding oil. This theory is demonstrated in some works by the fact that these particles tend to migrate from water to the organic phase when put together [133], [152], and that the mean size in suspension is much lower when a surfactant is used [65], [101], [142]. A beneficial side effect is that coated particles which were susceptible to oxidation are thus protected [25], [78], [79], [154].

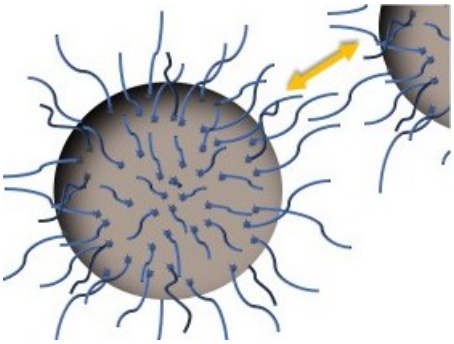

Figure 2.3. Steric repulsion between surfacted nanoparticles.

The treatment is often carried out above the rated temperature in order to assure the adsorption of these reagents [22], [26]–[32], [112], [113]. In the cases we reviewed related to dielectric nanofluids, the temperatures during surfactantion were approximately 80-90 °C [30], [31], [78]. Another important factor is the surfactant concentration. As it is shown in the Table 2.9 (in grams of surfactant per litre of fluid, volume percentage, millilitres of surfactant per gram of nanoparticle or weight percentage), the quantities of surfactant used during treatment were relatively low; it must be below the critical micelle concentration to avoid its own aggregation and negative consequences for fluid viscosity [39]. An optimal concentration from the point

of view of stability or nanoparticle size distribution can be achieved [65]. In some examples, the surfactantion process was repeated to increase the surfactant adsorption [25], [134].

Surfactants maintain the crystal structure of treated particles [142], [150] and slightly increase their size [142]; on the other hand, modifications of the pre-existing surface of particles also have been seen, by the addition of acid substances [46], [78], [119].

Table 2.9. Surfactant concentrations found in references.

Surfactant maximum concentration					
g/l	**2.5**				
	[27]				
%v	**0.25%**	**1.5%**		**4%**	
	[53]	[96]		[78]	
ml/g	**0.026**	**2**		**10**	
	[134]	[70]		[133]	
%w	**<1%**	**<1.5%**	**2-3%**	**22%**	**40%**
	[64]	[59]	[32]	[41]	[65]

Once the particles are ready after their surfactantion they must be recovered from the reaction solution. A number of methods were used in the papers we reviewed, useful also for their recovery after their synthesis, including: filtration [24], [33], [113], [150], centrifugation [24], [27]–[29], [101], [109], [113], [133], [134], [144], [146], [148]–[151], [154]–[156], and natural [152] or magnetic decantation [21], [22], [25], [31], [45], [78], [112], [113], [119], [142], [157], [158] for magnetic particles. Sometimes chemical agents were added to reduce the solubility of the particles in the solvent in order to enable their extraction [27], [134].

This step can be used to select specific particles. For example, during natural decantation, it is possible to take just the particles in the organic phase and to return those in the aqueous phase to the previous processes [133], [152].

Recovery is followed by different phases of washing to eliminate excess reagents and solvents, or to optimize the surfactant coating [21], [146]. During the formation of the surfactant coating, carboxylic groups bond chemically with the particle surface, this makes them lipophilic due to the hydrocarbon chains. However, if the saturation amount of surfactant is exceeded, these extra molecules interact physically with those attached to particles, through their chains, creating a second layer [25], [33], [36], [64] [96], [150], represented in Figure 2.4. For carboxylic groups facing the fluid [33], [36], [64], [150], this gives the particles a polar or hydrophilic nature which, although not suitable for addition to and sustenance in transformer oils, is sought for certain applications [25], [36].

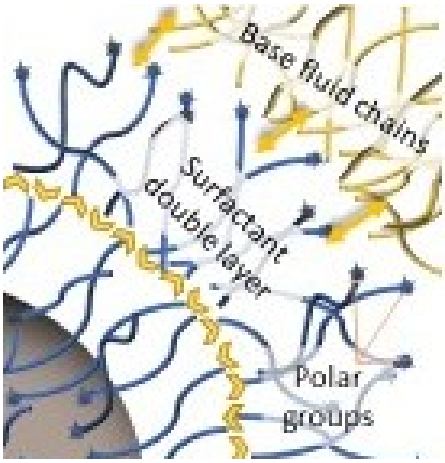

Figure 2.4. Hydrophilic double layer of surfactants and dielectric fluid.

The necessary amount of surfactant for each situation is difficult to know, as it depends on the composition, concentration, morphology, and size of the particles, so washing is a suitable way to remove the extra layer. Water [25], [45], [78], [109], [119], [149], [151], [157], [159], alcohol [24], [144] , organic solvents [112], [142], or a combination of them [21], [23], [26], [28], [29], [32], [101], [133], [146], [148], [150], [154], [155], [158], [160], are used in this step. After mixing and shaking, the nanoparticle must be recovered

again. To eliminate remnants from washing, or moisture in general, the particles are dried by heating them at temperatures up to 100 °C, in air or a vacuum, for between 12 and 72 hours [22], [23], [26]–[29], [31]–[33], [78], [101], [119], [133], [144], [146], [150]–[152], [155], [156], [160]. Alternatively, a nitrogen gas stream can be used for the same process [133]. Drying processes can affect the size distribution of nanoparticle flour, since they promote aggregation [30]. Particles are thereafter kept in the form of flour, or suspended as a concentrated nanofluid.

2.2. THERMAL CAPACITIES OF DIELECTRIC NANOFLUIDS

Although convection is the main mechanism of heat transport when fluids are the cooling medium, nanoparticles are included in the base fluids with the purpose of improving the contribution of thermal conduction. The thermal conductivity of solids is several times higher than that of fluids, by one or two orders of magnitude [53], so theoretically the thermal conductivity of a nanofluid would be intermediate between those of its components, an increase of as much as the solid fraction in suspension. Also, because the convective coefficient depends on the thermal conductivity of the cooling fluid [161], both may be enhanced by the presence of nanoparticles. Nevertheless, this presence could be detrimental to convection, which depends on the nanofluid's viscosity and evolution with temperature, but this parameter is affected by the nanoparticles. Additionally, improvements in conduction are constrained by the concentration limits set by the stability requirements. Again, a compromise solution between all of these parameters must be achieved.

Thus, since the proposal of cooling nanofluids, researchers have focused on demonstrating these tendencies, and have tried to determine how to achieve a meaningful improvement in conduction without harming convection, or any other essential properties of the base fluid.

Several direct measurements of the thermal conductivity of nanofluids have been done with samples based on a variety of cooling oils. The aim was not only to verify the effect

of nanoparticles on conductivity [23], but also to show how different variables affect it. Logically, one of the variables was the concentration of solids, but others, such as nanoparticle type, environmental conditions, and preparation method were also explored. These variations let researchers identify greater increases in conductivity, giving an idea of the potential improvement nanoparticles could bring. These results are shown in Table 2.10, where it can be noticed that, although there are examples where the variation was negative or below the confidence interval (5-10 %), most of the results show maximum increases of more than 20 %, and some are approximately 100 %. Some mathematical models support increases in the conductivity of oils by more than 500 % [31], [143]. To help with the comprehension of these results, the Table 2.11 summarises some characteristics of these nanofluids from previous sections of this review.

Table 2.10. Maximal thermal conductivity variation in oil-based cooling nanofluids respecting base fluid.

Maximal Δk (%)	**Reference**
<0	[60]
0-5	[23], [53], [65], [115]
5-10	[30], [42], [53]
20-50	[31], [33], [34], [41], [122], [124], [134], [144]
50-100	[113], [114]

Thus, several of the papers we reviewed support the theory that thermal conductivity grows in line with the nanoparticle concentration [31], [30], [33], [34], [53], [91], [113]–[115], [134], although there is not unanimity [60]. This trend is supported when the results from different sources, which use nanofluids that share most characteristics except the concentration of solids, are compared, as with AlN [30], [33].

Together, the research points out an optimal concentration, as the growth of conductivity decelerates at higher concentrations [30], [113]. Other studies show that

the growth in the conductivity is not linear before saturation, but grows at an increasing rate [114].

The variety of nanoparticles, or the pre-treatments they suffer, can condition these results. It has been shown that the conductivity variations of nanofluids with a similar concentration can differ due to changes in the particle characteristics, such as their composition [33], [34], [115], allotropic structures [23], or shape [33], [34], [114]. Some effects can be explained by the conductivity of the nanoparticles' bulk material [34], [115]; nevertheless, the lack of specific investigations comparing their effect on the function of the composition prevents us from making conclusions about which of them are better. Changes in conductivity may also be a result of differences in the nanoparticle size. In addition, when considering surfacted particles, it has been noticed that the surfactants themselves can increase the thermal conductivity of the base fluid; the higher the concentration, the bigger the increase [30], [33]. However, this effect is small compared to the nanoparticle effect on the base fluid [30].

Table 2.11. Nanofluids characteristics and their effects on thermal conductivity of base fluids.

Ref.	Base fluid	Nanoparticle	Concentration	Size	*k* variation
[23]	Mineral oil	TiO_2	0.075%v	18nm	1.20%
[30]	Mineral oil	AlN	<0.16%v	40 nm	7.00%
[31]	Engine oil	Fe_3O_4	<5%v	---	≈40%
[33]	Mineral oil	Al_2O_3	<4%v	13 nm	20.00%
		AlN		50 nm	20.00%
[34]	Mineral oil	NTC	<0.05%v	15 nm	25.00%
		Diamond		6 nm	20.00%
[40]	Mineral oil	Al_2O_3	5%v	---	38.00%
[41]	Mineral oil	Cu	<7.5%v	100 nm	43.00%
[42]	Parafinic oil	CNT	0.5 %v	10-30 nm	8.50%
[53]	Mineral oil	Al_2O_3	<1%v	<80 nm	≈7%
		SiO_2		<100 nm	≈3%
		SiC		<80 nm	≈10%
	Synthetic oil	Al_2O_3		<80 nm	≈5%
		SiO_2		<100 nm	≈3%
		SiC		<80 nm	≈5.5%
		Fe_2O_3		<100 nm	≈3%
[60]	Mineral oil	SiO_2	<0.1%w	15 nm	-1.60%
[113]	Mineral oil	$Mg_{0.40}Mn_{0.60}–xNi_xFe_2O_4$	<4%v	---	58.00%
[114]	Mineral oil	BN	<0.1%w	---	76.00%
[115]	Mineral oil	BN	<0.1% w	50 nm	≈1%
		Fe_3O_4		20 nm	≈0.5%
[122]	Mineral oil	Ag	<0.72%w	20 nm	≈30%
[124]	Mineral oil	CNT	<0.5%w	10-20 nm	22.70%
[133]	Mineral oil	TiO_2	<0.1%w	25 nm	≈0%
		Fullerene		70 nm	
[134]	Vegetal oil	Fe_2O_3	<0.014%w	10 nm	45.00%
[135]	Waste oil	SiC	<0,3%v	30 nm	23.00%
		TiO_2		10 nm	

Environmental effects on the thermal conductivity of nanofluids were also addressed. The natural tendency of the thermal conductivity of oils is to decrease as the temperature increases [115], [122], [134]. This was observed in some of the investigations with dielectric nanofluids [60], [113], [115], but the opposite behaviour was seen in others [91], [114], [134], as it was in some oils [122], [135]. Considering the magnitude of the conductivity variation with temperature, larger relative increases were observed in the base fluid at high temperatures [114], [134], with signs indicating the existence of an optimal temperature [134]. Nevertheless, other studies have shown linear variations, as is theoretically predicted [113], [115].

Magnetic fields positively affect the conductivity of nanofluids, for a determined concentration, and with a saturation tendency at higher fields [31]. The magnitude of this enhancement depends on the directions of the field and temperature gradients, and when they match each other it is maximal. It seems that particles are aligned according to the field direction, creating a preferential direction for heat transport by conduction, which is able to provide to increase the enhancements by five-fold [31].

These measurements were carried out with accurate equipment which was designed for conductivity analysis in other materials, mainly solids, but was adapted to fluid requirements. These were largely based on hot transient wires and discs [30], [31], [33] [34], [42], [53], [60], [113], [115], [122], [135], like the circuit represented in Figure 2.5, which are an electrical heat source and, at the same time, a probe. The thermal conductivity results were found by linking the changes in resistivity (R_3), voltage (V_0), and temperature in the wires due to the heat dissipation across the tested material. The temperature is controlled by measuring the electrical parameters of the circuit, and the thermal conductivity of the probe surrounding material can be obtained by comparing the evolution of the temperature and the amount of heat produced by the electrical circuit. Other experiments used the temperature oscillation technique [48], 3ω-wire

method [138], or laser flash method [23]. During the experiments, convection was generally limited in the samples by fast measurements and constrained fluxes of oil.

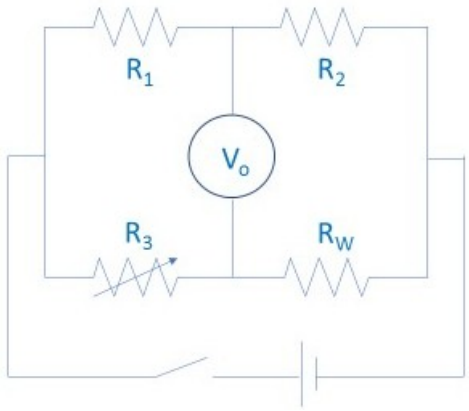

Figure 2.5. Hot transient wire scheme.

According to the literature, natural convection [112] and overall heat transfer [33], [64] are also enhanced by nanoparticles, with similar results to those seen for conductivity in terms of the concentration of nanoparticles [33] and surfactants [64]. More precisely, the improvement in conductivity was lower than that found in the overall heat transfer coefficient, pointing out an improvement in convection [33]. In the same way, the shape and composition of nanoparticles may also affect the heat transfer [33].

Characteristics that could conditionate the convection performance of a coolant oil, such as viscosity, especially with natural flux, were not generally harmed by the presence of nanoparticles. Although slight increases were found [33], [93], [97], [107], [123], they were just as frequent as those with no effects [23], [34], [49], [60], [63], [71], [110], [112], [114]. Indeed, reductions in the viscosity were also noticed [130], [135]. Researchers have demonstrated that viscosity depends on the nanoparticle concentration [107], [143] and shape [34], [114]. To ensure stability, nanofluids were prepared with low concentrations, and the particles were mainly spherical; it is reasonable that the viscosity was not significantly affected as a result. Another idea is that nanoparticles may act as a lubricant between the layers of fluid, as they remain oriented in the flux direction [34]. The viscosity of nanofluids decreases as the

temperature decreases, like with the base fluids [60], [97], [112]. Nevertheless, an essential modification was identified, which changed the behaviour of the base fluid from a Newtonian to a non-Newtonian fluid at a determinate concentration of nanoparticles [34], [122], [135] or at low temperatures [122], due to an increase in the number of interactions [114].

Heating tests with nanofluids samples were also done, controlling the temperatures in the fluid, isolators, and heaters. Here, nanofluids showed better cooling capacities, the temperatures measured in the tester components were lower [67], [92], [115] and those in coolant were higher [67], [134], than in tests carried out with the base fluids; the time required to reach these temperatures was also lower [134]. It was noticed that these differences became more pronounced at higher particle concentrations [67], [134], or when the base fluid was less thermally conductive [115].

Similar results were obtained in other studies with other base fluids such as water or ethylene-glycol, which showed improved conductivity [20], [35], [37], [43], [48], [136] and convection coefficients [43] as the concentration of particles increased. These results were dependant on the composition [42], [48], shape [44], [136], and size [37],[43] of the nanoparticles.

Explanations for these phenomena were given according to four main theories, represented in Figure 2.6. These are the Brownian movement of nanoparticles in fluids, particle-fluid interface behaviour, ballistic phonon transport, and higher thermal conductivity of temporary particle clusters [162], as mentioned earlier.

The first explanation justifies the improvements in the convection and its coefficient because of the Brownian movement of nanoparticles in the base fluid [19], [40], [41], [48], [37], [75], [91], [122], [135], [138], especially for spherical [138] and small [37] particles. This movement would be linked to the fourth explanation. According to this, the nanoparticles continuously form temporary clusters, due to their movement, that

create conductive paths for thermal transport [30], [38], [41], [42], [48], [91], [114], [124], [138]. Considering the second explanation, the molecules in the layers of fluid closest to the particles apparently tend to keep a more regular organization, resulting in behaviour more like that of solids [38], [40], [114], [115]. Finally, according to the third explanation, thermal phonons are able to have ballistic transport between close nanoparticles, due to their wavelength and the distances and diameters involved [38], [40], [75], [114], [115].

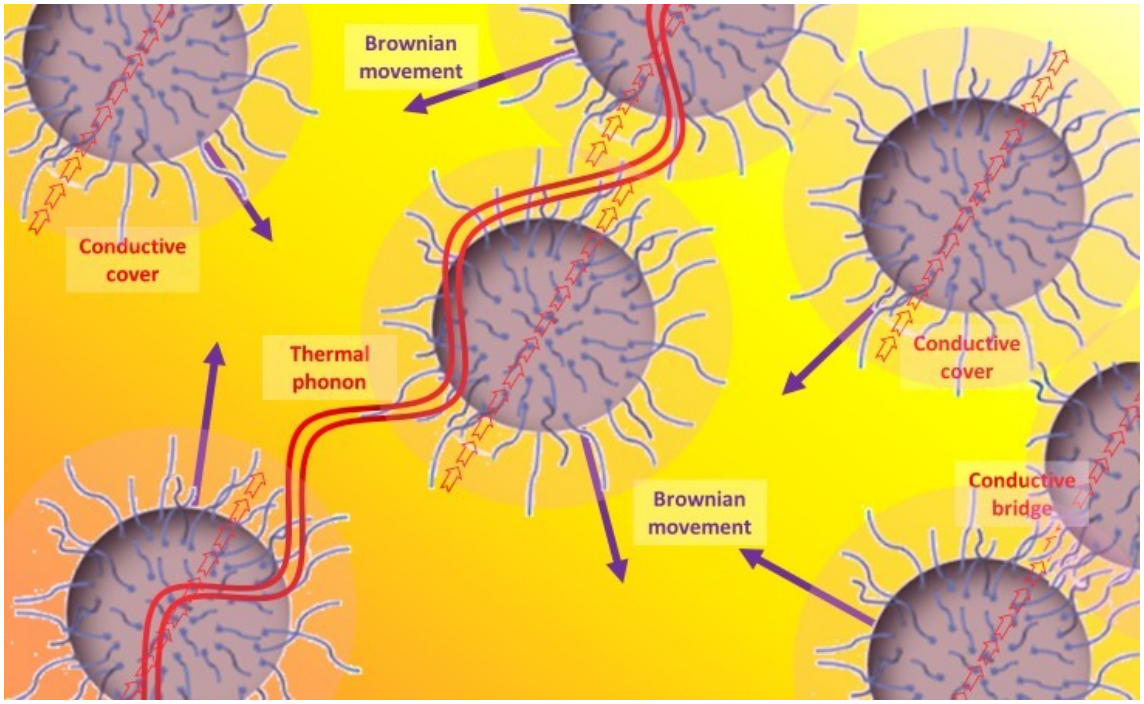

Figure 2.6. Heat transference mechanisms in nanofluids.

Increases in the dispersion concentration or temperature would enhance the magnitude of Brownian motion and temporary clustering [114], and can explain the behaviour observed with these parameters, when caution is taken not to promote settlement. The differences seen for different particle compositions may be due to their bulk material conductivities [34], [115], or because one kind of particle is more prone to maintain stability than others in specific circumstances [135].

Another property which has been studied is specific heat; it has been addressed by a few researchers, using dielectric oils. These results demonstrated that the specific heat

decreased when nanoparticles were added [92], [115], and the effect was more pronounced as the concentration of particles increased [113], [115] (as in aqueous nanofluids [47]), or when their thermal conductivity was bigger [115]. The specific heat also tended to increase with increasing temperature [92], [113].

2.3. DIELECTRIC PROPERTIES

In light of the application of nanofluids in power transformer cooling, the need to characterise their dielectric properties arose naturally. Dielectric cooling fluids must be able to withstand voltages greater than the rated values of the equipment in order to ensure the operation and safety of the components in case of an electrical fault.

This capacity was expected to decrease in dielectric nanofluids in comparison to the base fluids, due to the presence of nanoparticles, as occurs when transformer oils are not prefiltered in line with recommended standards [51], [81] or with microparticles [80], [97]. Nanoparticles are often more electrically conductive than transformer oils, so theoretically, this may harm the fluid's ability to hinder or delay discharges and streamers. However, the results were unexpectedly good, driving interest in this field of nanotechnology. This improvement in the dielectric properties was observed using many of the variety of tests available.

The dielectric strength represents the dielectric fluid capacity of withstanding voltage without the formation of a conductive channel through which an electric current may be established. This capacity is not constant; it depends on the magnitude of the electric field, as it might be sufficient to promote the ionization of fluid molecules and subsequent warming and gas formation, which finally translates to the enhancement of the electric conductivity, represented in Figure 2.7. During ionization, slow cations and fast electrons are created (a); the electrons tend to migrate towards the anode or positive pole, while the cations create a positively charged area. If the required conditions are fulfilled, this could enhance the local electric field, promoting more ionization in the surroundings and providing feedback to this process (b); this results in

the conductive zone spreading in the fluid, an effect known as streamers (c). When completed, a conductive channel of ions and gas is available, and discharge takes place (d). This process, mentioned in several references [54], [55], [57], [59], [69], [90], [95], [116], [118], [130], is supported by simulations [163], [164] in which an ionizing wave was observed by representing the estimated electric field, temperature, and electric net charge over time. Discharge occurs from a determined voltage, dependant on the dielectric media, known as the breakdown voltage (BDV).

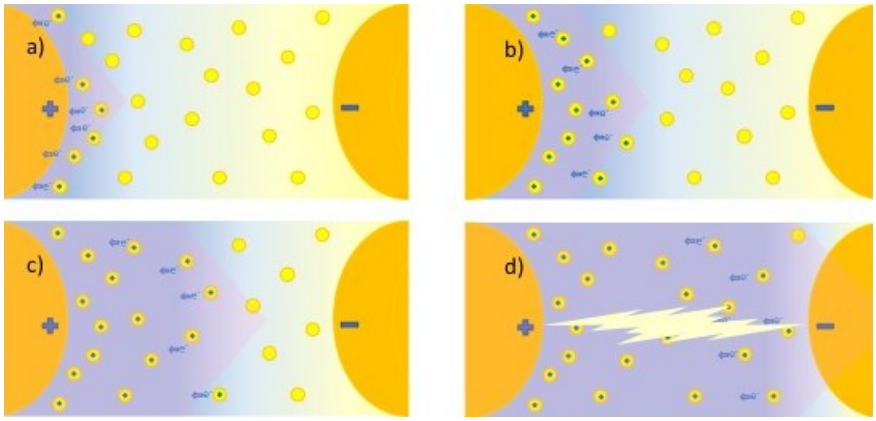

Figure 2.7. Streamer development and discharge in dielectric fluids.

Studies of the BDV have been developed by a narrow range of tests, to be representative of all possible types of dielectric fault. This includes direct (DC) or alternating current (AC) breakdown voltage tests, where samples of dielectric nanofluids are subjected to increasing voltages inside a cell until an electric arc appears between two electrodes, according to IEC 60156 standards for a lapse of time. Lightning impulse breakdown voltage tests are also common (IEC 60897), with the difference that, while the stresses in DC or AC breakdown tests are less acute, lightning impulse tests involve the application of higher voltages for shorter time intervals [73], [79], [89], [95], thus including this kind of failure in investigations. Finally, partial discharges are analysed (IEC 60270) by finding the voltage necessary for their appearance, called the partial discharge inception voltage (PDIV), where localised currents reach a determined magnitude as a function of the background noise [82], [83]. Once the PDIV is known, tests are carried

out at or above this voltage, measuring the magnitude and concurrency of discharges [49], [54], [70].

The following tables collect the results from these tests, carried out under different conditions. Starting with those from alternating current tests, the Table 2.12 shows the range of improvements reached in each of the studies reviewed. Dispersion in the conditions of nanofluids makes it difficult to notice if a specific component is more prone to greater increases in the breakdown voltages, although they seem more constrained in vegetal base fluids, as their starting BDVs are higher. It must be remembered that the breakdown voltages of the base fluids were already above the required values as they are applied in actual transformers, so any increase would be a step towards more reliable and powerful equipment. Although not all of the tests reflected improvements, most of them were more than 10 % higher than the estimated error of the measurement techniques.

In the Figure 2.8 the different breakdown voltage variations noticed in the reviewed works are represented, including the information about the composition of the nanoparticles used during the research (represented by the color of the spot in the graph), their concentration (volume percentage) and the type of base fluid (depending on the colors of the bibliographic reference number, black for mineral oils, green for natural esters). A deeper view is possible with this figure, as it is easy to notice the range of variations usually reached with the addition of nanoparticles, as well as which are the most common in this kind of works, and at which concentrations, or the lack of works carried out with natural esters as bases.

This appears more clearly when the results are refined by statistical methods. By adjusting the obtained data to statistic distributions (frequently Weibull [59], [60], [63], [71], [79], [87], [89], [99], [103], [109], [134], but not exclusively [130]), values for the low probability cases may be inferred. These, also in Table 2.12, represent the minimum voltages at which breakdown could take place, so they are very useful during the design

phases, as they represent the maximum voltage the dielectric can withstand without the risk of failure. Thus, equipment is designed with assigned values below these limits. When comparing these statistics from the base fluids with nanofluids, it can be seen that the improvements in the breakdown voltage are even better, with the majority over 20 %. Less frequently, DC breakdown voltage tests have been also developed, also showing enhanced dielectric strength when in nanofluids compared to the base fluids [73], [75], [84], [104], [115], [128].

Table 2.12. Maximal variations of AC breakdown voltage of nanofluids respecting base oils.

Maximal variation (%)	**AC BDV**	**AC BDV low probability**
<0	[30], [34], [81], [97], [165]	[165]
0-5	[67], [88]	[58]
5-10	[32], [56], [121], [130], [155]	[100]
10-20	[56], [58], [84], [87]–[89], [100], [103]–[105], [118]	[26]
20-50	[15], [23], [27]–[29], [49], [51], [56], [57], [59], [60], [63], [71], [87], [88]. [91], [97], [99], [103], [107], [109], [116], [127], [129], [131], [134]	[54], [84], [103], [104]
50-100	[60], [113]	[59], [63], [71], [99], [134], [165]
>100	[76], [96], [111]	

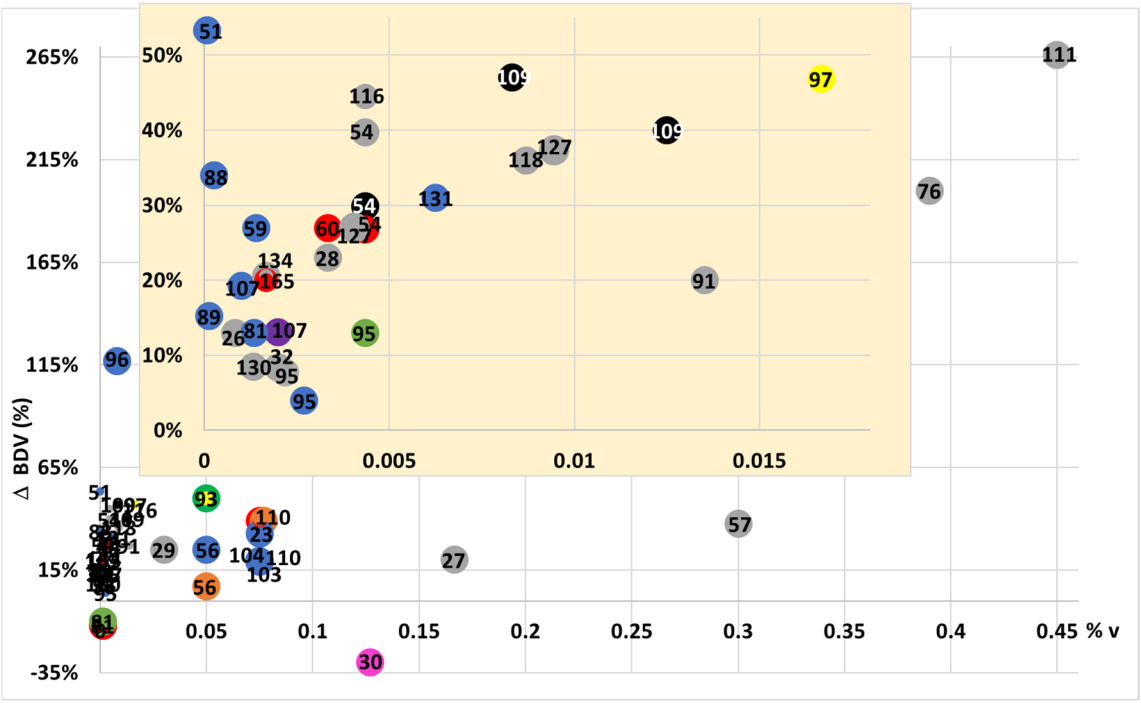

Figure 2.8. Comparative of the BDV maximal variations depending on the base fluid and the volumetric concentration and type of nanoparticles.

Similar results are collected in Table 2.13 and Table 2.14 relative to lightning impulse and partial discharge tests, respectively. The lightning impulse results can be separated into two groups based on their polarity. Standards require that these tests must be done using a needle/sphere configuration of electrodes [50], so these tests are driven by changing their polarity, what conditions the fault development due to their different geometry.

Thus, the results are named according to the polarity of the needle electrode. The negative impulse tests have been classified together with the positive ones, but the sign is opposite. One can see increases in both the voltages and times required for a positive streamer to appear; this means that dielectric nanofluids are not only able to withstand higher stresses, but they also take more time to develop failures, giving extra time to stop them. On the other hand, negative streamers show decreases in the voltages and times in most of the references.

This behaviour, on the whole, is satisfactory. Firstly, it is usual that lightning impulse voltages in base fluids are bigger when polarity is negative rather than positive.

Secondly, variations in the negative voltages with nanoparticles are softer than the positive ones, as can be seen in Table 2.13. Therefore, the use of nanoparticles provides an opportunity to improve the lower lightning impulse breakdown voltage in this kind of dielectric fluid, while the higher voltage decreases much less, or can even improve. Similar trends are observed with the times to streamer formation.

Table 2.13. Maximal variations of breakdown voltage and time to breakdown of nanofluids respecting base oils in lightning impulse tests.

Maximal variation (%)	**BDV + Impulse**	**Time to streamer**	**BDV – Impulse (-)**	**Time to streamer (-)**
<0	[79]	[79]	[27], [28], [30], [73], [132]	[27], [79]
0-10	[58], [87], [95], [117]	[95]	[15], [79], [117], [143]	[79], [143]
10-25	[55], [57], [73], [79], [81], [84], [88], [89], [95], [104], [105], [107], [129], [132]	[27], [79], [89], [95], [117]	[50], [79], [95]	[95], [117]
25-50	[27], [30], [50], [69], [85], [99], [100], [118], [132]	[143]	[79], [118]	[15], [95], [143]
50-100	[15], [28], [143]	[50], [79], [86], [104], [118]		[79]
>100		[15], [69], [143]		

Partial discharges seem constrained in oil nanofluids, as their PDIVs rise while their magnitude and concurrency decline, according to results in Table 2.14, where the

percentages for the partial discharge magnitude (PD) are negative. Nevertheless, here again, not all the results were positive [54], [70]; these cases show that, from a determined voltage, nanofluids changed their behaviour and their partial discharges went from being smaller to being larger than the base fluid ones in the same conditions. Also, for a voltage higher than the PDIV, a higher acceleration of the streamer velocity was observed in nanofluids, such that they reach fast-streamer speed at lower voltage than the respective base fluids [79].

Table 2.14. Maximal variations of partial discharge inception voltage and magnitude of discharges in nanofluids.

Variation (%)	**PDIV**	**PD (-)**
0-5		[61]
5-10	[49], [84], [85], [103], [104], [131]	
10-20	[61], [66]	[61], [84]
20-50	[15], [30], [66]	[66], [67], [104]
50-100	[54]	[66], [131]

There is a spread theory that tries to explain this behaviour of dielectric nanofluids based on the supposed capacity of nanoparticles to capture electrons in their surface [27], [28], [30], [51], [54], [56], [57], [62], [63], [69]–[73], [76], [79]–[81], [84]–[87], [89]–[91], [95], [99], [100], [103], [104], [107], [109], [111], [117], [118], [127], [130], [131], [134], [143], [163]–[165]. This may come from the polarization of nanoparticles with free charges under electric fields; this creates potential wells on the surface and leads field lines, and therefore electrons to nanoparticles, which are captured until saturation, as shown in Figure 2.9. In fact, an equilibrium between captures and liberations may be reached [71], [109], [163], which in practice, together with the lower mobility of particles, would cause

a delay in the migration of electrons and their effects, hindering the appearance of streamers. In the Figure 2.10 it is represented that the general charge at the ionization zone is neutralized due to this effect, as the positively charged base fluid molecules (yellow spots) are compensated by the negatively charged nanoparticles (grey spots).

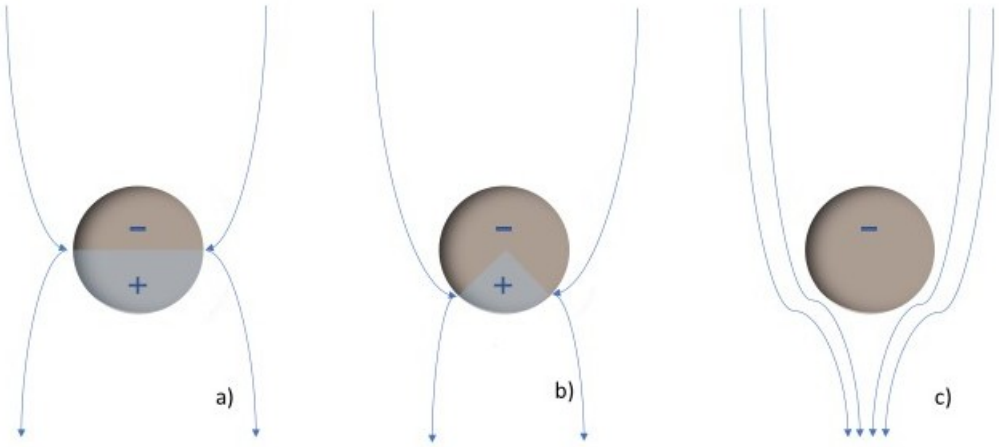

Figure 2.9. Polarization-charging of a nanoparticle under electric stress.

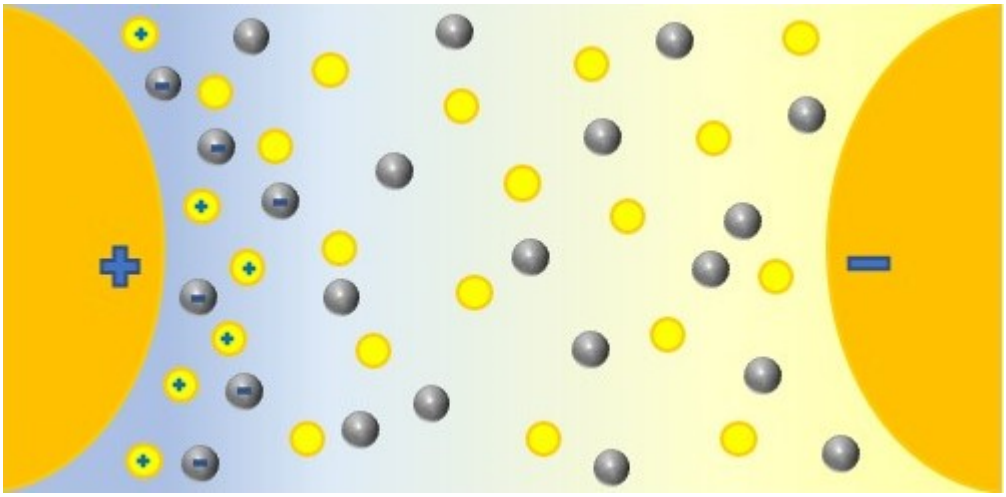

Figure 2.10. Capture of electrons by nanoparticles and delay of the streamer.

Theoretically, this capacity may depend on the particles easiness of polarization and depth of traps. These again depend on particle composition, specifically on their conductivity and permittivity, and their size, respectively. In the first place, traps should be available before electrons emergence, as soon as possible, so polarization time, represented by the relaxation time constant (τ_r), might be under streamer spreading time, in the order of nano to microseconds. According to Eq.1, particles with a higher

conductivity (σ_2) and reduced permittivity (ε_2) would be more suitable for application in dielectric base fluids, whose properties (σ_1 y ε_1) also affect the constant. In the second place, the deeper the wells, the harder it would be to scape for electrons and the bigger their capacity, being thus related to nanoparticles sizes, yet bigger particles present deeper wells [69]. It could also be beneficial from the point of view of saturation charge of each nanoparticle [69], as their surface increases with size, although on the whole total available surface of nanoparticles would be minor.

$$\tau_r = \frac{2\varepsilon_1 + \varepsilon_2}{2\sigma_1 + \sigma_2} \qquad \text{Eq.1}$$

Nevertheless, the particles included in dielectric fluids, collected in Table 2.7, were not only conductive but also semi-conductive or insulating, presenting also improvements of dielectric strength, even higher than those seen in similar conditions for conductive nanoparticles [69], [87], [89], [95], [110], [143]. It could be because polarization of these other kinds of particles takes place anyway, not with free charges, but by means of their own surface charges [69], [95]. This theory is supported by dielectric constant enhancement seen in reviewed articles, explained latterly, as it represents polarization ability.

Other sources link the capture capacity to the formation of a Stern double layer around the particles that may perform as a capacitor [80], [81], [89], [103]. Whatever the cause of electron trapping, its effects on the dielectric properties are clear, being a plausible explanation for the trends found in the test results. In AC and positive lightning impulse tests, the lower mobility of captured electrons should translate to a reduction in the local electric field enhancement at the anode, and thus the need for higher voltages and more time for streamer initiation [27], [56], [76], [86], [95], [99], [104], [134], [143]. In negative lightning impulse tests, when the needle (where the field is more accentuated) acts as cathode, negatively-charged particles may contribute to the enhancement of the field, reducing the dielectric strength [95], as was noticed in the papers here reviewed.

Partial discharges nourish themselves from electrons, so nanoparticles hinder their occurrence; hence, higher voltages become necessary [30], [54] and discharges are less frequent and lower [70].

To try and verify this theory, specific tests were done using measurements of the energy levels and trap density. These were the thermally stimulated current (TSC) [29], [30], [104]–[106], [131] and pulse electroacoustic (PEA) tests [28], [83], [105], [106], [131]. The first involves subjecting nanofluid samples to progressively increasing temperatures after they are stressed in a continuous electric field and cooled. These samples, placed in electric circuits as if they were capacitors, will release the electrons caught in potential traps as the temperature rises while the electric current is controlled. The results show that currents from nanofluids are much bigger than those from base fluids, what can be read as a confirmation of the presence of a larger number of traps on the nanoparticles' surface, although they are also present in base fluid [29], [30], [104], [105], [131]. Meanwhile, the second test measures the time evolution of samples which have been stressed by DC voltage, by using acoustic pressure waves that interact with field and charge [83], [106], [131]. In these tests, a lower density charge [131] and electric field [106], [131] were noticed in nanofluids compared to base fluid. When the stress ceased, the decay rates of the charge were larger in the nanofluids, showing an enhanced capacity to dissipate it [83], [105], [106]. Again, this appears to confirm the described theory according to the charge and field tendency, as the electrons would be able to dissipate by jumping from one particle to another according to the trapping-detrapping mechanism.

Simulations of the breakdown processes, which have been done using models that try to represent the behaviour of nanofluids, have also found differences compared to base fluids, reaching similar conclusions. Thus, in instant density-of-charge curves, while base fluids showed a rapid rise in the number of cations and electrons in the propagation wave front, nanofluids also experienced this phenomenon with anions together with a

reduction in the presence of free electrons. Moreover, it was seen how the wavefront progress was delayed at the same instant it was placed closer to the needle in the nanofluid simulations [163], [164], which also happened when plotting the maximal field [69], [163]. The electric potential between the electrodes was always bigger in the base fluid simulations [69], [163]. These effects were more pronounced when the relaxation time constant of the studied nanofluids was lower [69], [163], [164]. Here again, the capture capacity of nanoparticles seems to be a suitable explanation.

From these results the current interest of researchers in these kinds of investigations can be justified. However, they have not only focused on the effect of nanoparticles on the dielectric strength, but also on its dependence on other variables, as mentioned in previous sections. In this sense, it has been noticed that variations in the dielectric strength were more accentuated for more concentrated nanofluids, with bigger increases of AC [28]. [30], [32], [51], [54], [56], [57], [59], [60], [63], [67], [71], [80], [88], [89], [91], [95], [96], [99], [109]–[111], [113], [115], [118], [127], [134], DC [54], [73], [115] , and lightning impulse breakdown voltages [28], [30], [50], [55], [57], [73], [88], [89], [95], [99], [118]. This was also observed in the times to breakdown [95] and PDIV [30], [54], [70]. Partial discharges, for their part, were reduced as the presence of nanoparticles increased [67], [118]. These tendencies are noticeable when comparing research carried out with different concentrations ([55], [57] and [143]) ([89] and [95]).

Several researchers observed the existence of optimal concentrations at which the dielectric strength started to decrease. These results, collected in Table 2.15, belong to the lower gaps in the concentrations of the prepared nanofluids in the reviewed papers, showed in Table 2.4. The higher availability of traps may enhance electron capture when the concentration of nanoparticles is higher [109], until a determined point at which aggregation results in a reduction of the relative surface and a diminution of the capture capacity [32], [88], [89], [107], especially if stability is affected [134].

Table 2.15. Optimal concentrations of nanofluids respecting dielectric properties.

Optimal concentration	Reference
% volume	
< 0.05 %	[56]
0.05-0.5 %	[30], [55], [57]
0.5-1 %	[90], [111]
1-5 %	[31], [33], [72], [77], [78], [90], [97], [98], [112], [113], [137]
5-10 %	[41], [143]
20-40 %	[95]
% weight	
<0.01 %	[32], [51], [59], [88], [95], [107], [109], [134]
0.01-0.05 %	[54], [70], [95], [109], [116], [118]
0.05-0.1 %	[109]
g/l	
<0.1 g/l	[32], [51], [59], [70], [88], [95], [107]
0.1-1 g/l	[50], [54], [91], [95], [109], [116], [118], [134]
1-5 g/l	[56]

In one of analysed cases, the optimal concentration from the point of view of the dielectric strength was aligned with that of the maximum thermally stimulated current [30] This can even be taken to an extreme when aggregation leads to the formation of "electrically-conductive nanoparticles bridges" (Figure 2.11) [54], [55], [57], [72], [90], [95], [102], [111], [134], to the point where the breakdown voltage of the nanofluid is lower than that of the base fluid [134]. Another reason could be the fact that these

charged aggregates enhance the local electric field, promoting streamer occurrence [30], [54], [55].

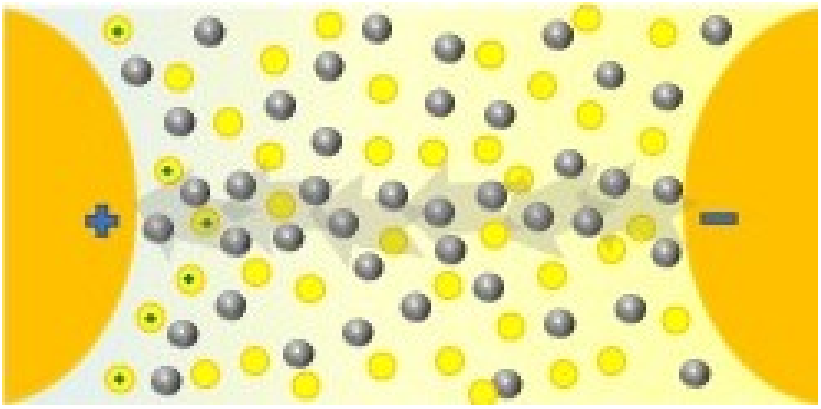

Figure 2.11. Conductive path of nanoparticles at high concentrations.

It has already been mentioned that, according to this theory, the size of the dispersed nanoparticles should condition the dielectric strength, relative to the surface of the solid fraction, and hence the number of available traps would increase as the size of the particles decreased [30], [109]. Nonetheless, TSC measurements have shown that the depth of traps increases as the size of nanoparticles increases [29]. Size may also affect the test results depending on the type of electric stresses applied. In the case of slow tests, for AC and DC, a larger amount of charge is launched than in lightning impulse or partial discharges. If the size distributions of nanoparticles have a large enough surface, it could be assumed that there would be traps for every charge. On the contrary, if particles were too big or in the case of aggregation, the relative surface would be comparatively low, and the positive effect of the particles on the dielectric strength may only be seen with the last two kinds of faults [30], [50]. As a result, a dependence on the nanoparticles mean size has been observed [134], with the breakdown voltages increasing with particle size [28], [29], [50], as well as with smaller sizes when comparing different investigations in which other parameters were alike ([27] and [28]) ([81] and [95]) ([89] and [95]). Thus, a compromise solution between the number and depth of traps together with the stability of the dispersion should be reached by controlling size

distribution in nanofluids, as suggested by the existence of an optimal size for the dielectric properties [50].

The surfactant effect, by itself over the base fluids, and over nanofluids, has also been addressed. In the first less frequent case, the results seem to depend on the surfactant and base fluid combination, as it has been observed with deterioration [53], no affectation [53], and improvement [30] of the dielectric strength. On the other side, most of studies reflect an improvement of this parameter in nanofluids due to the presence of surfactants [32], [80], [88], [113]; this can also be seen when comparing references with similar conditions ([81] and [88]) ([88] and [95]). This happens even though the surfactant layers reduce the depth of traps, as the highest potential is reached at the particle surface due to the reverse polarization of these coatings [29]. This behaviour could be explained by the aggregation avoidance provided by the surfactants that outweighs its drawbacks. Again, an optimal surfactant concentration seems to exist [32], which fits with the formation of simple or double layers and their consequences for the final behaviour of nanoparticles. In this case, it is to be noted that this concentration is approximately 2.7 % nanoparticles by mass content. Other determinants include the nanoparticle composition and properties, specifically their electric conductivity [54], [69], [79], [107], [109], [110], [113]–[115] and hydrophilicity [60], [61]; base fluid composition [73]; and concoction procedure [23], [134].

The concept of dielectric relaxation is comprised of different interdependent parameters that together build a non-destructive alternative for dielectric strength tests using breakdown voltage measurements, such as dielectric relaxation spectrometry [102]. This is based on the polarization of samples with time-dependent electric fields, which causes anisotropy and finally affects the relative permittivity or dielectric constant, volumetric resistivity, and dielectric dissipation factor [102], which are controlled. In reality, it is used as a supplement rather than an alternative, since most researchers apply both techniques, although not always completely.

Resistivity (and its opposite, conductivity) had been studied as a function of frequency [27], [28], [79], [129]; the resistivity decreases as the frequency increases. Results obtained from tests with thermal-dielectric nanofluids were inconclusive, as they present both increases [52], [79], [91], [94], [104], [113]–[115], [127] and decreases [27], [67], [107], [114], [115] in conductivity, and while the resistivity remained approximately constant at rated frequencies [28], [89], [129] , at short frequencies they registered higher resistivities than the base fluids [27], [28], [129]. This could be explained by the number of electrons launched at short cycles or high frequencies, as particles might not be capable of capturing them completely [27], [28].

The dielectric constant, that represents the capability of a material to become polarised, increases with the presence of nanoparticles [27], [28], [56], [79], [104], [108], [115], [129], [135], [143] and as the frequency rises [27], [28], [79], [129]. Equations for its calculation based on the properties and proportion of the nanofluids' components confirm this tendency [112], [113], [143], and indicate that it is larger with conductive particles [135], [143]. This also seems to depend also on size, as some theories relate to smaller particles with higher permittivities [28].

Finally, the dissipation factor (tan δ) analyses the dielectric losses of an insulator by representing how much the fluid's impedance deviates from the reactive component due to conductance and polarization losses [27]. It is a measurement of insulating quality, as it gets worse (its value increases) when pollutants, moisture, or products of degradation are present. In these nanofluids it shows erratic behaviour, as with resistivity, both increasing [28], [79], [91], [98], [108], [127], [143] and decreasing [27], [67], [129] compared to the base fluids, and decreasing as the frequency increases [28], [79], [108], [129].

According to the previous explanation, as they are interlinked, tan δ might increase when the conductivity or dielectric constant increases, as this would suggest conductivity or polarization losses, respectively. Despite this, dielectric oils are low

polarity fluids, so the contribution of these losses is negligible, so the prevailing effect is from resistivity changes [27], [67], [79], [107], [113]–[115], [129]. Variations in the resistivity and dissipation factor of different signs appeared together in several of the papers we reviewed [79], [91], [107], [114], [115], [127].

These three parameters are affected by the concentration of particles, which has been shown to accentuate their tendencies [52], [67], [75], [91], [98], [108], [113], [115], [127], [131], [135], [143]. Permittivity depends on the size of the solid fraction as they have been shown to vary contrarily [28]. Considering the particle composition, it seems logical that those which are more conductive translate into less resistive nanofluids, but there are results which support [114], [115] or deny [27], [94], [104] this behaviour.

2.4. APPLICATION OF NANOFLUIDS

Once the positive trends in the properties of thermal-dielectric nanofluids are checked, the focus of research will move to demonstrate their applicability in actual equipment. This will depend on their stability, environmental influence on fluid behaviour and properties, relationship with other components, and natural evolution with time under work conditions.

For this, it must be taken into account that nanofluids will have to support high temperatures, the presence of moisture and magnetic fields, as well as possible faults and stresses, all under the flow conditions determined by the type of cooling circuit.

2.4.1. Environmental conditions

It is compulsory to know how environmental conditions in equipment would affect the nanofluid under use, especially due to the presence of nanoparticles respecting base fluid. In this sense, some researches have committed part of its efforts to this objective.

It is known that moisture has perverse effects for dielectric properties since, as a conductive and polarizable substance that promotes ionization and electron appearance, its presence reduces dielectric strength of the fluid, saw in AC breakdown

voltage [15], [24], [26], [62], [63], [106], [109], [110], [116] and PDIV [24], [116] tests, although it does not affect lightning impulse results. Respecting influence of nanoparticles, it has been noticed that, when the dispersion is prepared with hydrophilic particles, they tend to withdraw water molecules from base fluid, and as a result an enhancement of dielectric strength is noticed [15], [54], [63], [106] , even more as higher are the concentration [63] or the moisture [15], [60], [63], [106] , to a point [26]. Additional evidences for this came from treatments with hydrophobic surfactants, as dielectric strength and gravimetric weight loss were less, what was read as lower quantities of water captured [60]. Also from TSC tests, as wetter dielectric nanofluids were able to release higher currents, so their capacity to capture electrons might be higher [106]. Other similar behaviours were found in [116] with ferrofluids over breakdown voltage and PDIV.

Temperature is a key factor. As cooling fluids get hot, especially in some places of transformer geometry, their dielectric strength increases, due to their lower viscosity and higher energy of electrons, which makes streamer formation difficult [115]. In nanofluids this tendency is promoted by also enhancement of the Brownian movement of particles, hindering aggregation and formation of preferential ways. This higher movement hinders also their polarization and promotes electrical conductivity, what is seen in lower permittivity [115] and resistivity [79], [115] and higher conductivity [52], [94] and dissipation factor [79], [114], [115]. Although the nanofluid behaviour was better at working temperatures, these also affects negatively stability of suspension of particles, promoting sedimentation, that may be offset at forced flow regimes.

Another environmental factor to consider is the presence of magnetic fields in equipment, especially when magnetic nanofluids are under study. Their magnetic properties are also affected by the presence of nanoparticles, and these changes translate finally into stability and thermal-dielectric properties. To measure it, magnetic susceptibility is useful, as it is the ratio between magnetization M and magnetic field H,

represented in magnetization curves M/H, obtained from magnetometers at different magnetic fields and temperatures.

Comparing these curves it can be seen that susceptibility of magnetic nanofluids grows respecting base fluids, even more as bigger concentrations they have, and that this parameter decreases as temperature rise [98], [123], [133], [166]. When surfactants are applied, this susceptibility decreases, due to a higher presence of non-magnetic material in the solid fraction [134], what happens in other revised references [25], [142], [149], [151], [158]. It has also been seen that this presence affects magnetic behaviour as it reduces interactions between particles. As a result, at rated temperatures the nanofluid behave as a superparamagnetic material, without hysteresis phenomenon, so remnant field is zero when the external field disappears [92], [133], [134]. As the particles kept separated one each other their magnetic domains recovered their aleatory distribution, what did not happen at low temperatures or without surfactants in the proper amount. This capacity would be useful to check which is the optimal concentration of surfactant capable of keeping the particles separated [133], [144].

When the external field is not zero, the particles tend to align with field lines, according to their dipoles, what translates in more powerful interactions, aggregation or formation of more orderly structures [31], [89], [102], unless their aleatory Brownian movement hinder these phenomena. This has been supported by acoustic spectroscopy tests, where acoustic attenuation is measured, as it varies with aggregation, showing their results anisotropy in attenuation respecting field direction and higher values as bigger is the magnitude of the field, and how it decreases as temperature grows [77], [153]. Moreover, these tendencies continued when the maximal field was removed, as a proof of hysteresis occurrence due to aggregation. Nevertheless, experimental tests have not found variations of concentration when samples are submitted to magnetic fields due to aggregation [68], [72].

This behaviour when exposed to magnetism must have influence in other properties of magnetic nanofluid. First, to their cooling capacity. In transformers, the dielectric fluid is under nonuniform magnetic field, and similarly when speaking about the temperature distribution. They appear magnetic forces when particles are magnetised [102], [123], [125], confirmed by simulations [78], [111], [120], [137], depending on field magnitude and temperature. These in radial direction [123] would contribute with convective cycles from coldest zones to coils [55], [57], [75], [92], [98], [120], [123], [125], [143], whenever in the their proximity the particles were demagnetized by reaching temperatures over Curie's, at which particles lose their magnetic susceptibility [123], [125], [167]. So that its contribution were considerable, it is recommended high pyromagnetic coefficient (variation of magnetization with temperature [123], [125]), low Curie's temperature, large thermal conductivity, a maximal saturation magnetization, low viscosity, all combined with enough concentration of particles [75], [123], [168]. The appearance of Lorentz forces as charged particles move under a variable magnetic field can also contribute to convection [75].

For its part, the thermal conductivity could be enhanced by alignment of particles, creating again preferent ways when concentrations and magnetic field magnitude are suitable, an anisotropy that supposes an increase of conductivity when thermal gradient and field are parallel and a decrease when perpendicular if conductive bridge is completed. If not, this enhancement is in every direction, but even more on the field one [31].

Finally, dielectric properties seem to be improved by external magnetic fields [50], [72] [75], [76], depending on field direction [50], [72], excepting in case of formation of the conductive bridge [90]. In case of permittivity occurs on the contrary, as it rises when electric and magnetic fields are parallel and sinks when are perpendicular [112].

2.4.2. Neighbouring relationship

It is important to consider the relationship between dielectric oils and other transformer components. The dielectric papers and pressboards that protect the coils must be impregnated by the oils while keeping or improving their isolating capacities [67], [107], but these are not the only requirements. The conservation of cellulosic components must be ensured; thus, the surrounding medium must not be aggressive from the chemical point of view. Another reason why the relationship between the fluid and paper is relevant, is that progressive surface discharges at their interface are considered to be the main cause of failure in transformers. This kind of fault causes cellulosic deterioration and the appearance of carbonized traces, this facilitates dielectric breakdown if the stress is high enough [82].

For this reason, some researchers have studied samples of nanofluids and base fluids in contact with previously dried dielectric papers [82], [83]. Firstly, they realised that particles tend to migrate toward the porous paper, as reflected in microscopy images [83]. A consequence and evidence of this was the change in the magnetism of the paper, from paramagnetism when dry to superparamagnetism, due to the presence of magnetic particles [68]. Once washed with oil, the paper returned to its initial condition, so the particles were not bonded to the paper.

The particles also had an effect on moisture. It is known that the presence of moisture is higher in cellulosics than in oil, but the water content of papers impregnated with nanofluid is comparatively low. This may have positive consequences on the dielectric properties of paper, as the increase in moisture translates to a larger dissipation factor at rated frequencies [169]. Their dielectric strength, measured with equipment designed for paper samples using techniques similar to those already mentioned, is also favoured according to results obtained for AC, DC, and lightning impulse breakdown voltages (+67, +6, and +19 to +31 %, respectively), PDIV (+6 to +12 %), and progressive discharge voltage (flashover) at the interface (+12 %) [82], [83]. The theory of traps is again capable

of explaining these results due to the presence of particles on the surface of the paper. The PEA and TSC tests also support this as the electric field is more homogeneous and lower; this also happened with the charge density, which was dispersed faster [82], [83]. The dissipation factor also improved as predicted [24], [134], especially as the concentration of particles increased [134].

2.4.3. Aging assessment

These tests have not only checked the initial stage of the nanofluid-paper combination, but also how these systems evolve with time under working conditions where they are submitted to electrical, chemical, mechanical, and thermal stresses. These stresses lead to the progressive degradation of hydrocarbon chains in these components, and the liberation of by-products such as water, acids, sludges, gases, and free electrons, which in turn feeds back the degradation. These substances harm the capacities of dielectrics, since they act as a focus of charge accumulation and distort the electric field, to a point that they do not fulfil the requirements, shortening the life expectancy of dielectrics and necessitating their replacement to avoid isolation failures that endanger the installations and their functioning.

Nevertheless, degradation processes take place over several years, so faster techniques to estimate the life expectancy of nanofluids and impregnated cellulosics became necessary. For this purpose, samples were submitted to accelerated thermal aging in different mass ratios of fluid/paper (10:1 or 20:1), dried and degassed, with presence of copper, and in an inert atmosphere, at temperatures several grades above the mean operating temperature in transformers [169], [170]. In these conditions, with same elements found in actual transformers, the samples needed less time to suffer the complete process of degradation. Periodically, parameters representative of the degradation progress, such as moisture, dissolved gasses, acidity, and degree of polymerization, were measured. Subsequently, by means of equations [62], [75], [85],

[171], the equivalent time of every measurement can be estimated at a determined temperature.

The results of tests done with aged samples of nanofluids and cellulosics, for periods between 1 and 500 days, at temperatures from 90 to 185°C, reflect similar behaviours to those seen in fresh nanofluids. The dielectric strength of an aged base fluid is enhanced by the presence of nanoparticles (Table 2.16) and the increases seen are larger than with fresh oils in AC [85], [100] and lightning impulse breakdown voltages [84], and PDIV [84], [85], [103] tests.

Table 2.16. Voltage enhancements seen in aged dielectric nanofluids.

Ref.	AC BDV	AC BDV at low probability	Lightning impulse BDV	PDIV
[51]	14%			
[62]	200%			
[68]	33.3%			
[74]	17.5%		49.4%	27.9%
[85]	40%		30%	10%
[84], [86], [103]	7.7%	11.4% at 1%	47.1%	12.2%
[93]	39.3%			
[100]	10.7%	19.5% at 5%	21.5%	

This situation again supports the theory of traps, as this effect would be explained by the lower degradation of nanofluids resulting from the capture of free electrons [84], with the additional contribution of water withdrawal [62]. The degree of polymerization (DP) of aged paper samples, which represents how well their molecular structure has been conserved, has also shown improvements [132] and deterioration [172], explained

respectively by the supposed capacity of the nanofluid to delay the degradation, and by the particles performing as hot spots on the surface of the paper.

In this same way, dielectric strength of transformer oils is harmed by successive electrical faults. This is why another kind of degradation tests consists in submitting samples to consecutive breakdowns checking their dielectric strength. In case of lightning impulse [57] or AC [134] voltages, it has been realised that samples are capable to keep their dielectric strength, with increases over the base fluid in the same conditions until 70%, and around 30% respecting fresh base fluid [57]. The reason given for this was that, as discharges occurred through particles, not the fluid, it kept protected from discharges effects [134].

2.5. CONCLUSIONS

Over the last two decades, since the rise of the idea of their application in power transformers, researchers have dedicated a great amount of effort to the search for efficient thermal-dielectric nanofluids. The main objective has always been to improve the performance of actual equipment and to allow the design of smaller, but more powerful, transformers in the future. To achieve this, it was first mandatory to demonstrate the beneficial effect of nanoparticles on their thermal and dielectric properties. Secondly, the parameters responsible for this effect had to be identified and optimized. Finally, the nanofluids needed to fulfil the applicability requirements.

Here much of the information published by researchers on this subject is collated, allowing us to reach conclusions about these issues, such as the confirmation of the higher thermal and dielectric capacities of nanofluids prepared with dielectric cooling fluids. Significant relative increases, frequently between 20 and 50 %, have been noticed in the thermal conductivity and breakdown voltages of nanofluids compared to their corresponding base fluids. However, variations in the first property pale in comparison to the second, taking into account the magnitude of the base-fluid thermal conductivity. Nevertheless, increases in the conductivity were sufficient to improve the global heat

transference or convection coefficients, according to the scarce experimental data available. The consecution of improvements in both thermal and dielectric properties is required in order to justify the addition of nanoparticles to transformer coolant fluids.

The enhancement of these properties can also be optimized with proper design and preparation of the nanofluids; this dependence has been verified for parameters such as the concentration, size, shape, and composition of the nanoparticles. The first characteristic is of particular importance, as both the thermal and dielectric capacities have shown to grow with the concentration of the nanoparticles. This is why most researchers have studied its effects on the final properties of the nanofluid, noticing the existence of optimal concentrations above which an excessive presence of the solid fraction is detrimental. Nevertheless, this limitation on nanofluids is not adverse, as it also comes from stability constraints, related to the applicability of nanofluids. Thus, fortunately, the requirements for stability are not in competition with those of the thermal-dielectric properties, as the range of concentrations is limited by both.

Stability is the first condition required of dispersions, so their improved properties persist over time; it requires their control, as well as treatments that make the particles suitable for dielectric base fluids. Again, the use of surfactants does not appear to be detrimental to other aspects of their performance. Results show that most stabilities are under the mean residence time in actual transformers, although they have been studied under static conditions, not in working cooling circuits. A bigger effort in this sense is needed.

The great number of existing variables in the preparation processes of thermal-dielectric nanofluids makes it challenging to find an optimized methodology which is suitable for the production of dispersions for transformer applications. This includes not only the production of nanoparticles, their characteristics, properties, and surface treatments mentioned above, but also how are they carried out, such as the base fluid, as well as how the particles are added and dispersed into it.

Several processes have already been established. According to the vast majority of these, nanofluids were prepared following a two-step method, probably due to the difficulty of using mineral oils or natural esters as the synthesis medium for nanoparticles; or the dispersion of small and spherical nanoparticles in low concentrations, by a combination of mechanical shaking and ultrasound.

Considering the methods still under discussion, from the information collected here, the beneficial effects of the use of surfactants can be observed when used in proper concentrations and chosen specifically for a determined nanofluid based on its components. The length of organic chains, stability against temperature, and the design of the surfactantion procedure all affect the result. The contact between particles and surfactants must be ensured, for example by putting them together before the addition of the base fluid. Similarly, enhanced bonds between the nanoparticles and surfactants can be achieved applying heat during the treatment. To avoid formation of double surfactant layers, excess surfactant should be removed by washing with organic solvents and recovering the particles, a step which can be useful to select those particles to add to the base fluid. Once a surfacted powder is obtained, and considering the final use of the nanoparticles, drying under a vacuum or inert atmosphere is convenient.

The dispersion of particles must be optimized, beyond the combination of different mechanisms. Heating of samples during large sonications may result in the breaking of bonds between the surfactants and solid surfaces; this can be prevented by periodic stops or cooling systems. Another drying step, to remove moisture absorbed during handling, is also useful in the elimination of bubbles.

Thus, a suitable process for the preparation of nanofluids for the cooling and isolation of transformers, from the point of view of stability, is shown in the Figure 2.12.

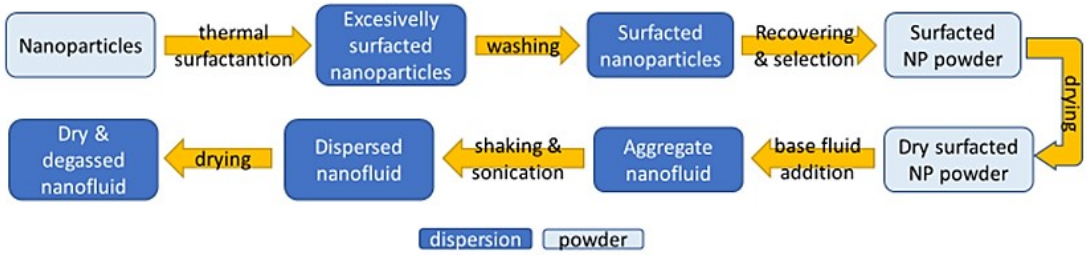

Figure 2.12. Preparation method for dielectric nanofluids with improved stability.

Each step of this proposed general procedure has been independently shown to be effective, but they must be tested together while considering the recommendations with respect to the nanoparticle, surfactant, and nanofluid characteristics. Different compositions, concentrations, base fluids, surfactants, dispersion times, and temperatures should also be tested, adjusting the method for every combination. Of course, once the effectiveness of this methodology for the stability of nanofluids has been demonstrated, these stable nanofluids must be submitted to characterization tests to ensure that their enhanced properties remain. Their existence and perdurability, intimately linked to durable suspensions, are requisites to support the applicability of nanofluids in transformers. Time-evolution studies of the properties may also be needed.

Considering applicability, despite the current stability of dispersions, regarding other factors the nanofluids have shown positive tendencies. It has been noticed that the environmental conditions during work in actual equipment do not represent problems, but advantages, for these nanofluids, as their properties would be even enhanced respecting the base fluids with the same conditions of temperature or moisture, excepting if higher temperatures (over 80°C) harm the stability or the surfactants integrity or if the magnetic fields promote aggregation. Similarly, it occurs with relationship between nanofluids and cellulosics, as the presence of nanoparticles also seems to improve cellulosics properties, and the resistance to aging caused by stress, at least in the case of oils.

The confirmation of the enhanced characteristics of dielectric nanofluids, by the consecution of samples with demonstrated thermal-dielectric properties and stability, would represent a definitive step in this field. So, during the following years, the researches should focus on the consecution of this efficient preparation methodology for nanofluids, and the confirmation of their theoretical properties. Once this is achieved, it will be necessary to check the behaviour of the thermal-dielectric nanofluids in pilot plants and transformers under working conditions.

In parallel, other aspects which have been comparatively less demonstrated than others, and parameters whose effects are still uncertain, like size or shape, should remain under investigation in an attempt to confirm their influence, especially over global heat transfer capacities. The range of particle compositions may be broadened. For this, the synthesis of ad hoc particles may be helpful. In the same sense, efforts to demonstrate whether the presence of particles definitively promotes or decelerates paper aging must be strengthened.

CHAPTER 3:

MATERIALS AND METHODS

3. MATERIALS AND METHODS

In this section it is described the experimental study carried out for analyzing the suitability of different candidate nanofluids for their application in transformers, not only focussing on a mere characterization of their properties as it is usual, but also including the study of an actual application case. First, it is explained the preparation method applied and also the components of the nanofluids are described. This is followed by the description of the methods and equipment used during the characterization of the nanofluids, from both the dielectric and thermal point of view. Finally, the experimental setup where the nanofluids are tested and the test conditions are presented.

3.1. NANOPARTICLES AND BASE FLUID. PREPARATION OF THE NANOFLUIDS

The properties of the vegetal base fluid selected for this research, according to its manufacturer, are shown in Table 3.1. Regarding the standards, the recommended thresholds to be fulfilled by this kind of dielectric fluids, in fresh conditions, are collected in Table 3.2 [173]. These values are, on the whole, upper thresholds, excepting those relative to the flash point or the breakdown voltage, as in these cases the values shown are lower thresholds and must be outweighed. In the case of this last property the threshold is set for unused and untreated natural esters, as delivered by the providers. By comparing the data in both tables, the chosen natural ester meets the criteria set out in the standards.

The solid fraction of the nanofluids is composed by four different high-purity spherical nanoparticles (Fe_2O_3, TiO_2, ZnO and CuO). According to the manufacturers, these have a mean size between 10 and 50 nm of diameter. This has been confirmed by Transmission Electron Microscopy (TEM) (Figure 3.1). According these images, among the nanoparticles, the Fe_2O_3 is the one with the most homogeneous size distribution, and with a smaller mean size. On the contrary, ZnO and CuO seem to present the larger nanoparticle size, but also more dispersion in this parameter.

Table 3.1. Main properties of the vegetal base fluid.

Density (20°C)(kg/m^3)	910
Kinematic viscosity (40°C)(m^2/s)	$<5\cdot10^{-5}$
Thermal conductivity (25°C)(W/K·m)	0.1691
Dissipation factor (Tan δ)	<0.05
AC Breakdown Voltage (kV)	>35
Acidity (mg KOH/g)	0.02
Moisture content (mg/kg)	100
Flash Point (°C)	334
Pour Point (°C)	-21
Appearance	Clear and bright

Table 3.2. Threshold values for fresh dielectric natural esters (IEC 62770).

Property	**Threshold value**
Density (20°C)(kg/m^3)	1000
Kinematic viscosity (40°C)(mm^2/s)	50
Moisture content (mg/kg)	200
Acidity (mg KOH/g)	0.06
Pour Point (°C)	-10
Flash Point (°C)	250
Appearance	Free of sediments and suspended matter
Dissipation factor at 50 Hz	0.05
AC Breakdown Voltage (kV)	35

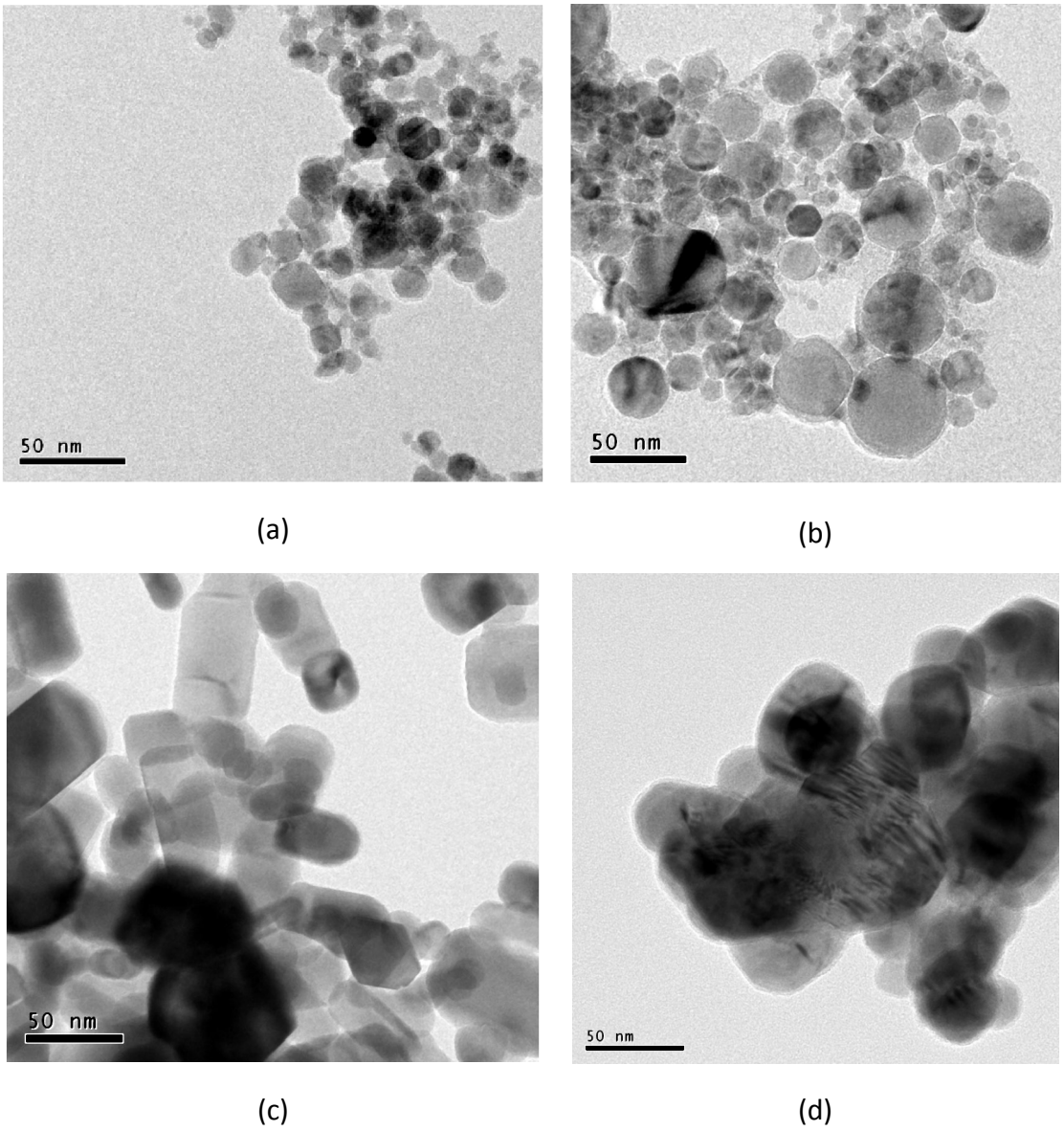

Figure 3.1. TEM images of the nanoparticles: a)Fe_2O_3 b)TiO_2 c)ZnO d)CuO

The preparation of the samples follows the two-step method typically used in this kind of works. A certain amount of nanoparticles is added carefully to the natural ester contained in an Erlenmeyer flask, and then the mixture is set under mechanic stirring during 15 minutes, followed by 12 hours under treatment with ultrasounds in a water bath, with the samples contained in closed bottles (Figure 3.2). With this procedure a proper distribution of the solid fraction is warranted.

Although during the preparation the samples are exposed to the environment, these are not submitted to any step of drying. They are just kept static for another 12 hours to dissipate any bubble arose during the process.

The selected nanoparticle concentrations for the characterization of nanofluids properties are between 0.1 and 1.0 kg/m^3, depending on the nanoparticle composition. As can be seen in Table 2.15, from the dielectric point of view, this is the range in which the optimal concentrations are usually located. Once the natural ester base fluid and the nanofluids to be tested are prepared following this method, the tests to measure their properties are carried out by duplicate, following the methods set in the IEC standards, when the latter are available.

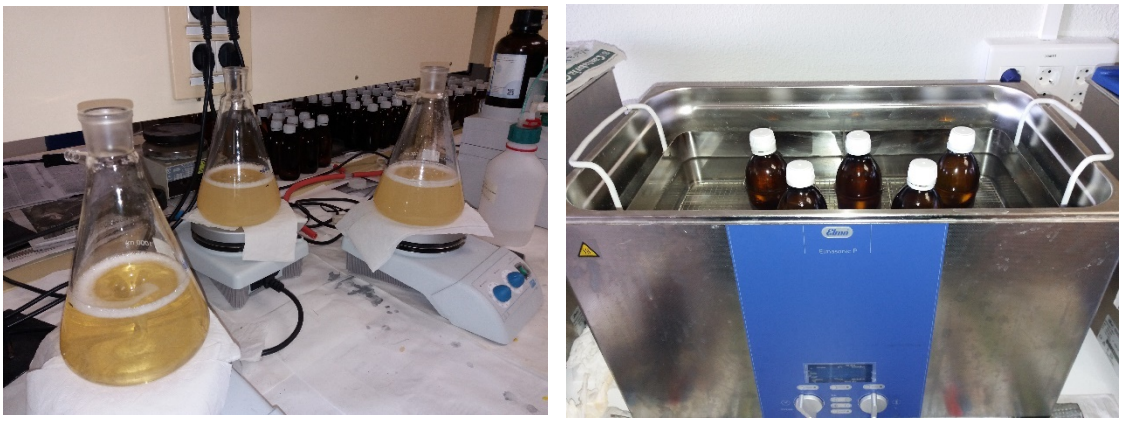

(a) (b)

Figure 3.2. Preparation of the nanofluids by magnetic stirring (a) and ultrasonication (b).

3.2. TEST METHODS

3.2.1. Physical properties

The thermal conductivity is measured at different temperatures using a *KD2 Pro Thermal properties analyzer* (5% uncertainty). As it was explained in the section 2.2 this is the most spread equipment for this purpose in the related scientific literature. It is based on the relationship between the temperature and the electrical variables in the wires. The probe is introduced into the oven through a butterfly door in the back part (Figure 3.3) and placed inside sealed vials with the samples to test. To avoid the effect of any bubble

inside the vials, these are set upside down. Also, to prevent any movement and to center the probe in the sample, it is blocked with a fabric tape. With the oven closed, once it reaches the desired temperature (323K) the analyzer is connected and takes a thermal conductivity measurement every 15 minutes while samples cool down slowly to ambient temperature inside the oven.

Figure 3.3. Disposition of the KD2 Pro sensor inserted in a sample vial and inside the oven.

To determine the viscosity of the samples a rotatory viscometer *Haake Viscotester 550* (0.5% uncertainty) is used. It presents a rotatory head or rotor placed in a specimen holder. The substance to be tested is located in the measuring gap of the sensor system between the rotor and the holder (Figure 3.4). The rotor is rotated at a preset speed (n). The substance to be measured exerts a resistance to this rotational movement (due to its viscosity) which becomes apparent as a (braking) torque value (Md) applied to the measuring shaft of the *HAAKE Viscotester 550*. The dynamic viscosity is measured at different temperatures using 50 ml of sample for each test. The sample temperature is controlled by an external fluid circuit linked to a thermostatic bath.

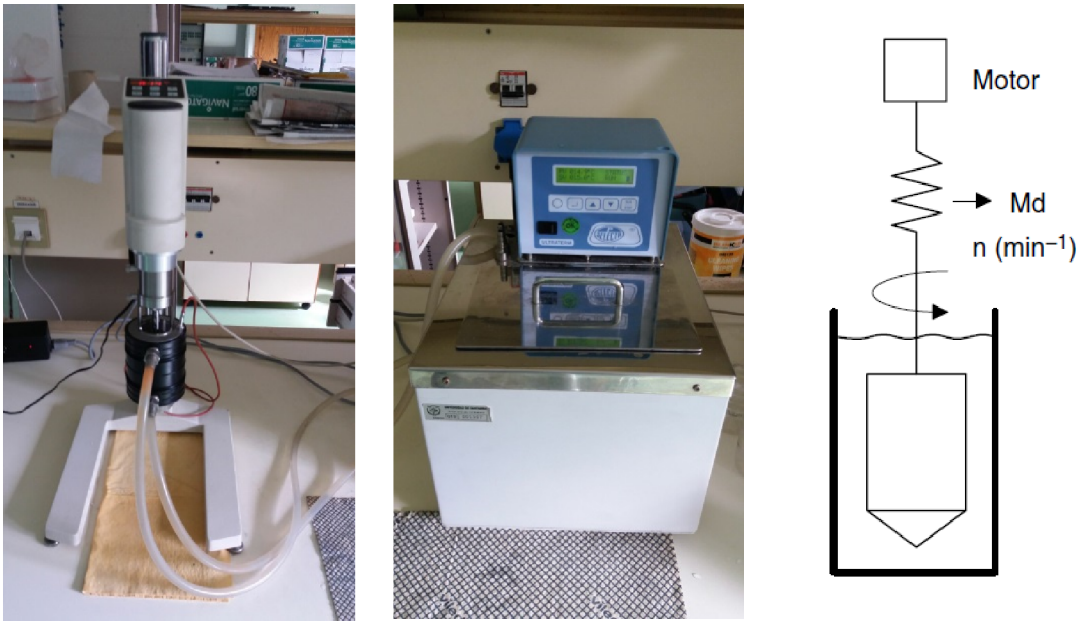

Figure 3.4. Pictures of the Haake 550 rotatory viscotester and the isothermal bath. Scheme of the rotatory system.

The software of the viscotester calculates automatically the dynamic viscosity, entering both the Md and the n, and two geometric factors f and M, according to the Eq.2.

$$\eta = \frac{f \cdot Md}{M \cdot n} \qquad \text{Eq.2.}$$

f is calculated using the length (L) and radius (Ri) of the rotor in SI units (Eq.3) while M depends on the radius of the rotor and the holder (Ri and Ra respectively), also in SI units(Eq.4).

$$f = \frac{0.01}{2\pi \cdot L \cdot R_i^2} \qquad \text{Eq.3.}$$

$$M = \frac{\pi}{15} \frac{R_a^2}{R_a^2 - R_i^2} \qquad \text{Eq.4.}$$

The rotating head used in these tests was the *MV3*. The characteristics of this head are shown in the Figure 3.5. With these characteristics, f and M for the *MV3* rotor result in 111.0 Pa/N·cm and 0.440 min/s, respectively.

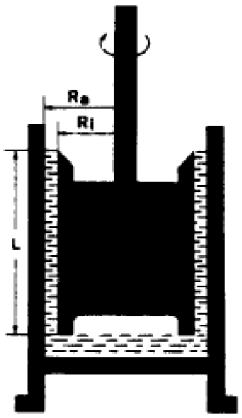

Sensor System	MV1	MV2	MV3
System No.:	*3*	*4*	*5*
Inner Cylinder (Rotor)			
Radius R_i (mm)	20.04	18.4	15.2
Height L (mm)	60.0	60.0	60.0
Outer Cylinder (Cup)			
Radius R_a (mm)	21.0	21.0	21.0
Radii Ratio R_a/R_i	1.05	1.14	1.38
Gap Width (mm)	0.96	2.6	5.8
Sample Volume V (cm^3)	34.0	46.0	66.0
Temperature (°C)		-30 / 100	
System Factors			
f (Pa/Ncm)	65.7	76.8	111.0
M (min/s)	2.340	0.900	0.440

Figure 3.5. Dimensions of the rotor and the cylindrical holder of the Haake 550.

Regarding the density variation with temperature, it is estimated with a density meter *Mettler Toledo DM40* (0.1 kg/m^3 measurement error)(Figure 3.6) at six different temperatures between 293 and 343K. This equipment is based on the vibrating body method. A U-shaped glass tube is periodically vibrated using electromagnetic fields. The volume of the tube at different temperatures is known, as also the amplitude of the periodic movement. The frequency depends on the mass in this available volume. That is, it depends on the density of the fluid. The higher the density and the mass, the lower the frequency, as higher values of these parameters hinder the movement of the tube. This frequency is registered optically and converted to the sample density.

Figure 3.6. Capillary density meter Metler Toledo DM40.

The equipment is calibrated with samples of fluids with known densities, as those of water or air. The frequencies of their vibrations are taken as references. This equipment has the capacity to adequate and control the sample temperature required by itself.

3.2.2. Dielectric properties

Different dielectric properties are measured. The AC breakdown voltage is a parameter sensitive to the characteristics of the tested fluid. The presence of suspended particles or moisture affects this parameter and is thus indicative of the necessity of treatments in those oils under working conditions. This is why it is frequently measured during the characterization of dielectric oils, always according to the strict requirements set in the standard IEC 60156:2018 [174]. The measurement method is based on the application of an increasing AC voltage to an oil sample, in steps of 2 kV/s, until the breakdown occurs. The breakdown is noticed due to the formation of an electric arc between the electrodes that are immersed in the sample. At this moment the voltage is extinguished, the electric circuit is automatically opened and the result is calculated by the root mean square (RMS) of the AC voltage before the arc appears.

The geometry and materials of the test cell and electrodes, the amount of sample or the intensity of the stirring is set in the standard. The electrodes must be composed by polished stainless steel, bronze or brass, with diameters between 12.5 and 13 mm in the horizontal axis, covered by at least 40 mm of sample and placed at least 12 mm far away of any other element in the cell. The distance between the electrodes is set in 2.5 mm (Figure 3.7).

In this thesis, the AC breakdown voltage is determined by a *BAUR DPA 75* dielectric oil tester (Figure 3.8). According to methodology fixed in,also used in the equipment setup [174], an oil sample of 400 ml at ambient temperature is utilized. Every tested sample is subjected to six consecutive voltage breakdowns that are separated in time one minute. During this minute, the sample is stirred. The final result is got calculating the mean value of these six consecutive tests (accuracy <1 kV).

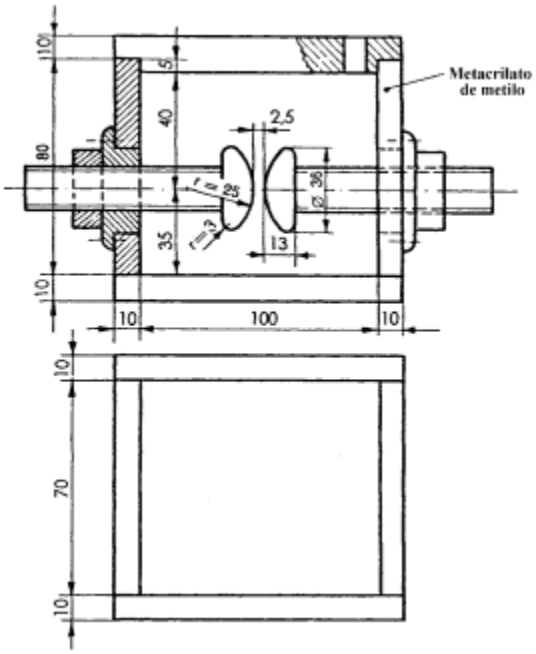

Figure 3.7. Example of test cell and electrodes geometries shown in the IEC standard.

(a) (b) (c)

Figure 3.8. (a) Oil tester BAUR DPA 75, (b) Oil tester BAUR DTL, (c) Karl-Fischer Titrator Metrohm 899.

Other usual dielectric parameters tested in transformer oil samples are the relative permittivity, the loss factor (tan δ) and the DC resistivity. While the permittivity represents the tendency of a material to be polarized under an electrical field (in this case compared with the air permittivity), and the resistivity how strongly a material is opposed to the circulation of electrical current, the loss or dielectric dissipation factor is a more abstract parameter. It is known that an electric insulator is equivalent to a capacitor, and that there is not a perfect insulator. This means that an insulator under

voltage is always crossed by a small and mainly capacitive leakage current. The loss factor quantifies how much an insulator differs from the ideal capacitive behaviour. It measures the magnitude of the active component of the current by means of the tangent of the angle (δ). This angle is that formed by the reactive component of the current and the current itself (I_C and I in the Figure 3.9, respectively). The factor depends on the voltage polarity and also on the conductivity of the medium, so that changes in the resistivity or in the permittivity are also reflected on the loss factor.

These properties are able to indicate the degree of pollution reached by an oil during its time under working conditions in a transformer. Therefore, their values can be used to determine the insulation degree of a transformer oil and also to detect in advance any risk of insulation failure in this equipment. The presence of pollutants, reduces the resistivity of the oil, increases their ease of polarization and alienates the performance of the isolator from the ideal one. While the relative permittivity is only affected by an important presence of pollutants, the loss factor and the resistivity are also injured at low concentrations. In the same way, these properties are also affected by the temperature or, in the case of the permittivity or the loss factor, by the frequency of the alternating current.

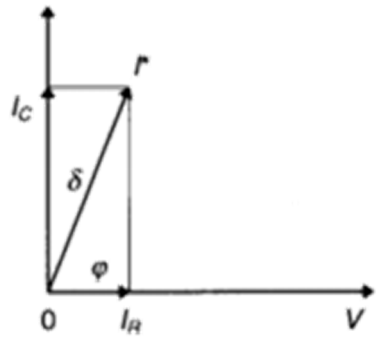

Figure 3.9. Dielectric dissipation angle δ.

The tests order must also be considered. Both the relative permittivity and the loss factor of an oil sample could be modified if this sample has suffered direct currents in first place. Thus, the resistivity test of a sample must be the last one, after short-

circuiting the electrodes for at least one minute after the AC tests. In fact, the testers carry out this procedure by default.

The relative permittivity ε_x is obtained by comparing the electric capacities of the test cell (between its electrodes) at three situations: empty (C_a), full of a fluid with known permittivity ε_n (C_n) and with the sample to be tested (C_x). To carry out this test, the AC frequency must be between 40 and 62 Hz and the temperature of the samples must be the same. The Eq.5 shows the mathematical relationship among these three capacities and the relative permittivity of the reference fluid to result in the relative permittivity of the oils tested.

$$\boldsymbol{\varepsilon_x = \frac{C_x - \left(C_a - \frac{C_n - C_a}{\varepsilon_n - 1}\right)}{C_e}} \qquad \text{Eq.5.}$$

The dielectric dissipation factor (DDF), or tan δ, could be obtained from the power factor PF (cos φ) of the leakage current across the oil using the Eq.6, and it is approximately equal to the sine δ. If the PF is under 0.05 the loss factor can be considered directly equal.

$$\boldsymbol{PF = \frac{DDF}{\sqrt{1 + (DDF)^2}}} \qquad \text{Eq.6.}$$

During the loss factor tests the sample should be subjected to an electric field between 0.03 and 1 kV/mm, with a sample temperature of 90°C and at a frequency between 40 and 62 Hz. Nonetheless, the result obtained during the test at a frequency out of this range could be corrected by the Eq.7.

$$\boldsymbol{tan\ \delta_{f1} = \left(tan\ \delta_{f2}\right)\frac{f_2}{f_1}} \qquad \text{Eq.7.}$$

The transversal resistivity of a isolating fluid at direct current, in Ω·m, represents the relationship between the intensity of the continuous electric field and the stationary value of the current density across the material. Nevertheless, the pass of a direct current (contrary to alternating current) changes with time the caracteristics of the fluid,

due to the migration of charges in the material. As a consequence, the resistivity in that case is not real, unless the measurement is done at such low voltages and with the rapidly enough so this phenomenon is negligible. The standard IEC 60247 [175] sets that the DC voltage should be enough to subject the fluid to an electric field of 250 V/mm for 60 ± 2 seconds. This field is applied twice to the same fluid sample with inverted polarity, with an intermediate time gap of five minutes in which the cell electrodes are short-circuited. The electric field (V), the current (I) that circulates through the fluid and the cell constant (K) allow to calculate the resistivity ρ using the Eq.8. Eq.9 states the dependence of the cell constant K on the capacity of the empty cell C_a.

$$\boldsymbol{\rho = K\frac{V}{I}} \qquad \text{Eq.8.}$$

$$\boldsymbol{K = 0.113 \cdot C_a} \qquad \text{Eq.9.}$$

Huge discrepancies among the results obtained at the different polarities (if existing) may point out an inadequate maintenance of the cell.

In this thesis, a *BAUR DTL 2a* (Figure 3.8), which has been set up according to [175], is used to measure the resistivity, relative permittivity and the loss factor.

3.2.3. Moisture content

The moisture content is also controlled, since the dielectric properties depend on this parameter. According to the standard IEC 60814 [176], the Karl-Fischer titration is applied in a *Metrohm 899* coulombmeter. This equipment is shown in Figure 3.8.

The Karl-Fischer titration is based on the reaction between the water of an oil sample with iodine, sulfur oxide, an organic base and alcohol, in an organic tampon medium. The reactions are shown in Eq.10 and Eq.11.

$$\boldsymbol{H_2O + I_2 + SO_2 + 3C_5H_5N \rightarrow 2C_5H_5N.HI + C_5H_5N.SO_3} \qquad \text{Eq.10.}$$

$$\boldsymbol{C_5H_5N.SO_3 + CH_3OH \rightarrow C_5H_5NH.SO_4CH_3} \qquad \text{Eq.11.}$$

The iodine used in the previous reactions is produced electrolytically from its ions in the electrolyte and controlled by means of a coulombmetric assessment, proportional to the current circulating through the cell electrodes, according to Eq.12.

$$2I^- - 2e^- \rightarrow I_2 \qquad \text{Eq.12.}$$

The quantity of electrons needed to produce the iodine that reacts with the water of the sample, is yielded by controlling the current through the electrode jointly with the reaction time, thus obtaining stoichiometrically its concentration in parts per million.

This is carried out with a Karl-Fischer coulometer (Figure 3.10). It presents an electrolytic cell with two compartments separated by a porous diaphragm. The anodic compartment (a) contains both the reaction solution and the sample, that are continuously stirred (g), while the cathodic one (e) contains an anhydrous reactive. While one electrode applies a constant alternating current that generates the iodine (e), the other measures the potential at the anodic fluid (f). When the water is consumed and the iodine increases its concentration the voltage suffers an important drop . This instant is detected by the equipment, thus obtaining the reaction time [176], [177].

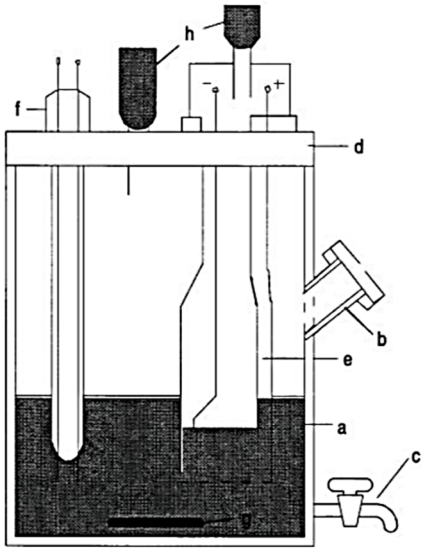

Figure 3.10. Karl-Fischer titrator cell scheme.

The equipment calculates the moisture content of the sample (in mass, m_2) and its concentration. This depends on the weight of sample introduced into the cell (M) and on the usual moisture content of the cell without sample (m_1), according to the Eq.13.

$$\boldsymbol{water\ content\ (weight\ \%)} = \frac{\boldsymbol{m_2 - m_1}}{\boldsymbol{M}} \boldsymbol{10^{-4}} \qquad \text{Eq.13.}$$

3.2.4. Cooling Capacity. Experimental setup.

Following the experiment used by *Patel et al.* [178], an experimental setup was developed to study the cooling performance. The most promising nanofluids among those studied have been tested by comparison with the base oil (natural ester). This task has been made on an experimental platform that was previously used in a previous work, [179].

The experimental setup is formed by a distribution transformer (800 VA, 115/230V) (Figure 3.11) placed inside a stainless steel tank. The dimensions of this casing are 20 cm × 20 cm × 20 cm. The platform temperatures are monitored by four probes located in strategic places of the transformer (top, bottom, iron and windings). The Figure 3.11 shows, approximately, the location of the four probes. This can be observed in more detail in the Figure 3.12, together with the constructive materials. Also, an external probe was used to measure the ambient temperature, taken as reference. The measurement and recording of the temperatures are made by a microcontroller (Arduino) and an Integrated Development Environment (IDE). The samples (about 6.5 liters each) are poured into the casing until the transformer is completely covered with coolant. The sample movement inside the tank is driven only by natural convection.

The samples were tested using three different load levels whose load indexes C (C=0.7, C=1, C=1.3). This coefficient quantifies the power level that the transformer offers regarding the rated power. That is, if this coefficient is equal to one means the power provided by the transformer is the rated power. In the same way, if this coefficient is

higher or smaller than one, the power provided by the transformer is respectively higher or smaller than the rated power, i.e., at C=1.3 the power level is 30% higher than the rated one.

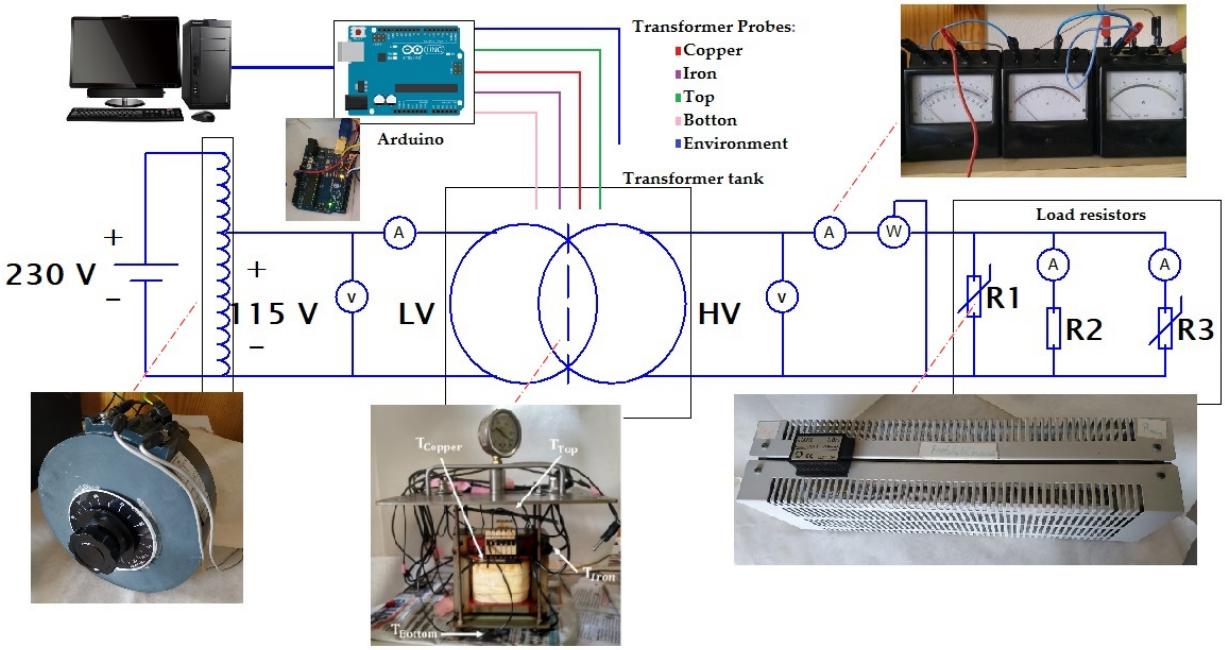

Figure 3.11. Connection scheme of the experimental platform.

The load levels are reached by controlling three variable resistors equal to that shown in the scheme of Figure 3.11. In Table 3.3 the currents, voltages and resistances applied during the tests for each load index are summarized. The thermal-hydraulic study of the samples is assured using these load levels. In fact, the temperatures that are achieved in the overload regime are close to those found in real transformers.

The temperatures of the probes are caught every five seconds during the tests until the steady-state is reached and are available during the process. The stability criteria followed is the one defined in the IEC 60076-2 [180], that establishes this condition is reached when the variation of the top oil's temperature rises below 1 $K \cdot h^{-1}$ over a consecutive period of 3 hours.

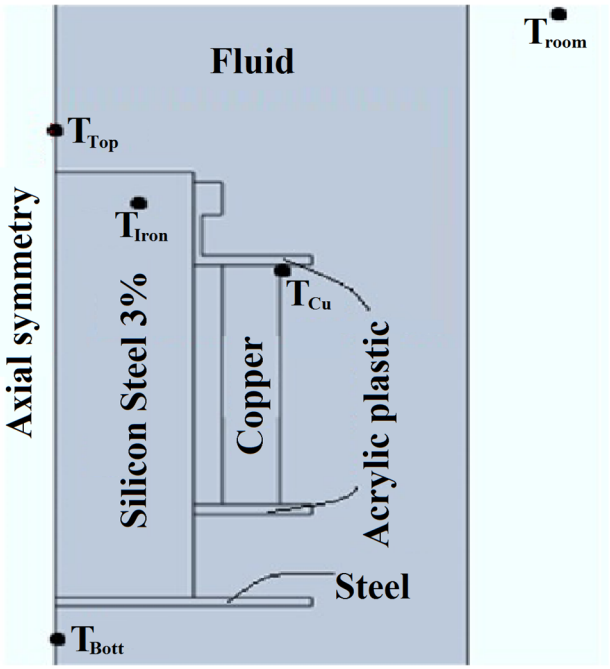

Figure 3.12. Section of the experimental transformer in the setup.

Table 3.3. Circuit parameters during the load tests.

Overload C=1.3; P=1040 W	
Primary winding	Secondary winding
I_p=9 A V_p=115 V	I_s=4.5 A V_s= 230 V $R_{eq.s}$=51.11 Ω
Rated power C=1; P=800 W	
Primary winding	Secondary winding
I_p=6.96 A V_p=115 V	I_s=3.48 A V_s= 230 V $R_{eq.s}$=65.71 Ω
Underload C=0.7; P=560 W	
Primary winding	Secondary winding
I_p=4.87 A V_p=115 V	I_s=2.43 A V_s= 230 V $R_{eq.s}$=94.46 Ω

CHAPTER 4:

RESULTS

4. RESULTS

The characterization of the main properties of the prepared nanofluids, from both the dielectric and thermal point of view, is presented in this section. Also, the results of the application of the best nanofluids from these standpoints in an experimental setup are collected and analysed.

4.1. DIELECTRIC CHARACTERIZATION OF NANOFLUIDS AND BASE OIL

A first step in this thesis consisted in the determination of the suitability of the different nanoparticles proposed to be studied regarding their dielectric properties. Four different nanofluids have been prepared and tested, to infer the optimal nanoparticle concentration regarding their dielectric properties in each case, or even if these nanoparticles are adequate to be added to a dielectric fluid for its enhancement.

4.1.1. Breakdown Voltage

Searching for the aforementioned goal, nanofluids with concentrations of 0.1, 0.2, 0.5, 0.7 and 1.0 kg/m^3 of TiO_2, ZnO and CuO nanoparticles were prepared and their dielectric strength tested, by mean of standard BDV tests.

The BDV distributions obtained in these tests are shown in the Figures 4.1-3 for the base fluid and the different nanoparticles (TiO_2, ZnO and CuO respectively), together with the mean values for each concentration. Even more, not only the mean values of this parameter for each concentration are presented, but also their average percentage variation regarding the value obtained with the base fluid is shown. As can be seen in these three figures, on the whole, the presence of the nanoparticles supposes a profit for the insulating capacity of the base fluid.

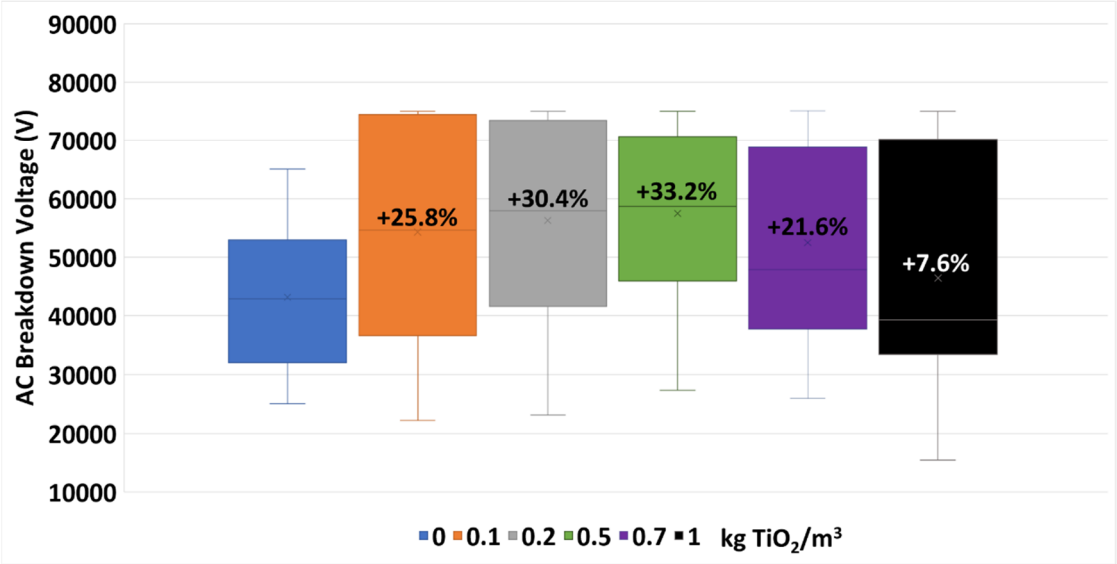

Figure 4.1. Breakdown voltage test results of the TiO_2 nanofluids and the base fluid.

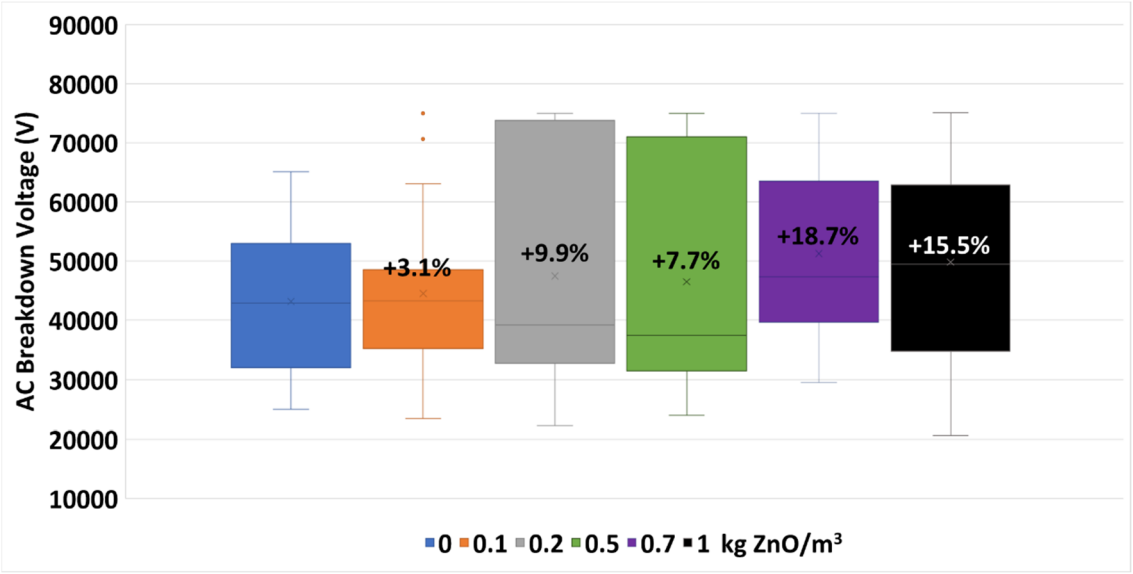

Figure 4.2. Breakdown voltage test results of the ZnO nanofluids and the base fluid.

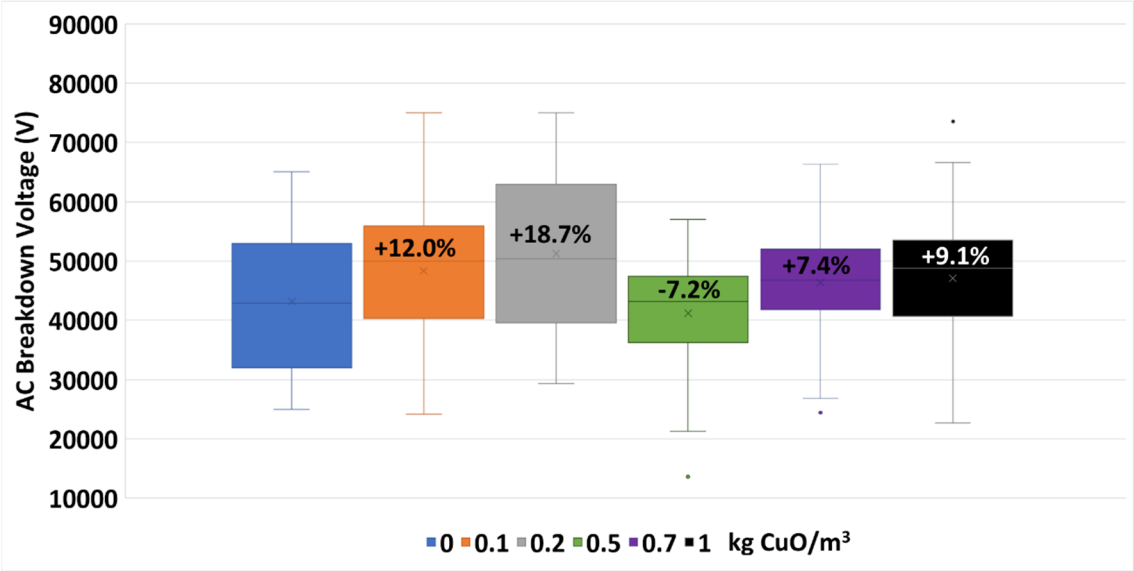

Figure 4.3. Breakdown voltage test results of the CuO nanofluids and the base fluid.

In Figures 4.4-6 the mean moisture content is represented in each case. As it was mentioned in the section 2.4.1, water, as a polar substance, eases the transmission of charges in the oil, and reduces the voltage that the samples are capable to withstand [15], [24], [26]. Thus, the measurement of the moisture content in the samples is mandatory if the comparison of BDVs of the different samples is planned.

In this case, the moisture graphs show how the content is always around 200 or 300 ppm, similar with the three nanoparticles. This level is considerable but usual considering the nature of the base fluid (natural ester, more hygroscopic than a mineral oil) and the absence of drying during the preparation of the samples. It can be seen also that the nanofluids, in general, present higher moisture levels respecting the base fluid, although they were subjected to the same preparation steps. This could be because the hygroscopic nature of the nanoparticles

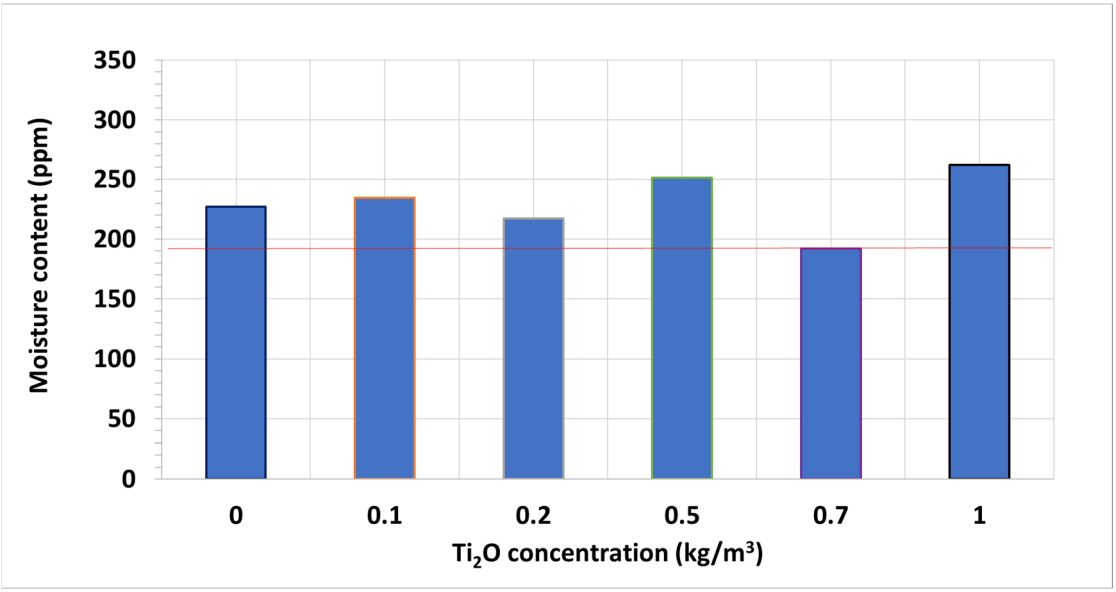

Figure 4.4. Mean moisture content of tested TiO_2 nanofluid samples.

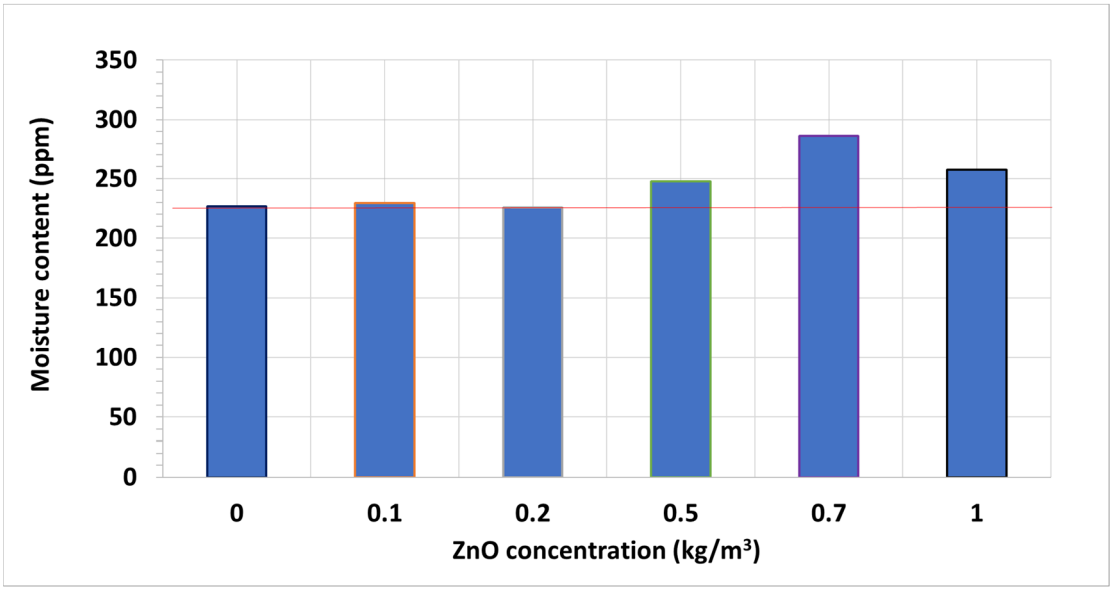

Figure 4.5. Mean moisture content of tested ZnO nanofluids.

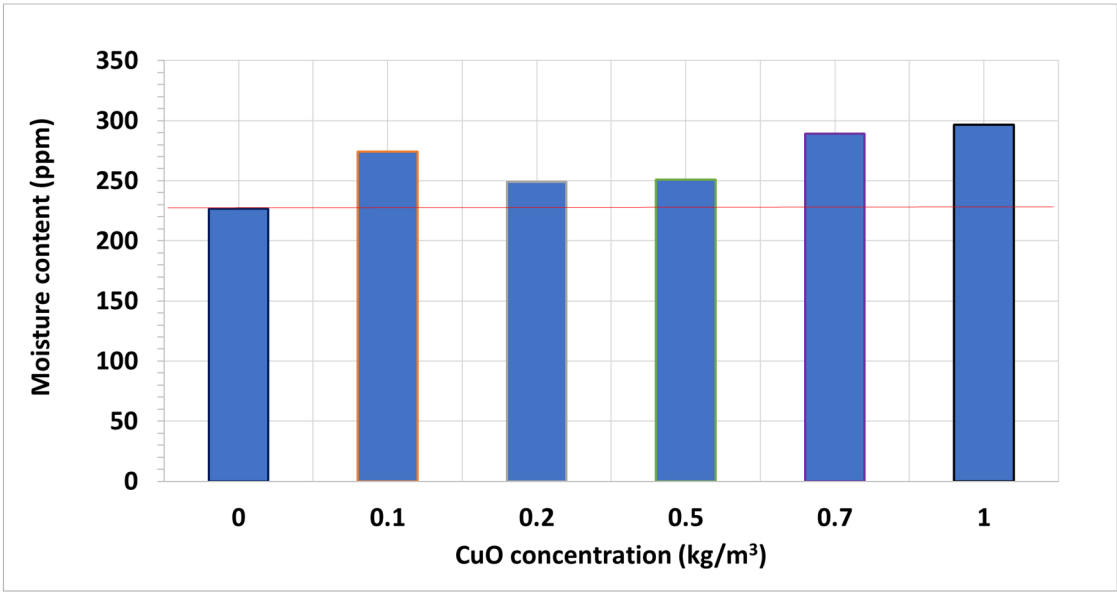

Figure 4.6. Mean moisture content of tested CuO nanofluid samples.

A deeper analyses of these results nonetheless reflects that only the TiO_2 nanoparticles seem capable to enhance the BDV of the base fluid in accordance with what was seen in the available bibliography and explained in the section 2.3. Here it is mentioned the dependence of the BDV variation on the nanoparticle concentration and the existence of optimal concentrations. It is usually noticed that the BDV improves progressively as the concentration rises, up to the optimal concentration, and that from this point the BDV starts to decrease [54]–[57]. In this case, as it can be seen in Figure 4.1, the mean breakdown voltage of the base fluid is clearly improved in all the TiO_2 concentrations, but the effect is more pronounced al the lower concentrations and also more pronounced as the concentration rises, with a maximum enhancement of 33.2 % at 0.5 kg/m^3. At larger concentrations the effect is lost progressively, especially at 1.0 kg/m^3, with an improvement of breakdown voltage of only 7.6 %. Thus, according to the literature, it has been noticed the existence of an optimal concentration.

This occurs even though most of the nanofluid samples have slightly larger contents of moisture respecting the base fluid one (Figure 4.4). These samples, with the same moisture contents, may have shown improvements even more pronounced respecting the base fluid, according to the literature [109], [110]. Additionally, the sample with the

optimal concentration is also the second one with the largest moisture, while the closer-concentration samples present the lower moisture contents, under the base fluid one. Thus, the optimal-concentration nanofluid may have been more noticeable with the same moisture contents. Regarding the 1 kg/m^3 nanofluid sample, although it presents the largest moisture, this is no really far from some of the preceding samples. Therefore, the fall in breakdown voltage respecting the other nanofluids is not only attributable to the moisture, and it is also due to an excessive concentration of nanoparticles.

The results with the other two nanoparticles seem more erratic. Neither the CuO nor the ZnO show a similar clear tendency as the TiO_2. In both cases, especially with the CuO, although the BDVs are improved, their evolution with the nanoparticle concentration are not monotonous before and after the optimal point.

Thus, with the ZnO nanoparticles (Figure 4.2), the BDV increases with the concentration up to 0.7 kg/m^3, with an improvement of 18.7%, but this tendency is broken at 0.5 kg/m^3, as its BDV is under those seen in the close samples. This is not explainable considering the moisture (Figure 4.5), as the optimal concentration sample is also that with the highest water content and, regarding the sample concerned (0.5 kg/m^3), its moisture level is more similar to the 0.2 kg/m^3 sample.

With the CuO the situation is similar (Figure 4.3), as the best concentration seems to be 0.2 kg/m^3 with an improvement of 18.7%, but the immediately closest concentration reflects a decrease of -7.2% respecting the BDV of the base fluid. Again, at higher concentrations than 0.7 kg/m^3 the BDV results start to improve that obtained with the base fluid. Regarding their moisture levels, those samples with such huge differences in their BDVs (0.2 and 0.5 kg/m^3) present almost the same moisture content (Figure 4.6).

An explanation for this behaviour could come from their size distribution. As can be seen in the section 3.1 (Figure 3.1), they are the ZnO and CuO the nanoparticles with a larger mean size and a less homogeneous size distribution. Also, it is explained in the section

2.3 the dependence of the capture capacity of the nanoparticles on their size, regarding the depth and number of available potential wells, and the supposed existence of optimal sizes [28], [29], [50]. The use of nanoparticles with a wider range of diameters could boost the inherent uncertainty of these tests, as the capture of the electrons depends on the size of the nanoparticles. That is, if during the test development, a nanoparticles fraction with sizes far from the optimal one were eventually located between the electrodes, the results would be affected, showing a lower resistance to dielectric breakdown On the contrary, the results could be improved by the presence of a fraction with sizes closer to the optimal one. If this occurs, could suppose the appearance of erratic behaviours regarding the evolution of the dielectric strength with the concentration normally seen in the bibliography, as this is the case. These phenomena could translate in an erratic behaviour of the dielectric strength evolution with the concentration.

According to these results, although improvements in the three cases have been registered, only the TiO_2 nanoparticles seem to behave in a confidable way, with a clearly-identifiable optimal concentration regarding the dielectric strength of the nanofluid, at 0.5 kg/m^3. Nevertheless, the remaining tests were also carried out with CuO and ZnO nanofluids, to check how other properties are affected by them. Also, in view of the previous results, another nanoparticle was included in the study, from one of the iron species which gave such good results in other works [127], [129], [134].

After performing the same preparation process, with the same base oil, samples of Fe_2O_3 nanofluids were tested. In this case the concentration range was narrower, as the optimal concentrations appeared at lower concentrations in the other cases. The BDV results for the base fluid and the nanofluid samples are summarized in the Figure 4.7.

Firstly, it must be pointed out that the BDV values obtained in this set of samples are lower than those of the previous nanofluids, which is noticed even when comparing the values of BDV obtained with the base fluid. This could be explained not only by the

higher moisture content of these samples (Figure 4.8, above 300 ppm), but also due to a possible evolution of the base fluid with the time while exposed to air, as all the nanofluid samples tested were produced with oil from the same vessel but with months of difference. Some of these BDV values are lower than the one specified by the manufacturer for the base oil, probably due to the same reasons.

Secondly, the average BDV of the base fluid is improved with Fe_2O_3 nanoparticles. This fact occurs especially at with the lower concentrations, with a maximum enhancement of 15.1% at 0.2 kg/m^3. On the other hand, as in the case of TiO_2, this improvement effect is lost progressively and continuously with larger concentrations, showing even BDVs lower than that of the base fluid. According to Figure 4.8, these improvements occur again with samples with slightly larger moisture contents regarding than that of the base fluid. Once more, if the moisture content would have been the same, these improvements may have been even more pronounced. Another possible effect of the moisture seems to appear in the range of the BDV distribution. Thus, the sample with more moisture (0.3 kg/m^3) presents lower maximum and minimum BDV values respecting close drier samples (0.2 and 0.4 kg/m^3).

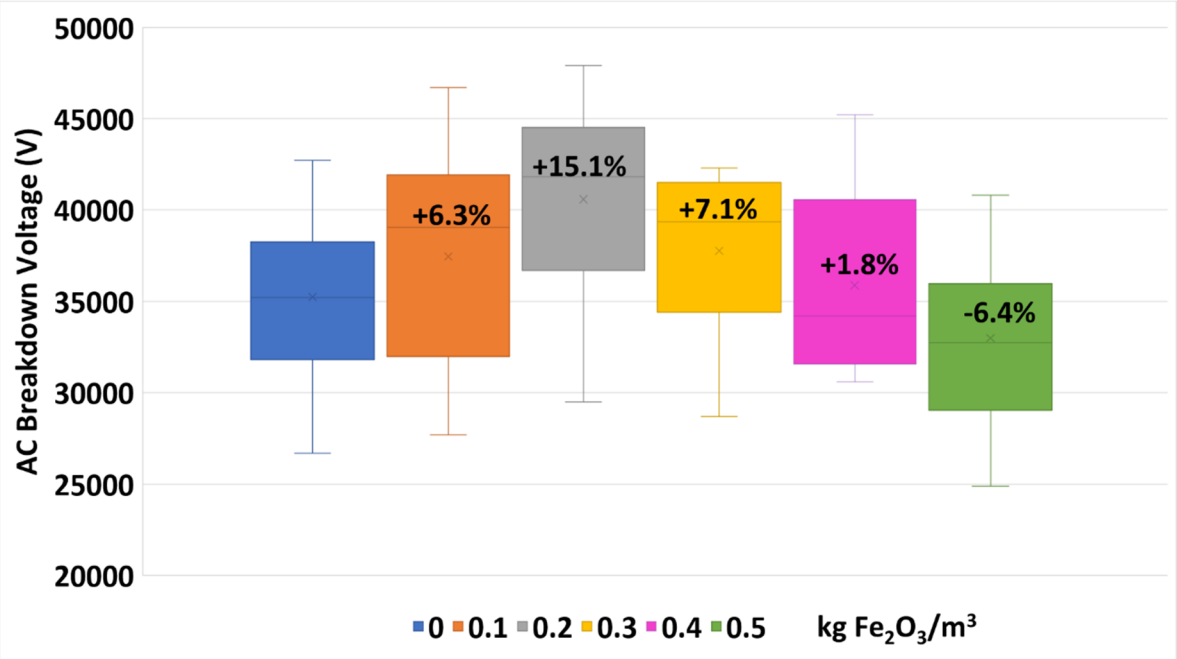

Figure 4.7. Dielectric strength results of the Fe_2O_3 nanofluids tested.

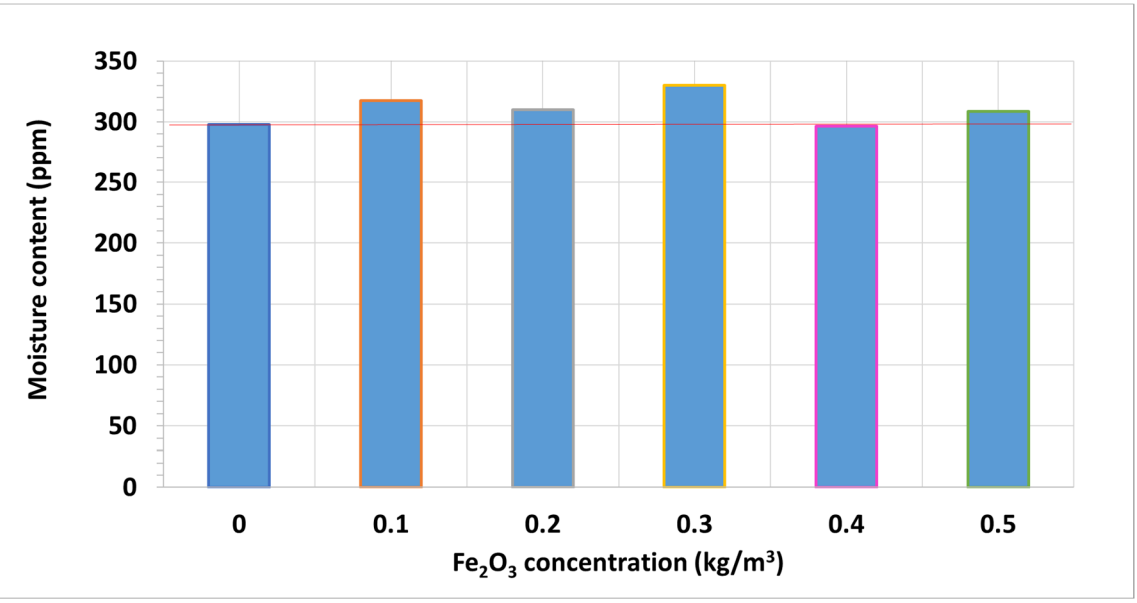

Figure 4.8. Mean moisture content of tested Fe_2O_3 nanofluid samples.

Finally, the comparison of the improvements achieved with TiO_2 and Fe_2O_3 nanoparticles points out a better performance of the former. The percentage enhancement with TiO_2 nanoparticles is double than that with Fe_2O_3 at the optimal concentrations, even though the reference BDV is also higher. Despite the differences in their moisture content, other experiences with similar nanoparticles have demonstrated the capacity of these nanofluids to improve their performance as more water molecules are present [15], [65], [106]. The worse performance of the maghemite is then not attributable to the moisture.

Among the great dispersion of the breakdown voltage test results in this kind of researches, noticeable in the Figure 2.8, some of these works were carried out under similar conditions and show similar results to this research. Thus, *Peppas et al.* [134] studied vegetal-oil-based dielectric nanofluids of maghemite, at concentrations under 0.14 g/l, close to the optimal here noticed, with a BDV improvement of 20.6%. With magnetite, at a lower concentration the variation was 8.5% [130]. *Zhong et al.* were dedicated to titania nanoparticles, also with vegetal base fluids [131]. They noticed an improvement of BDV close to 30%, around 0.3 g/l of nanoparticle. With mineral oils there are also similar results both with titania [59] or iron oxides [91], [118].

4.1.2. Dielectric dissipation factor and DC resistivity

Other dielectric parameters such as the Dielectric Dissipation factor (or loss factor) and the DC resistivity of the TiO_2 and Fe_2O_3 samples have been also studied and their results are presented in Figures 4.9-10. These are usually represented together with the dielectric strength in this kind of works, for comparison purpose [27], [28], [56].

As can be seen in these figures, while the dielectric dissipation factor increases with the concentration of nanoparticles, the resistivity is affected in an opposite way. This reverse effect of the nanoparticles on these properties and their interdependence has already been noticed in other researches [79], [127] and explained in the section 3.2.2.

Thus, in the Figure 4.10, as the presence of conductive nanoparticles (Fe_2O_3) rises, the resistivity of the nanofluid falls, reaching up to 50% drop with the highest concentration. On the contrary, in the same situation, the semiconductive TiO_2 nanoparticles suppose a slight increase of the resistivity (Figure 4.9). This increment reaches up to a 10%, even although in the highest case the TiO_2 concentration doubles the one with Fe_2O_3.

In the mentioned figures, it is remarkable how the larger affectation of the loss factor belongs to the conductive nanoparticle (Fe_2O_3), as its value doubles with the concentration. On the opposite, with the semiconductive nanoparticle (TiO_2) it grows only up to a 20%, although the concentration regarding the largest one of the Fe_2O_3 is double.

According to this, the larger variations of resistivity and dissipation factor are produced with the same kind of nanoparticle, those with conductive nature (Fe_2O_3). This also meets with the previous BDV results, as the nanoparticle capable of a better enhancement of this parameter in the base fluid (TiO_2) presents also an improvement on its resistivity and a lower increasement of the loss factor.

Another event to be pointed out is the discrepancy between the results of the two test rounds regarding the resistivity and the loss factor of the base fluid. Comparatively,

those carried out latterly (Fe_2O_3 nanofluid tests) have lower resistivity and higher tan δ, in a similar way to that seen before in the BDV tests.

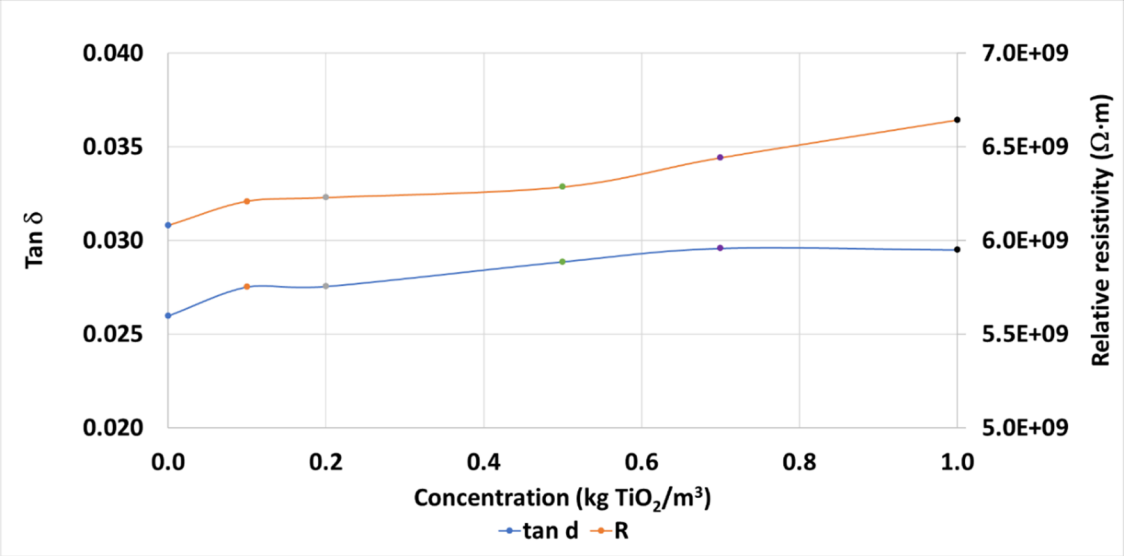

Figure 4.9. Dissipation factor and relative resistivity of TiO_2 nanofluid samples.

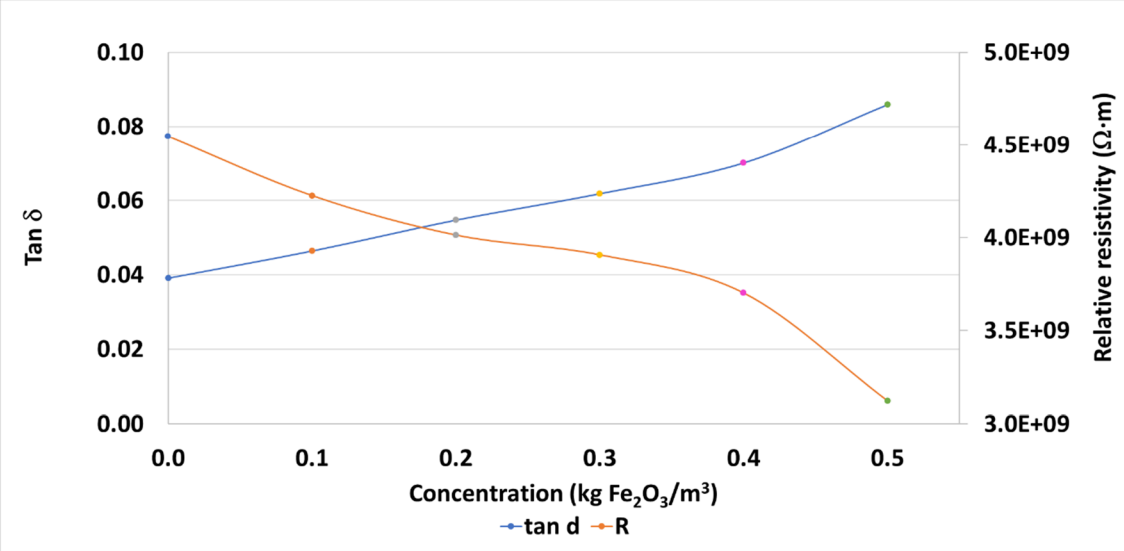

Figure 4.10. Dissipation factor and relative resistivity of Fe_2O_3 nanofluid samples.

For its part, the tests with the other nanoparticles give more erratic results back. Although the nature of CuO and ZnO are conductive and semiconductive respectively, the resistivity of the nanofluids results to be generally deep enhanced, even more at higher concentrations, and their loss factors seem to decrease in considering a general view of the graphs (Figures 4.11-12). This is contrary to what was seen with the other

nanoparticles, also conductive and semiconductive. In addition, the evolution of the tan δ of the CuO nanofluids does not show any coherent tendency, with continuous up and down events. This deepens in the erratic situation already seen with these nanoparticles with their BDVs, whose results do not even meet with those just explained if comparing sample by sample, on the contrary to with the other two nanoparticles.

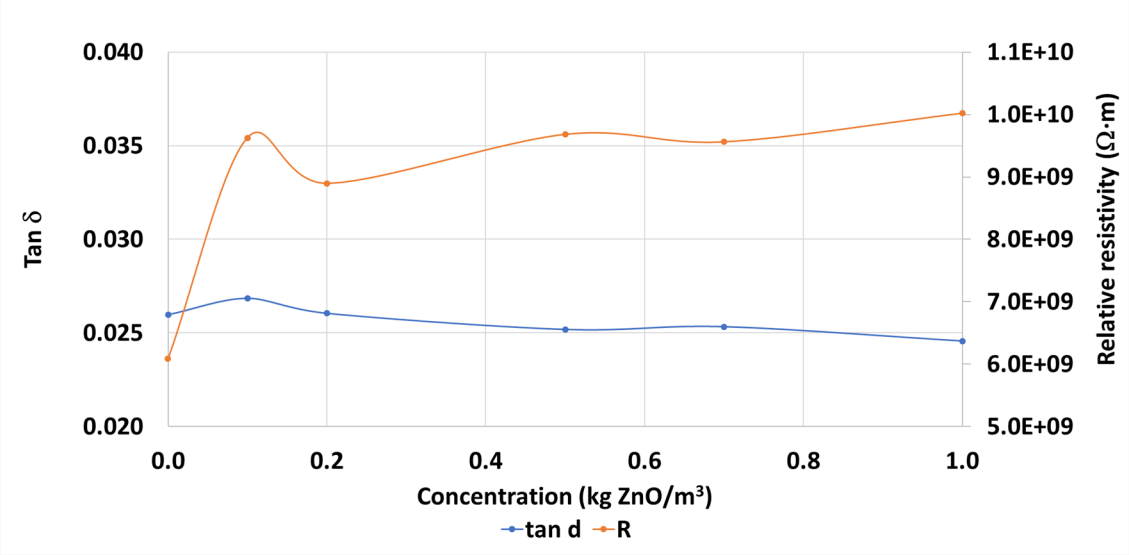

Figure 4.11. Dissipation factor and relative resistivity of ZnO nanofluid samples.

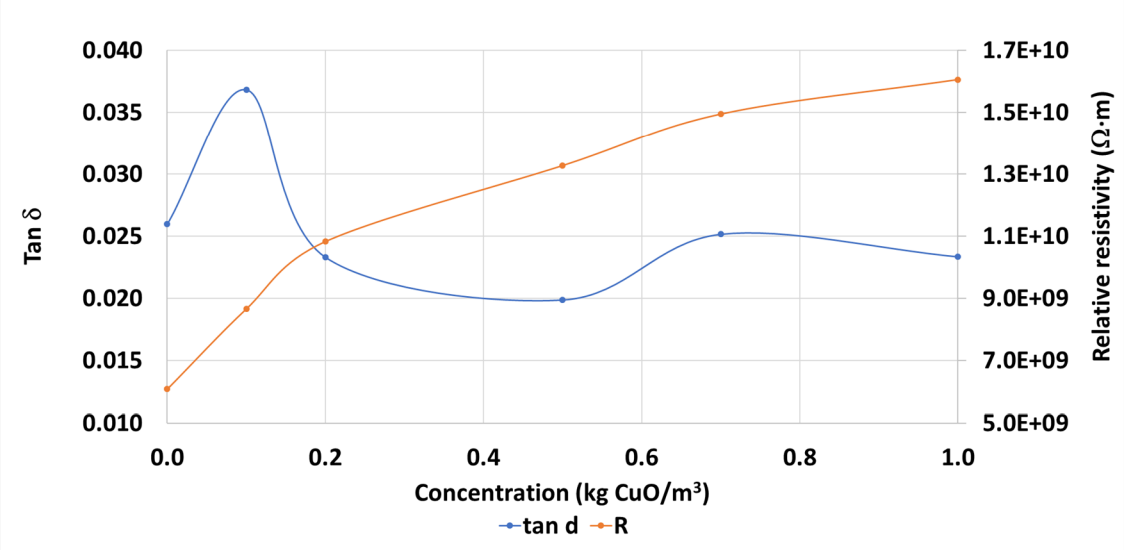

Figure 4.12. Dissipation factor and relative resistivity of CuO nanofluid samples.

4.2. THERMAL CHARACTERIZATION OF NANOFLUIDS AND BASE OIL

In the study of the suitability of the nanofluids, once done the dielectric characterization of the samples (with the TiO_2 nanofluids showing a better behaviour), the subsequent step was the determination of their thermal properties. To be more specific, they have been characterized the thermal conductivity and those temperature-dependent physical properties that also condition the performance of the nanofluids as coolant, as the density and the viscosity. For this, identical samples of base fluid and nanofluids at the same concentrations have been prepared and tested.

4.2.1. Thermal conductivity

This property has been measured according to the most common method, already explained in the section 3.2.1. Thus, the samples of base fluid and nanofluids were placed inside an oven at different temperatures and tested using a *KD2 Pro* tester. The data registered by this equipment has been represented in the Figures 4.13-16, together with their tendency lines and the uncertainty gap of the tests (red dashed lines). The experimental results of the base fluid are used as a reference to calculate this uncertainty gap, considering the experimental error provided by the tester manufacturer (±5%).

As can be seen in the aforementioned figures, no effect of the nanoparticles on the base-fluid thermal conductivity can be noticed. The conductivity values of the nanofluids are in the estimated error gap, at any of the concentrations and temperatures studied, and the tendency lines almost overlap. In view of these results, it can be pointed out that the thermal conductivity is not affected by the addition of these nanoparticles at the proposed concentrations. The foregoing contradicts what it is stated in most references available at similar conditions (Tables 2.10-11).

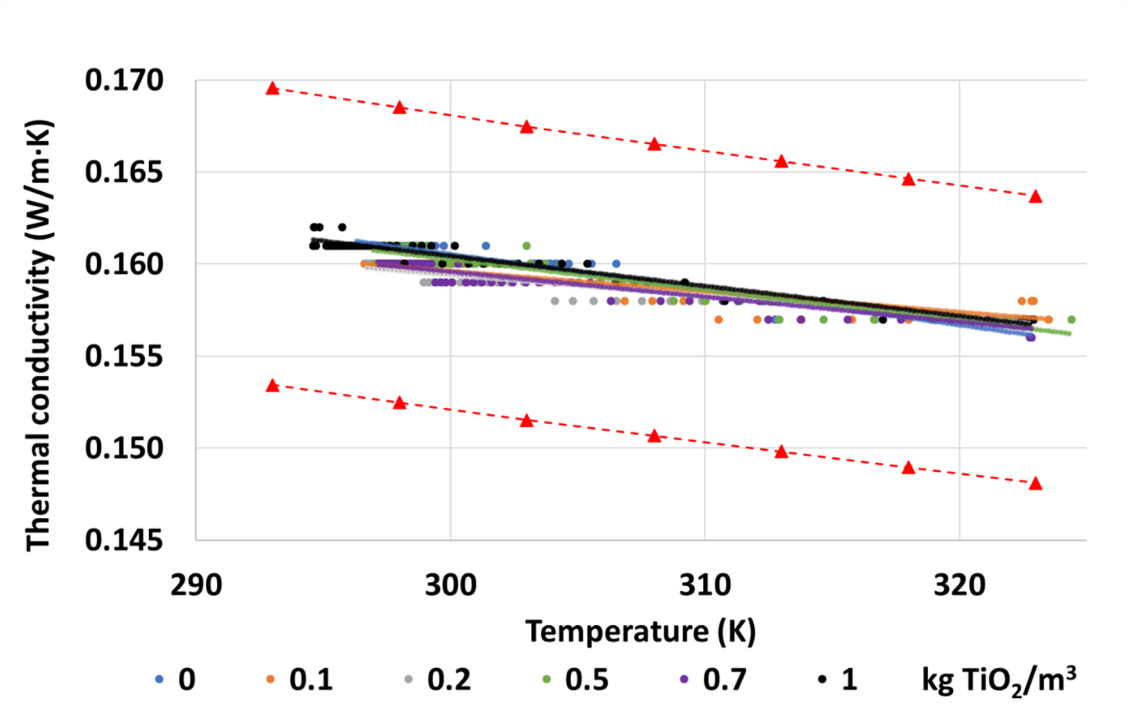

Figure 4.13. Thermal conductivity of the tested samples of TiO_2 nanofluids.

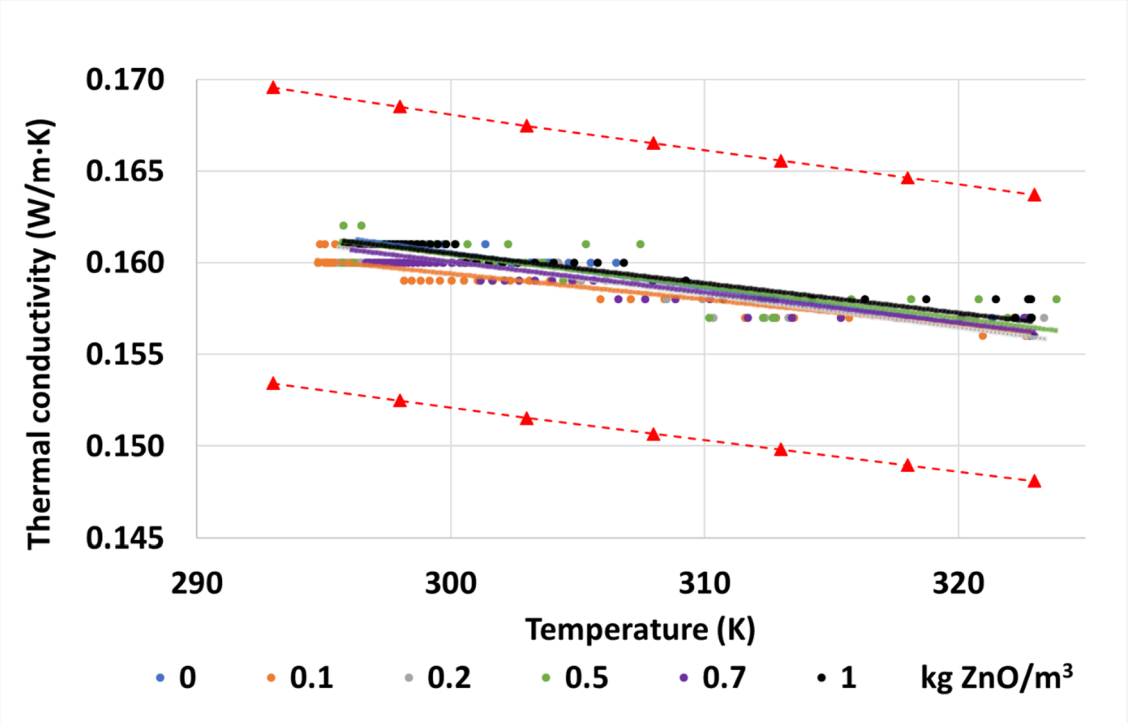

Figure 4.14. Thermal conductivity of the tested samples of ZnO nanofluids.

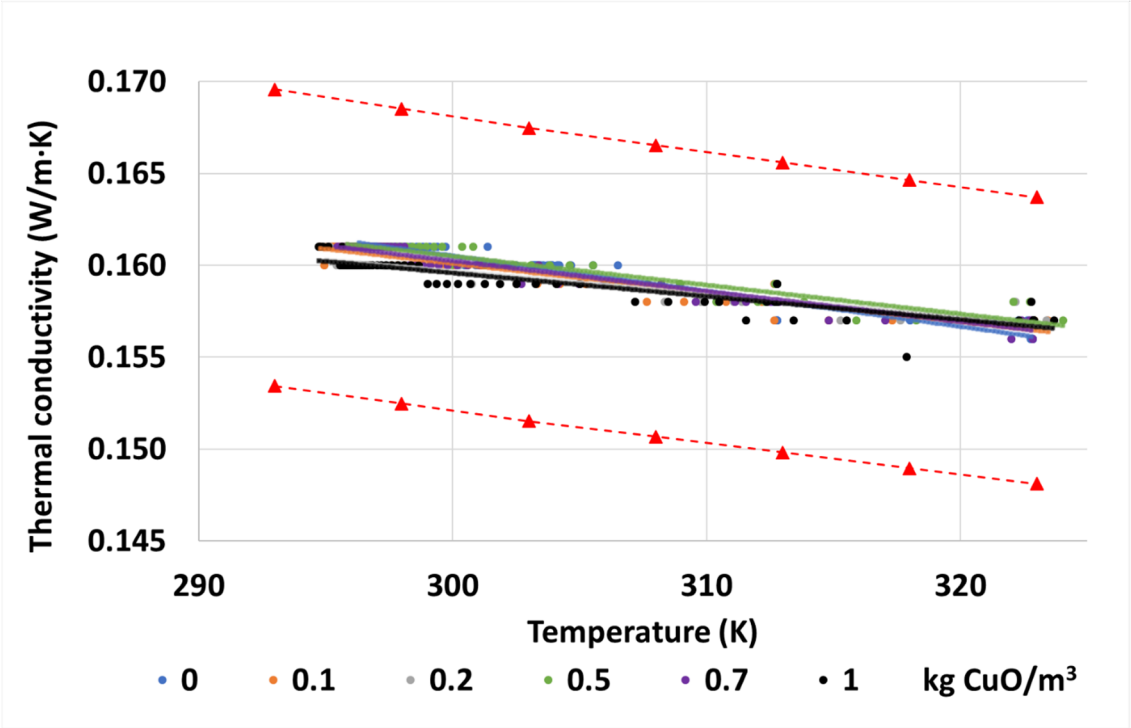

Figure 4.15. Thermal conductivity of the tested samples of CuO nanofluids.

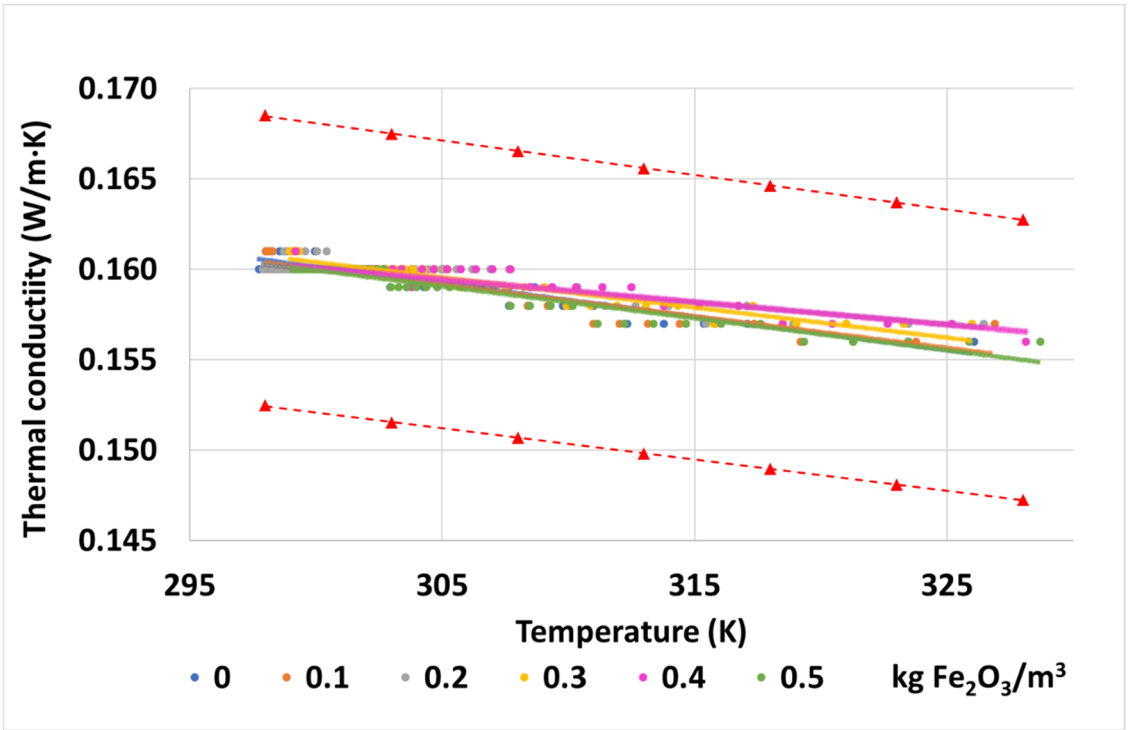

Figure 4.16. Thermal conductivity of the tested samples of Fe_2O_3 nanofluids.

An additional set of tests was carried out at higher concentrations with Fe_2O_3, since this nanoparticle has the larger bulk thermal conductivity of all nanoparticles analysed (Table 2.6). Four additional samples of Fe_2O_3 nanofluid at concentrations between 5 and 40 kg/m^3 were prepared and tested. These concentrations are well above those usually tested in this kind of research. They are also beyond the optimal concentration noticed from the dielectric standpoint. Therefore, they are not suitable for their application in a transformer.

The thermal conductivities of these samples, at different temperatures, are shown in Figure 4.17. In this case the effect of the nanoparticles on this property seems to occur, as the thermal conductivity results of the samples with concentrations of 20 and 40 kg/m^3 differ from those obtained with the base fluid and the Fe_2O_3 nanofluids with 5 and 10 kg/m^3. Nevertheless, these results are still inside the uncertainty gap set for the *KD2* tester and cannot be accepted as a suitable demonstration of the improvement of the thermal conductivity. Again, this is against the thermal-conductivity improvements found in other similar works.

Summarizing, this property cannot be considered during the selection of the optimal concentration of the different nanofluids, since it seems not to be affected by the addition of nanoparticles. In other words, this decision must rely only on the dielectric properties. Therefore, the optimal concentrations are 0.2 kg/m^3 for the Fe_2O_3 nanofluid and 0.5 kg/m^3 for the TiO_2 nanofluid, those with the largest improvement of BDV. Regarding the other species, with the same criteria, they have been chosen 0.7 kg/m^3 for the ZnO nanofluid and 0.2 kg/m^3 for the CuO nanofluid. Nevertheless, strictly speaking, these last cannot be considered optimal concentrations as the evolution of their BDVs with the nanoparticle concentration is not monotonous.

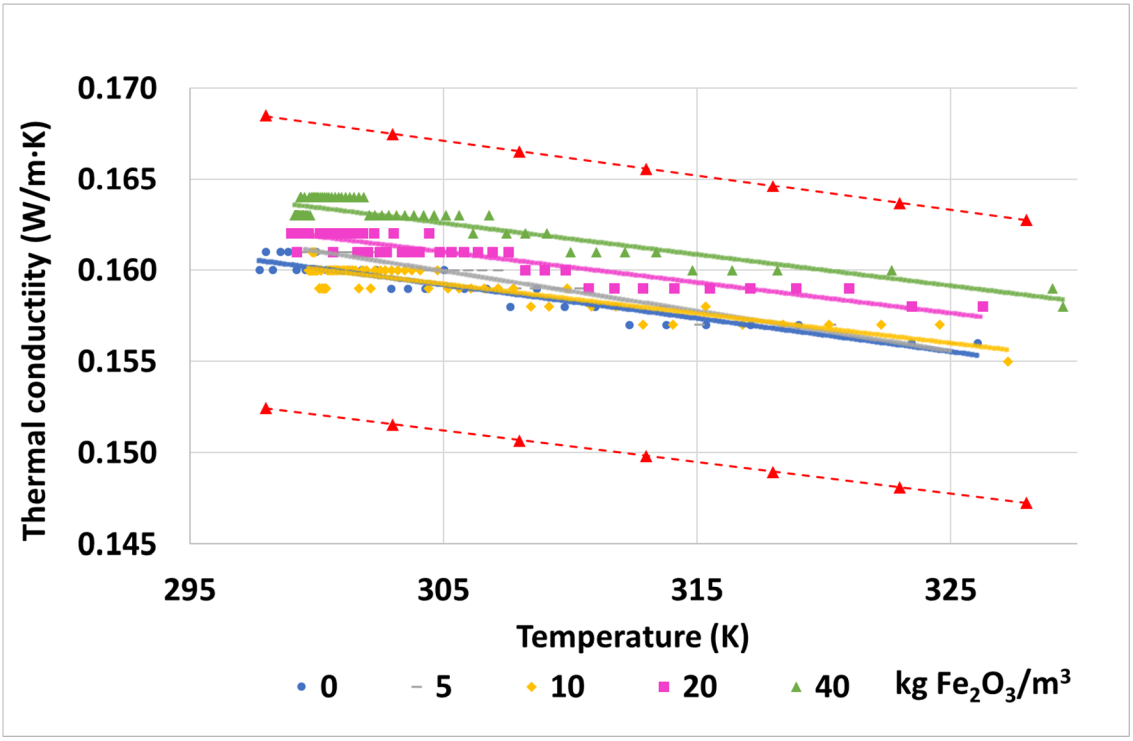

Figure 4.17. Thermal conductivity of Fe_2O_3 nanofluid with large concentrations.

4.2.2. Temperature-dependent physical properties: density and viscosity

Regarding the temperature-dependent properties that can condition the cooling capacity of the resulting nanofluids, their viscosity and density were measured at different temperatures.

First, it is necessary to point out that the results of both properties surpass the testers uncertainty gaps (slashed red lines in Figures 4.18-25). That is, the measures can be considered reliable. Bearing this in mind, while the densities meet the calculation according the amount of nanoparticles added and the volume of base fluid in each case (Figures 4.18-21), the viscosities vary up to a 5.7% with the Fe_2O_3 and up to a 7.2% with the TiO_2 (Figures 4.22-23). A similar situation occurs with the ZnO and the CuO nanoparticles (Figures 4.24-25), with variations up to 6.6 and 8.3 % respectively. In practically all the cases, the viscosities show quite a logical tendency with the nanoparticle concentration, and also with the temperature if they are compared with the information given by the base fluid manufacturer. Also, the largest viscosity variations seem to occur with the nanoparticles of larger mean size. Finally, considering

the concentrations that showed the largest BDVs, the viscosity of the ferrofluid is increased up to a 3%, 3.5%, 5.1% and 8.1% in the case of the Fe_2O_3, TiO_2, ZnO and CuO nanofluids, respectively. Despite the increase in viscosities, all of them fulfil the requirement set in the standard IEC 62770 for natural esters [173], as they are under 5·10-5 m^2/s at 40°C (Table 3.2). These values confirm the selected optimal concentrations, as no one of them presents an excessive increase of viscosity, as it happened in other works [60], [63], [71].

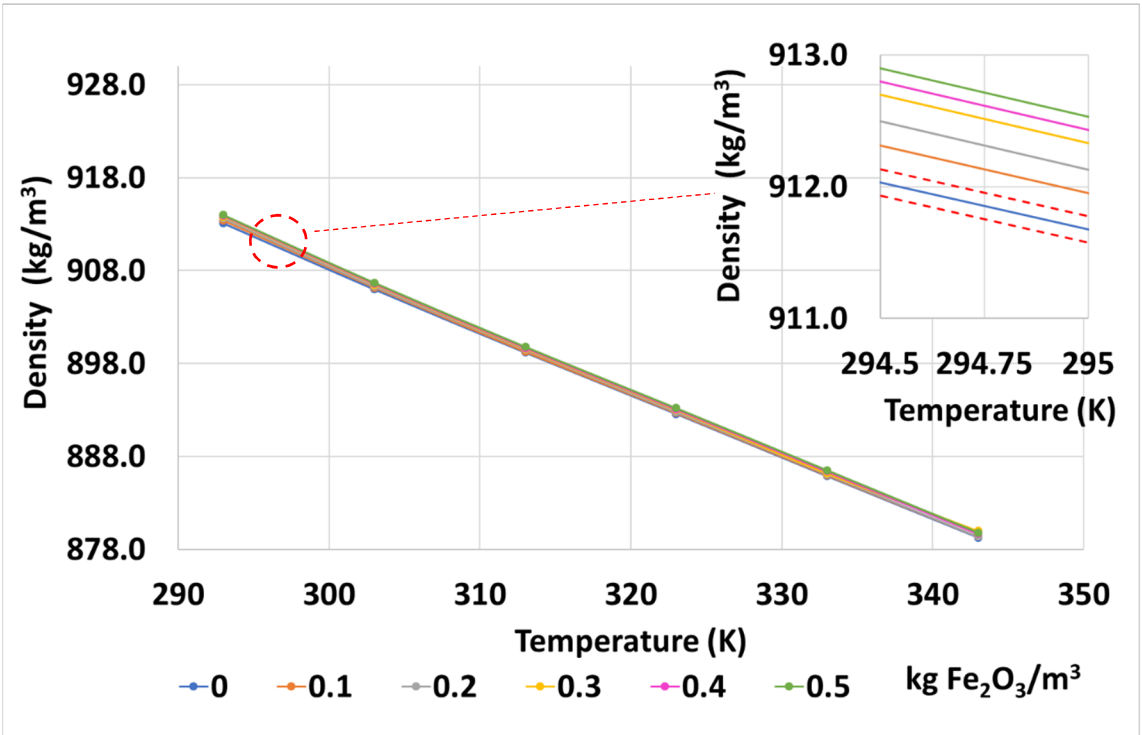

Figure 4.18. Evolution with temperature of the Fe_2O_3 nanofluids densities.

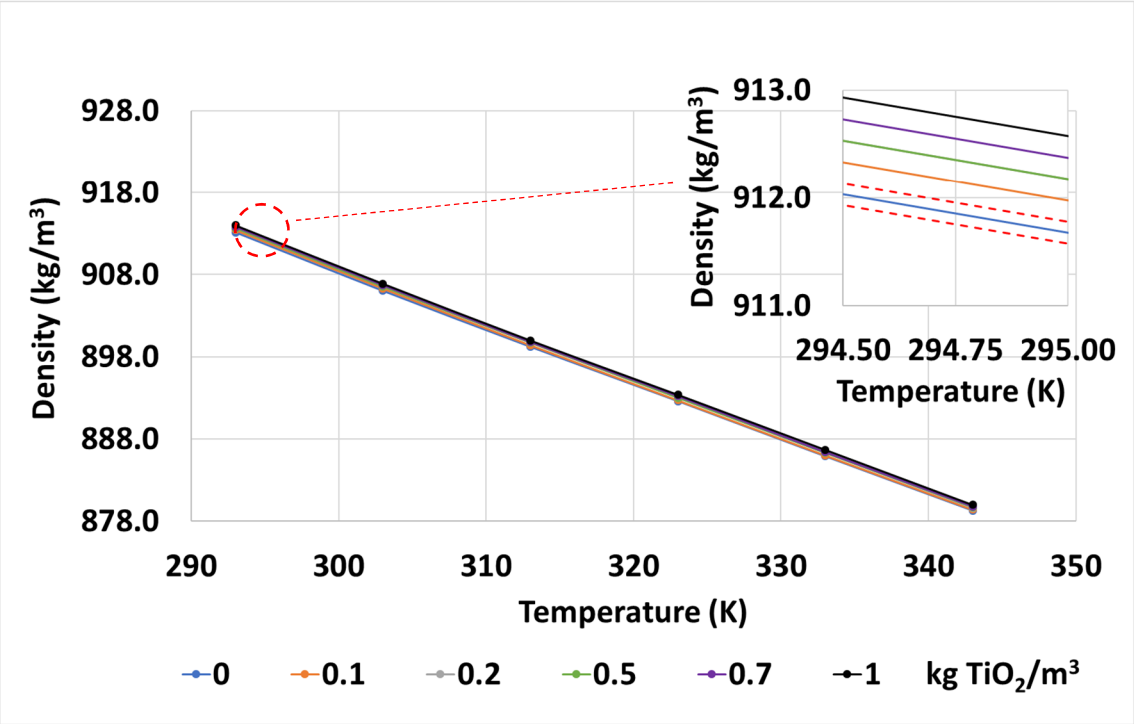

Figure 4.19. Evolution with temperature of the TiO_2 nanofluids densities.

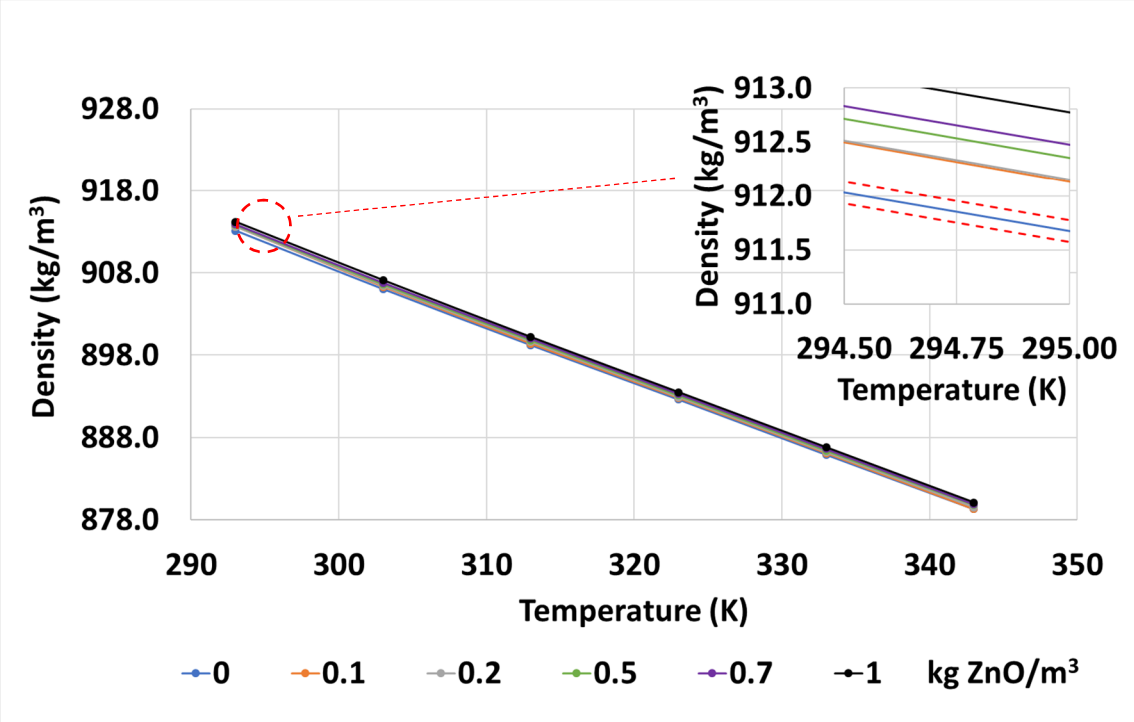

Figure 4.20. Evolution with temperature of the ZnO nanofluids densities.

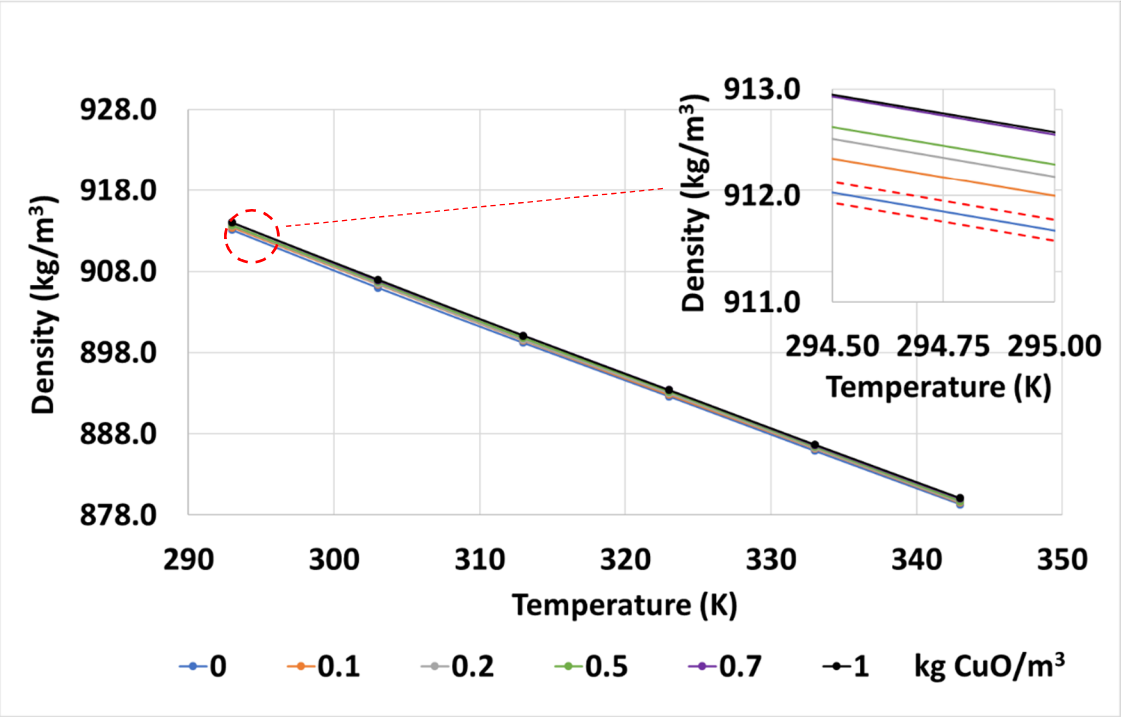

Figure 4.21. Evolution with temperature of the CuO nanofluids densities.

Summarizing, once again, as occurring with thermal conductivity, the effect of the nanoparticles on density or viscosity is limited due to the low concentrations used. By the addition of these nanoparticles it has not happened an important detriment on these properties while at the same time an improvement of the dielectric properties has been achieved. This may suppose, together with the stability on thermal conductivity, that the cooling capacity of the base fluid is almost kept constant when the particles are added, especially with Fe_2O_3 and TiO_2. According to all the above, the inferred optimal concentrations are selected to use them in an experimental setup in order to determine their cooling capacity.

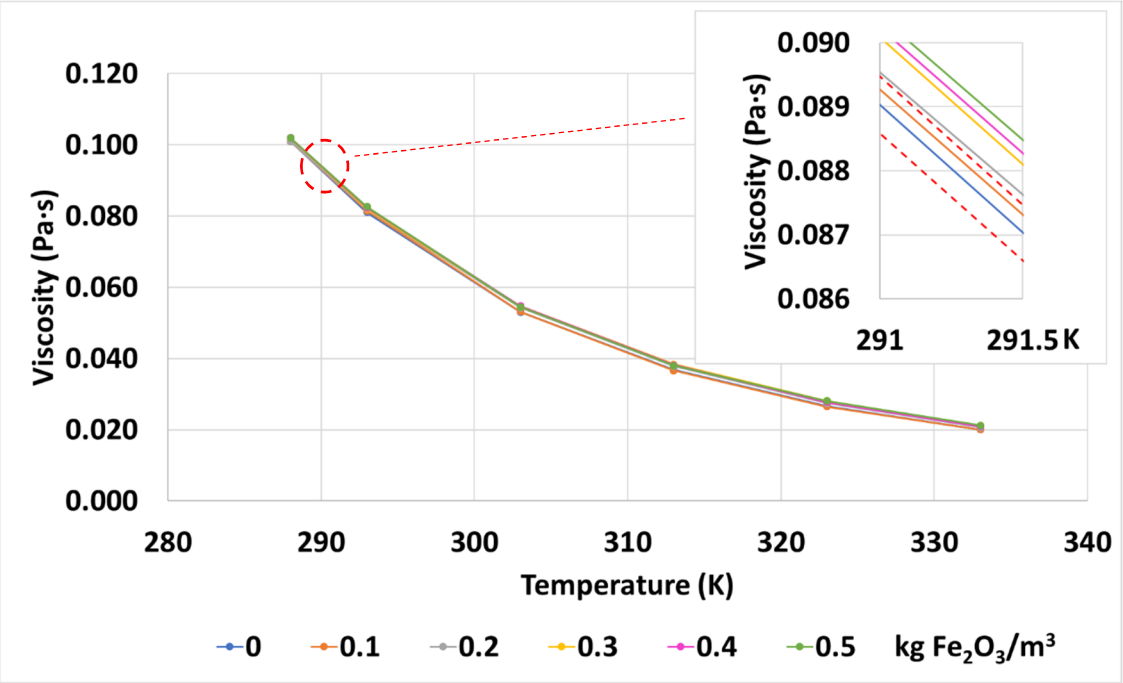

Figure 4.22. Evolution with temperature of the Fe_2O_3 nanofluids dynamic viscosities.

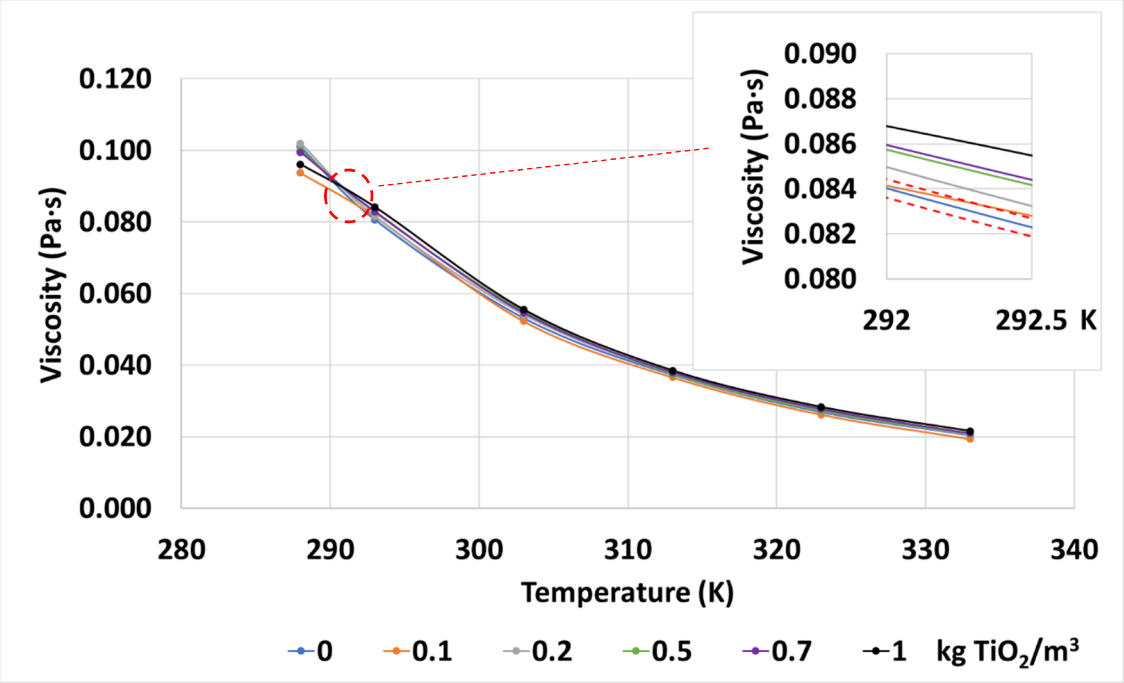

Figure 4.23. Evolution with temperature of the TiO_2 nanofluids dynamic viscosities.

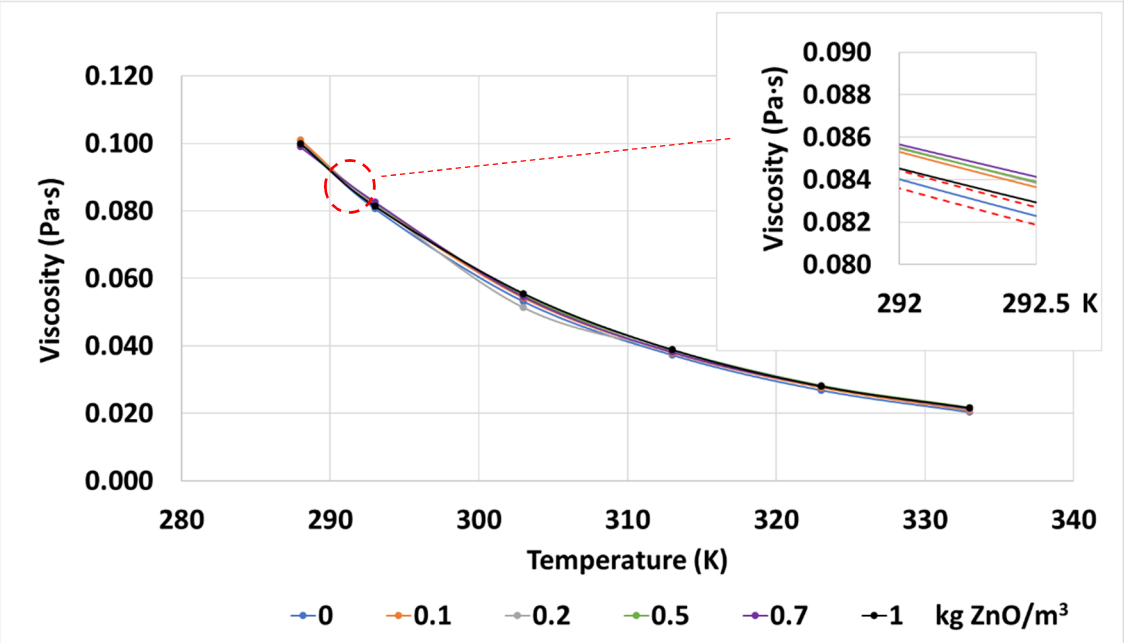

Figure 4.24. Evolution with temperature of the ZnO nanofluids dynamic viscosities.

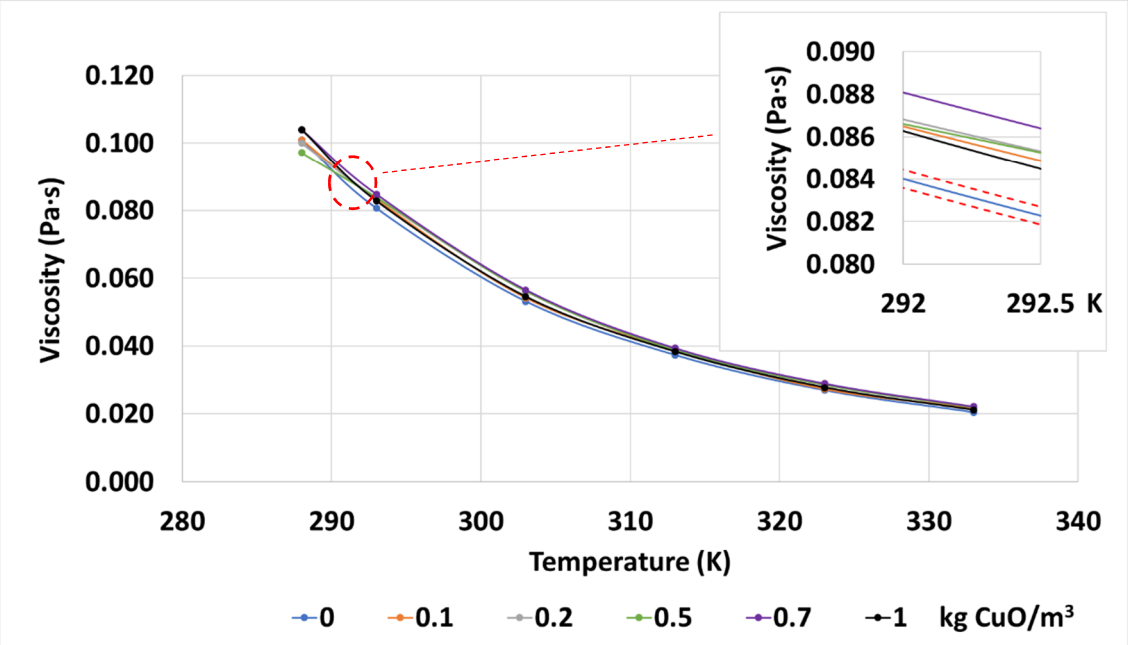

Figure 4.25. Evolution with temperature of the CuO nanofluids dynamic viscosities.

4.3. EXPERIMENTAL SETUP

Based on the knowledge obtained in the previous stages of the research the optimal concentrations according to the measured properties, those to be added to the experimental platform were 0.2 kg/m^3 for the Fe_2O_3 nanofluid and 0.5 kg/m^3 for the TiO_2 nanofluid. 0.7 kg/m^3 and 0.2 kg/m^3 were selected for the ZnO and CuO nanofluids.

Samples of these nanofluids and of the base fluid were prepared in the necessary amount and used in the cooling of a single-phase transformer The setup of the experimental platform utilized to carry out this task has been explained in the section 3.2.4.

The results obtained from this platform are shown in Table 4.1. To be more specific, the temperature gradients of the probes relative to the ambient temperature are presented, once the temperature stability criteria were fulfilled, for the natural ester base fluid and the optimal nanofluids. As it can be seen in this table, and in Figures 4.26-29, the temperature increase is generally lower when the ferrofluid is used as cooling fluid. However, these gradients are usually higher with the other nanofluids, especially with the CuO and ZnO nanoparticles at some of the load levels applied.

Table 4.1. Temperature gradients registered with different load regimes and fluids.

C	Fluid	ΔT_{Top}	ΔT_{Cu}	ΔT_{Iron}	ΔT_{Bottom}
1.3	**Base fluid**	32.7	36.6	36.6	25.6
	0.2 kg/m^3 Fe_2O_3	28.6	32.5	32.6	22.4
	0.5 kg/m^3 TiO_2	32.6	36.7	36.6	28.3
	0.7 kg/m^3 ZnO	38.1	42.4	42.0	28.3
	0.2 kg/m3 CuO	37.2	41.7	41.1	26.8
1	**Base fluid**	25.6	28.5	29.6	20.4
	0.2 kg/m^3 Fe_2O_3	23.9	27.2	28.1	20.1
	0.5 kg/m^3 TiO_2	26.5	29.6	30.4	23.9
	0.7 kg/m^3 ZnO	27.0	30.9	31.6	20.4
	0.2 kg/m^3 CuO	27.6	31.1	31.8	20.7
0.7	**Base fluid**	19.9	21.9	24.4	16.8
	0.2 kg/m^3 Fe_2O_3	18.9	21.4	23.8	17.2
	0.5 kg/m^3 TiO_2	20.2	22.2	24.4	18.8
	0.7 kg/m^3 ZnO	20.7	23.2	25.2	16.2
	0.2 kg/m3 CuO	24.0	26.7	28.8	19.3

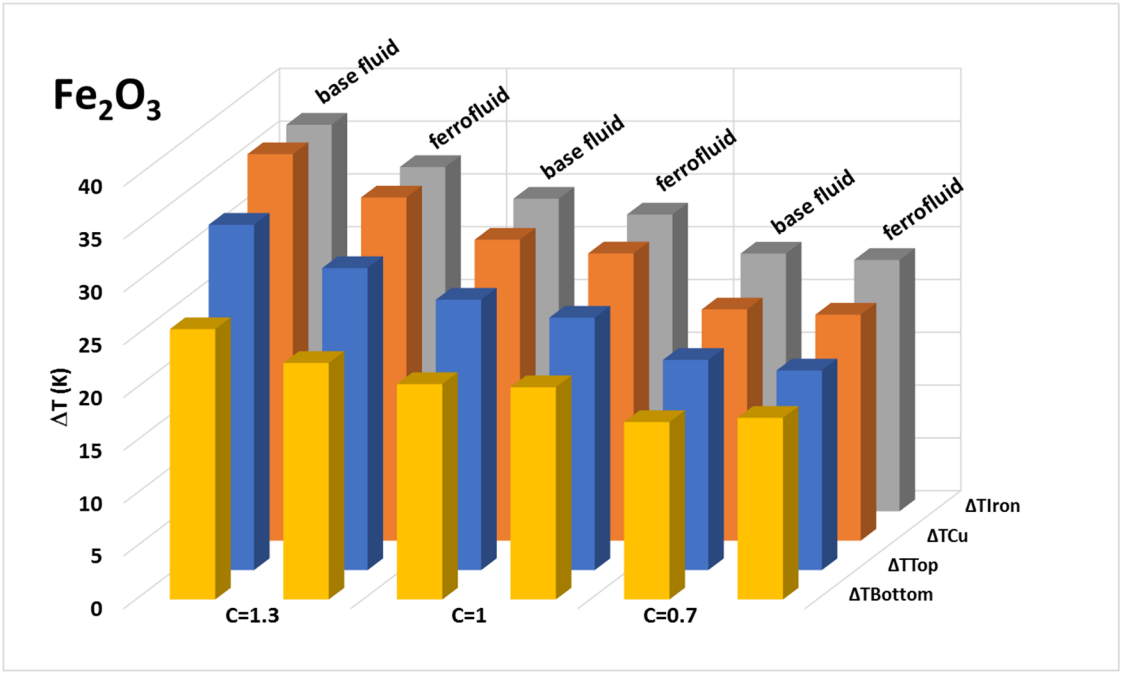

Figure 4.26. Comparison of the temperature gradients of the base fluid with those of the ferrofluid.

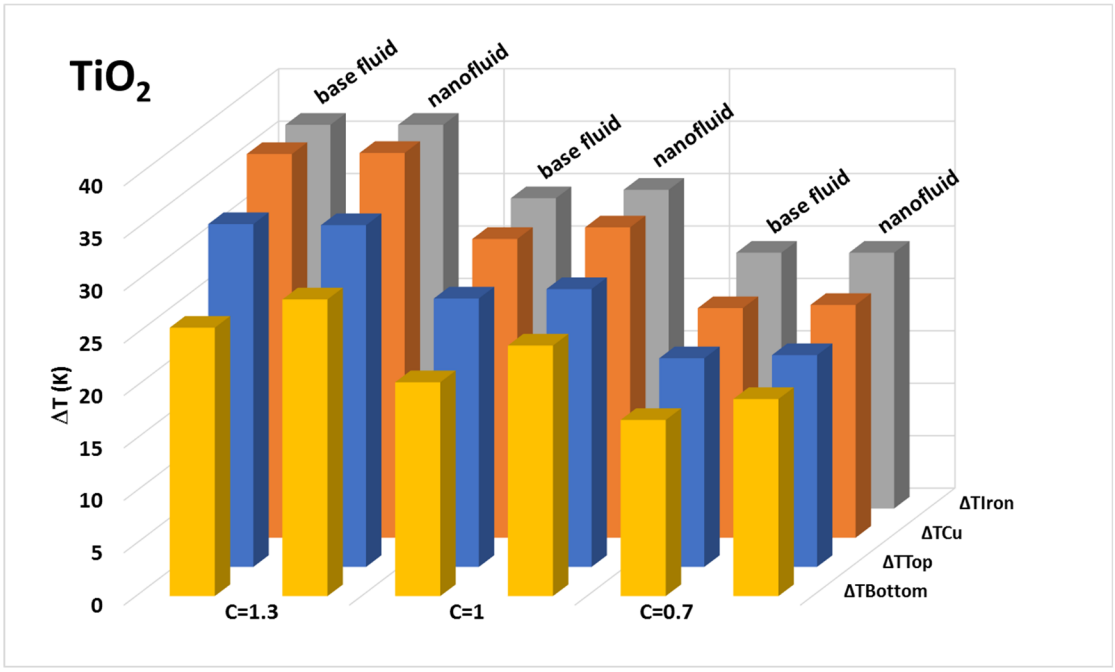

Figure 4.27. Comparison of the temperature gradients of the base fluid with those of the TiO_2 nanofluid.

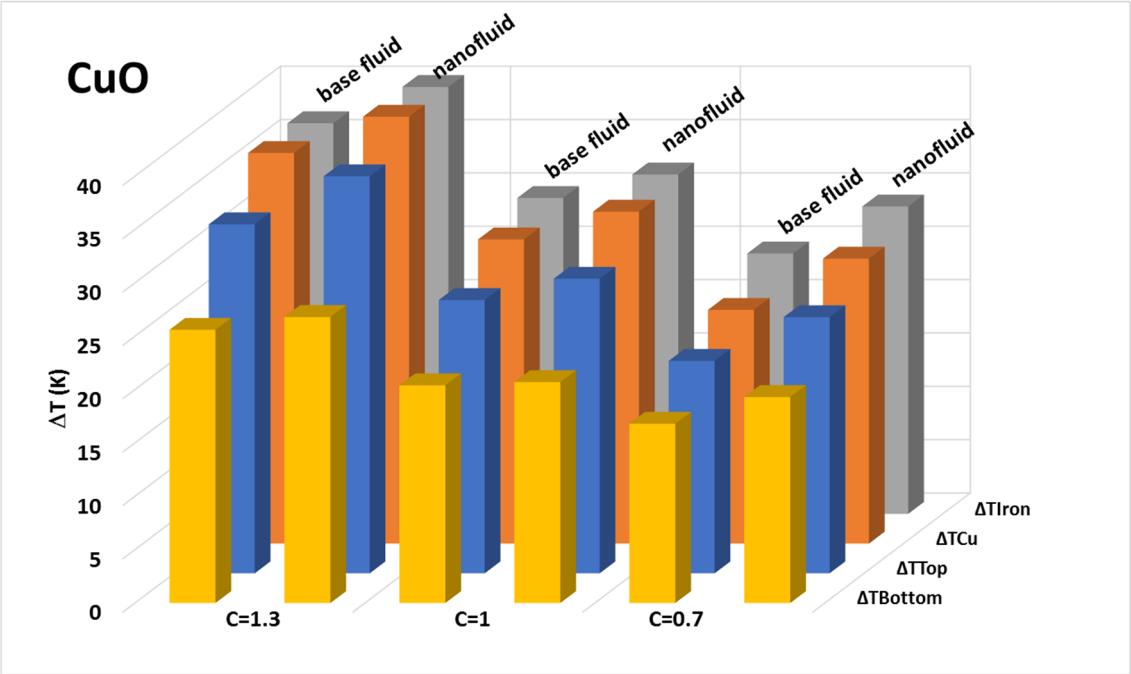

Figure 4.28. Comparison of the temperature gradients of the base fluid with those of the CuO nanofluid.

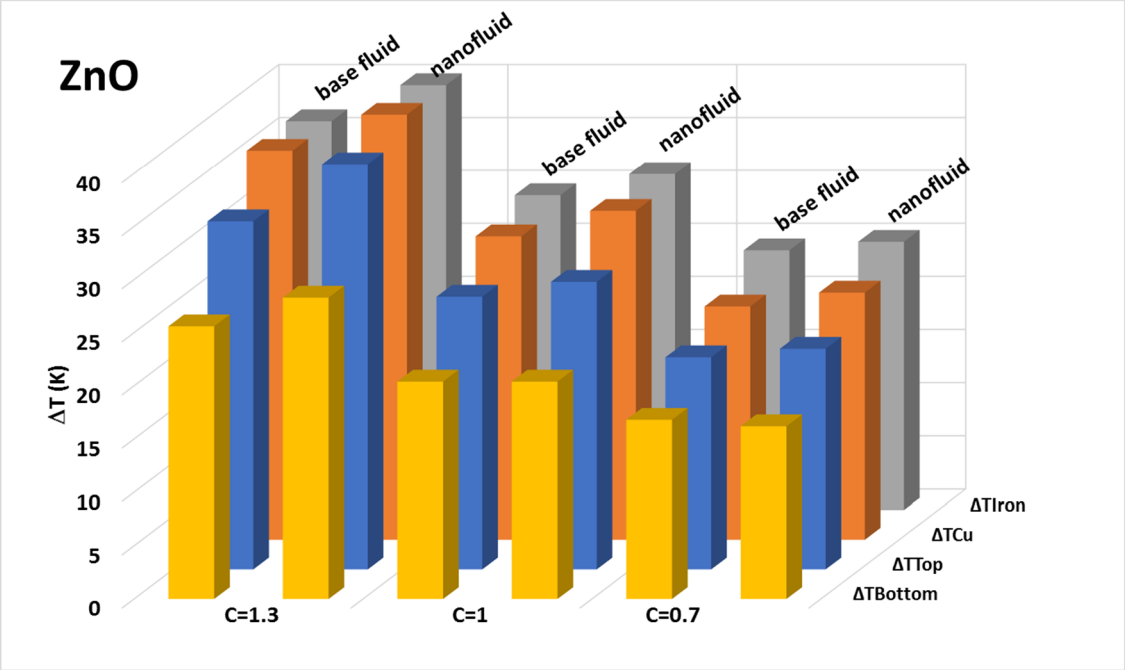

Figure 4.29. Comparison of the temperature gradients of the base fluid with those of the ZnO nanofluid.

As can be seen in Figure 4.26, the higher differences between the ferrofluid gradients and those of the base fluid occur in the overload regime (more heat to dissipate),

decreasing with the decrement of the load rate. In fact, these differences are practically null with the underload regime. As shown in Figure 4.30, this is more noticeable in the gradients obtained where the temperatures are also larger, as at the windings, ΔT_{Cu}. This figure includes the variation of the gradient of the nanofluid in %.

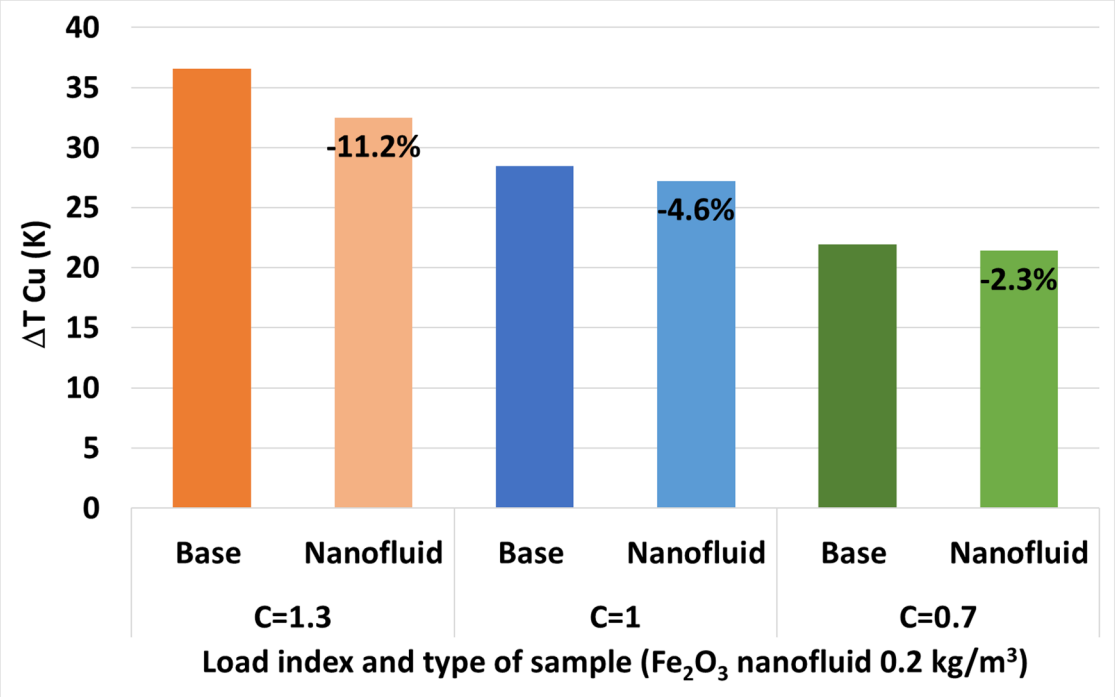

Figure 4.30. Comparison of the temperature gradients of the base fluid with those of the ferrofluid registered in the windings.

On the other hand, in the case of titania, these differences (shown in Figure 4.27, but also in Figures 4.31-32) are shorter with the largest load level. An explanation for this different behaviour could come from the combined effect of temperature and nanoparticles on the viscosity. Thus, as can be seen in Figure 4.33, the influence of the nanoparticles on the viscosity variation of the 0.5 kg/m^3 TiO_2 nanofluid regarding the base fluid is pretty similar in the range of temperatures from 293 K to 303 K. However, with higher temperatures close to 313K, this variation is reduced in such a way that the viscosity measured is inside the error gap (red dashed lines) of the viscometer. Therefore, if the viscosity is less enhanced at 313K (approximately the temperature at the overload regime of the three hotter probes), it could be reasonable to find that the deterioration of the cooling is less pronounced.

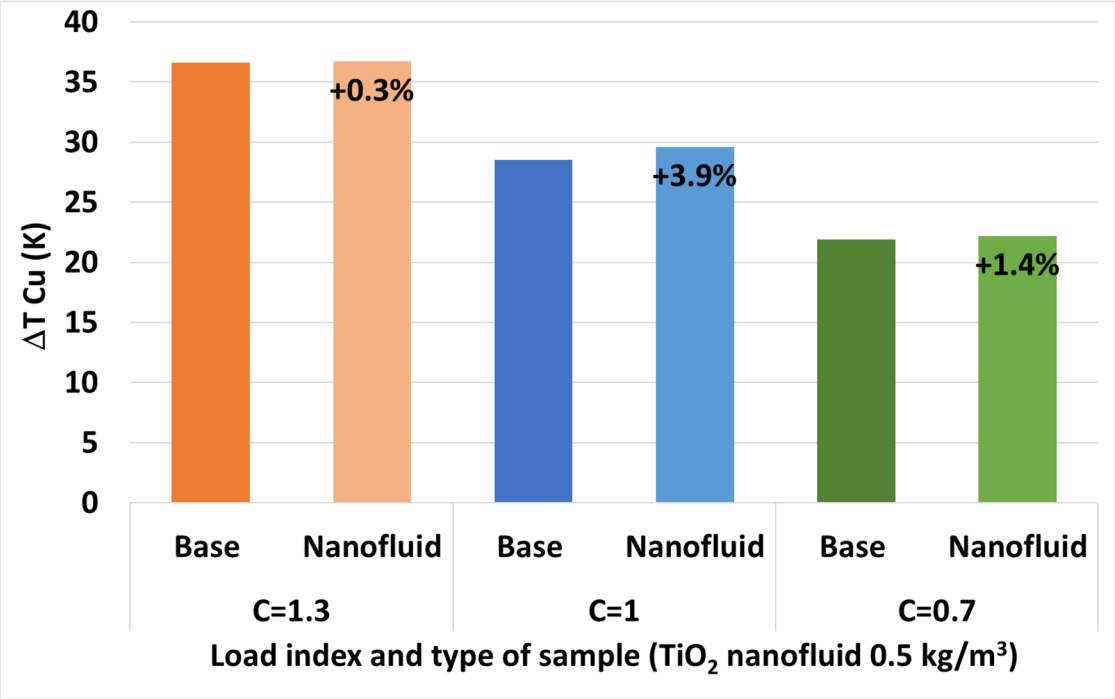

Figure 4.31. Comparison of the temperature gradients in the windings with the base fluid and the TiO_2 nanofluid.

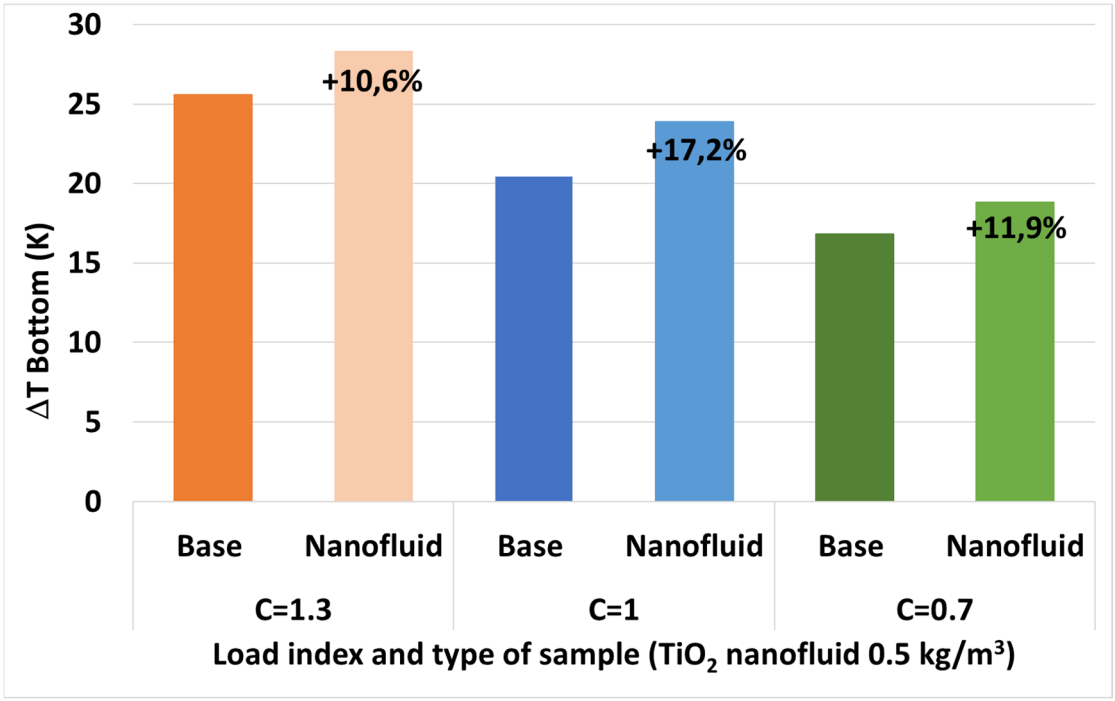

Figure 4.32. Comparison of the temperature gradients registered at the bottom with the base fluid and the TiO_2 nanofluid.

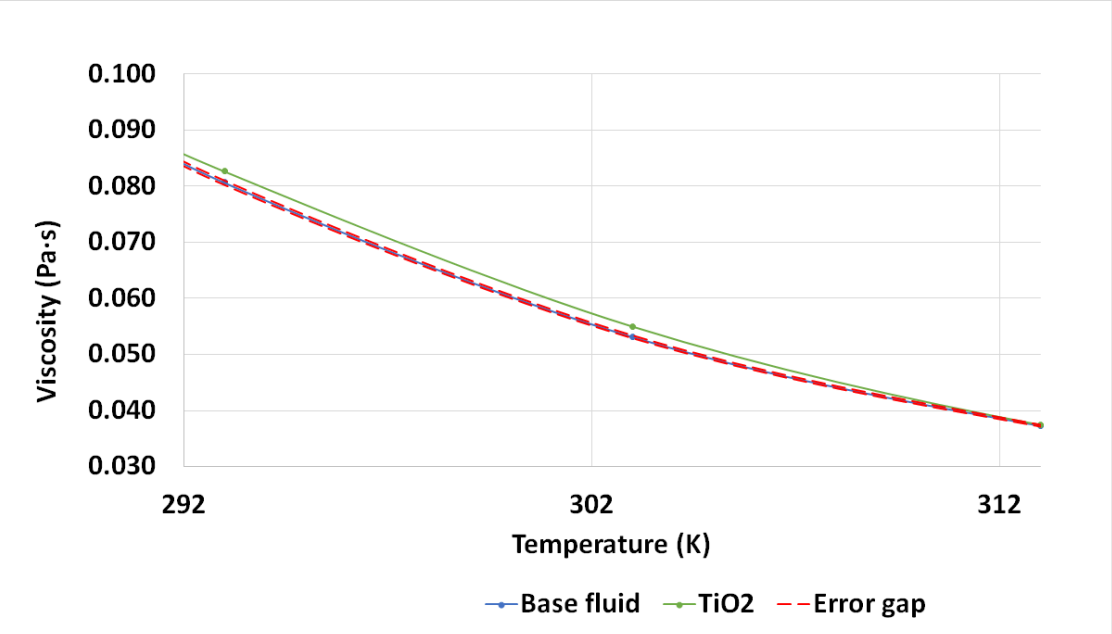

Figure 4.33. Viscosities of the base fluid and of the optimal TiO_2 nanofluid in the temperatures range of the cooling test.

Nevertheless, it must be considered the limited effect of the nanoparticles on the viscosity found during the characterization of the nanofluids due to the low concentrations applied. Thus, viscosity variations between 2.5 and 3.5% could not be enough to produce these cooling differences, especially the largest ones.

The joint action of the nanoparticles sedimentation and viscosity could explain these differences. It is known that the nanoparticles tend to fall with time to the bottom of the vessels due to the gravity forces, even in stabilized nanofluids. If so, this would translate in a higher viscosity that hinders even more the cooling in the bottom, together with a lighter viscosity in the upper parts. This is what it is seen in the bottom probe results, in which the differences between the TiO_2 nanofluid and the base fluid are, in every case, much larger than in the other probes, but they are closer among the load regimes, as can be noticed in Figures 4.31-32. In addition, sedimentation has been noticed during the tests, as after each test a thin film of nanoparticles always appeared on the horizontal surfaces of the transformer. However, this sedimentation was far from complete, as this fact may have supposed the inexistence of differences in the

temperatures of the upper probes at the lowest load regimes between the base fluid and the nanofluid.

Consequently, a reasonable explanation for these results with the TiO_2 optimal nanofluid is a combination of the occurrence of an actual and limited sedimentation of the nanoparticles, together with the limitation of their effect on the viscosity with the temperature.

These phenomena occur in the same way with a concentration of maghemite of 0.2 kg/m^3. However, in this case, the effect of the increase of viscosity at test temperatures because of the particles (from 2.3 to 4.9%) or their sedimentation seem to be despicable. The temperatures of the probes with the ferrofluid are always lower than with the base fluid, excepting at the bottom at the lowest load level, probably due to the adverse effect of the sedimentation (Table 4.1).

Regarding the other two species studied, their behaviour is in general worse than the one showed by the TiO_2 nanofluid, especially with the larger loads (Figures 4.34-35). Although these nanofluids presents a slightly larger viscosity respecting the TiO_2 nanofluid in the temperature range studied (Figure 4.36), these limited variations (around 2.5% for the ZnO and from 4 to 6% with the CuO regarding the base fluid viscosity) do not seem to be enough by themselves to explain the differences in their cooling performance, especially at the larger load levels.

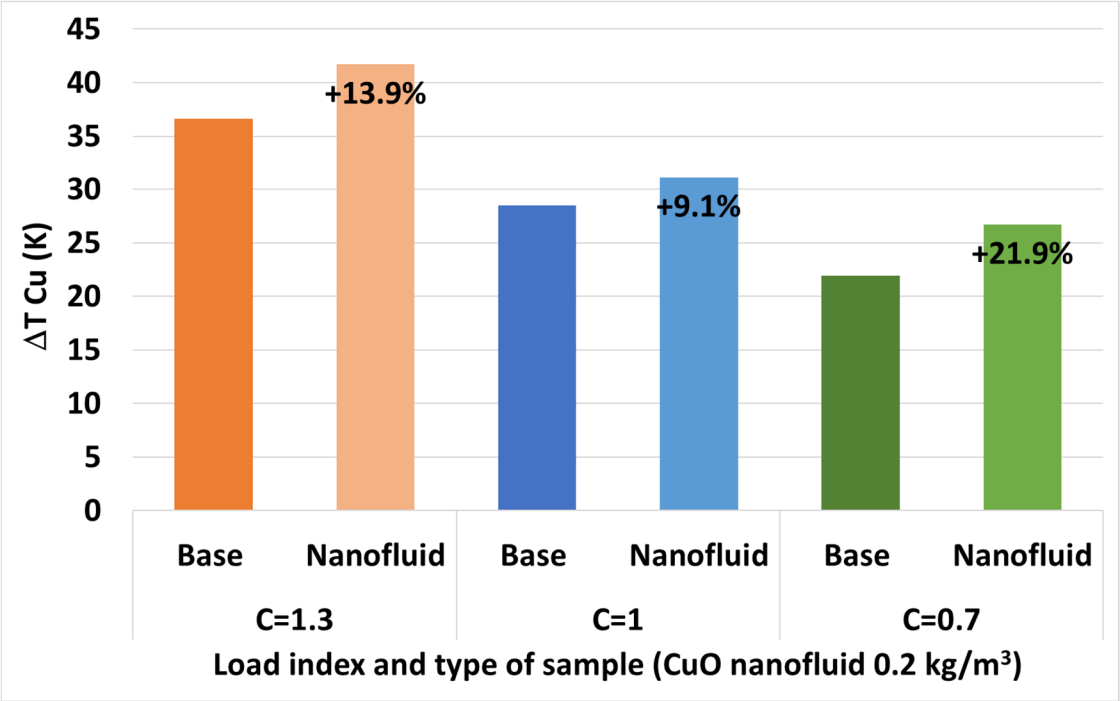

Figure 4.34. Comparison of the temperature gradients in the windings with the base fluid and the CuO nanofluid.

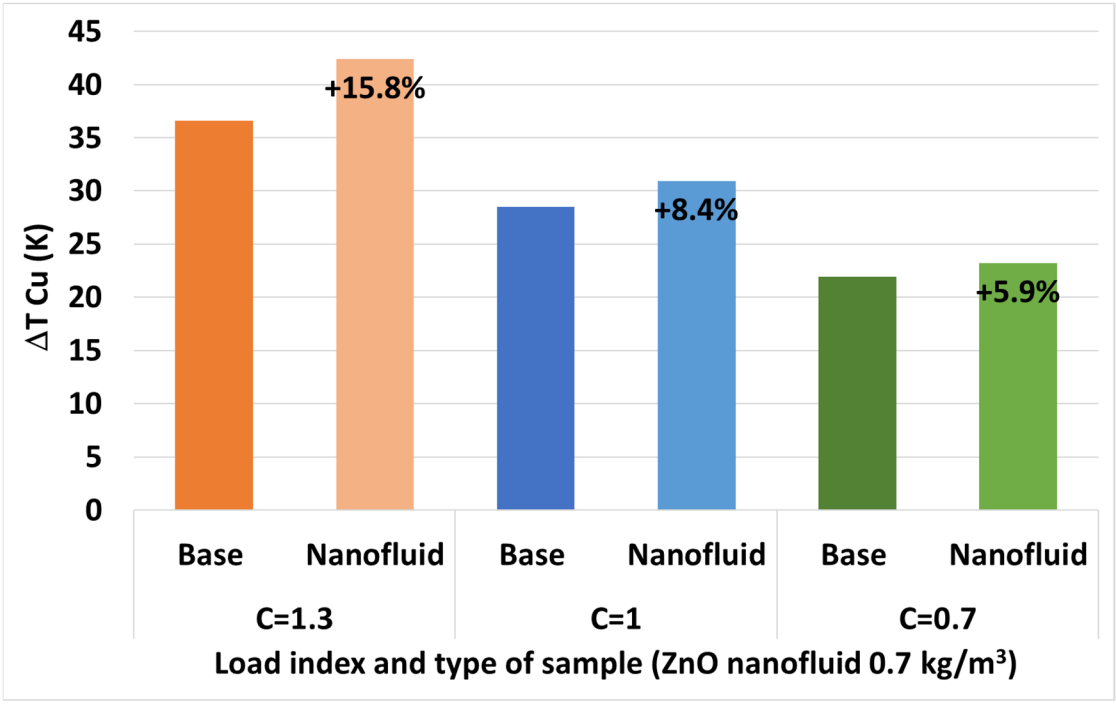

Figure 4.35. Comparison of the temperature gradients in the windings with the base fluid and the ZnO nanofluid.

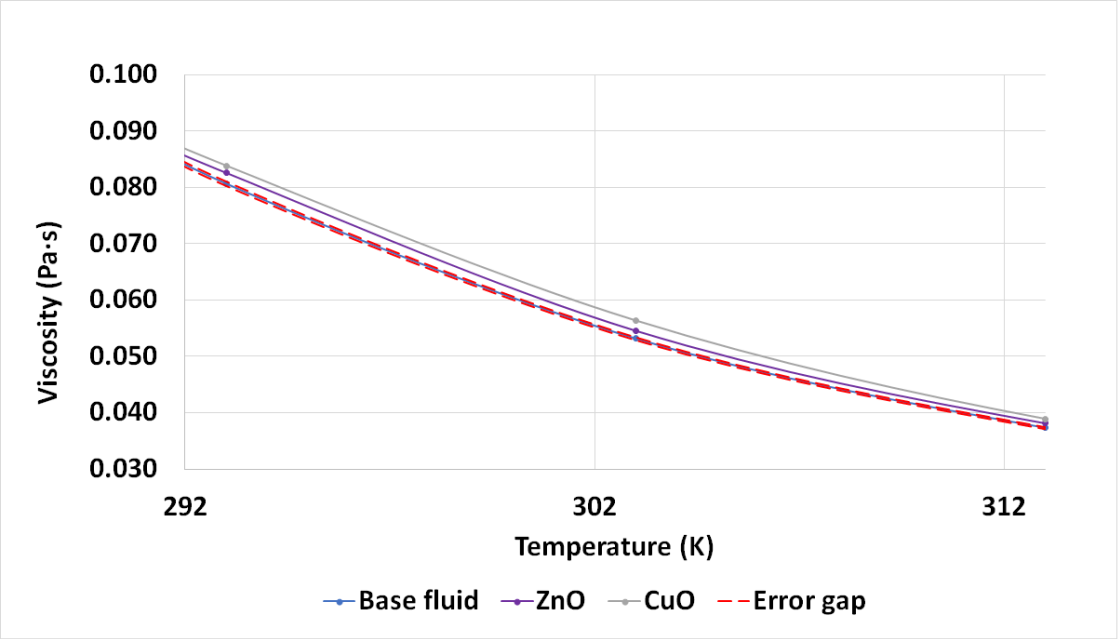

Figure 4.36. Viscosities of the base fluid and of the optimal ZnO and CuO nanofluids in the temperature range of the cooling test.

The different thermal behaviour of these nanofluids, together with the absence of a significative improvement of their thermal conductivity, point out the existence of an additional mechanism in the ferrofluid improving its cooling capacity.

A feasible explanation of the higher cooling capacity of ferrofluids is the interaction between the ferrofluid and the magnetic field generated by the transformer. This has been noticed and explained in other works and in the section 2.4.1: the existence of a thermomagnetic convection produced by additional buoyancy forces caused by the different magnetic susceptibilities of the hotter parts regarding the colder ones of the ferrofluid [92], [178]. This difference raises when the amount of heat dissipated increases, as the magnetic susceptibility decreases with the temperature.

This theory is also compatible with the results of the experimental setup with the TiO_2, CuO and ZnO optimal nanofluids. These nanoparticles present similar characteristics than the Fe_2O_3 respecting size, shape or bulk thermal conductivity, and they affect also in a similar way several properties here characterized as thermal conductivity, density or viscosity. Their main differences are in the magnetic susceptibility and electric

conductivity. Thus, the different thermal behaviour of the nanofluids in the experimental platform may be caused by these two properties. As non-magnetic particles, the absence of interaction with the magnetic field generated by the transformer is expected in the case of TiO_2, CuO and ZnO nanoparticles. The appearance of thermo-magnetic convection with the Fe_2O_3 nanoparticles and its inexistence with the other could be enough to explain their behaviour.

CHAPTER 5:

CONCLUSIONS

5. CONCLUSIONS

The present section collects the general conclusions of this thesis and summarises its main contributions. Then, they are listed the articles related with this thesis published in international journals an in international conference proceedings. The third section presents the funding received to carry out this work and the international stays in foreign institutions. Finally, future research lines derived from this thesis are also suggested.

5.1. GENERAL CONCLUSIONS

This research assesses the thermal and dielectric performance of several nanofluids in order to be used in electric transformers, focusing on their main properties. The revision of the available information in this field reflects lack of knowledge regarding the application of dielectric nanofluids in existing devices, even at laboratory scale. Even more, this lack is more pronounced with those oils expected to substitute mineral oils at transformers in the mid-term, the biodegradable natural esters. Consequently, deepening in the knowledge of the natural ester-based nanofluids and their application in transformers were set as objectives of this thesis. To carry out this task, several combinations of nanofluids have been characterized, and those with the best characteristics have been tested in an experimental setup.

In this sense, according to the results obtained during the dielectric characterization, it can be stated:

- Among the commercial nanoparticles used only the Fe_2O_3 and TiO_2 species have demonstrated clearly and reliably that they improve the BDV of the natural ester used as base fluid, especially the last one.
- The dependence of the BDV on the moisture content or the Fe_2O_3 and TiO_2 nanoparticle concentration have shown to be as explained in the related literature.

- The optimal concentrations from the dielectric point of view were 0.2 kg/m^3 of Fe_2O_3 and 0.5 kg/m^3 of TiO_2, again in the range usually found in other researches and with similar results.
- In the case of CuO and ZnO nanoparticles, their influence on the BDV is not so clear, although improvements have been also noticed. This could be due to their less homogenous distribution of sizes.
- The above conclusions are corroborated when considering the other dielectric properties measured, dielectric dissipation factor and resistivity.
- In short, the metal oxide nanoparticles added in low concentrations have demonstrated to be capable of improving the dielectric properties of transformer alternative oils.

Regarding the thermal-physical properties, some conclusions can be stated:

- Unlike density and thermal conductivity, the viscosity seems to be the only property really affected by the presence of nanoparticles with the concentrations studied. In any case, these viscosity variations are limited, and the nanofluids fulfil the limit value set for fresh natural esters in the standard.
- Thus, the thermal properties do not condition the cooling capacity of the fluid and the selection of the optimal concentrations was done based on the dielectric properties.

Finally, some findings obtained from the experimental setup can be presented:

- The thermal characterization collides in part with the experimental results. Although the results tend to confirm a worst cooling when the TiO_2, ZnO and CuO nanofluids are used (cooling behaviour consistent with the thermal properties tested, especially in the case of the last two nanoparticles), the performance of the Fe_2O_3 nanofluid is the opposite. The temperatures found with this fluid are, in general, lower than those obtained with the base fluid, even though the

viscosity is higher, and the thermal conductivity is kept. This occurs more pronounced as higher is the load level of the transformer (as the temperatures are higher) and at those probes with the highest temperatures.

- The magnetic nature of the Fe_2O_3 nanoparticles, together with a best cooling performance at higher temperatures and the absence of this improvement with the other nanoparticles, seem to support the existence of thermal-magnetic buoyancy forces that improve the convection in the tank.

5.2. MAIN CONTRIBUTIONS

During this work a review of the state of the art in dielectric nanofluids for transformers has been carried out. Based on it, an experimental research has been designed and developed. The original contributions of the work can be found below:

- As a result of the information collected in the reviewed literature, an optimized preparation method has been proposed.
- Among the nanoparticles proposed, those that are more suitable have been found based on the characterization of their dielectric and thermal properties, together with their optimal concentrations
- The optimal nanofluids have been tested in an actual transformer to find their cooling capacity. The presence of buoyancy forces beyond those relative to the natural thermal convection seems to appear with the maghemite nanoparticles. Their magnetic nature, on the contrary to the other species, point out the thermo-magnetic nature of these buoyancy forces.

5.3. PUBLICATIONS

Part of the results of this thesis has been published in form of the following research and conference papers:

- C. Olmo, C. Méndez, F. Ortiz, F. Delgado, R. Valiente and P. Werle, "Maghemite Nanofluid Based on Natural Ester: Cooling and Insulation Properties

Assessment," in *IEEE Access*, vol. 7, pp. 145851-145860, 2019. doi: 10.1109/ACCESS.2019.2945547.

- C. Olmo, I. Fernandez, A. Santisteban, C. Mendez, F. Ortiz and A. Ortiz, "Effect of maghemite nanoparticles on insulation and cooling behaviour of a natural ester used in power transformers,"*2019 IEEE 20th International Conference on Dielectric Liquids (ICDL)*, Roma, Italy, 2019, pp. 1-4. doi: 10.1109/ICDL.2019.8796817.

- C. Olmo, I. Fernández, F. Ortiz, C.J. Renedo, S. Pérez, "Dielectric properties enhancement of vegetal transformer oil with TiO_2, CuO and ZnO nanoparticles," International Conference on Renewable Energies and Power Quality (ICREPQ'18), Salamanca, Spain, 2018, pp. 623-627. doi: 10.24084/repqj16.412.

Other works derived from this thesis are currently under revision:

- C. Olmo, I. Fernández, F. Ortiz, C. J. Renedo, A. Ortiz, Fernando Delgado, "Search for Suitable Thermal-dielectric Nanofluids for Transformers – A Review"

- C. Olmo, C. Méndez, F. Ortiz, F. Delgado, A. Santisteban, I. Fernández, "Non-magnetic Nanofluids Based on Natural Ester: Cooling and Insulation Properties Assessment,"

These results have been also used in other investigations of the research group, as:

- A. Santisteban, C. Olmo, C. Méndez, F. Delgado, C. J. Renedo and F. Ortiz, "Cooling Performance of Different Dielectric Fluids Containing Nanoparticles in a Transformer Winding," *2019 IEEE 20th International Conference on Dielectric Liquids (ICDL)*, Roma, Italy, 2019, pp. 1-4. doi: 10.1109/ICDL.2019.8796516.

5.4. STAYS AND FUNDING RECEIVED

Part of this investigation has been carried out in collaboration with other research institutions during the following research stays:

- Institution: Leibniz Universität Hannover, Hochspannungstechnik und Asset Management - Schering-Institut, Hannover, Germany. Start date: 15/08/2018. End date: 15/11/2018 (3 months). Supported by the University of Cantabria. Name of the grant: Aids for the realization of short research stays by researchers in predoctoral training.

- Institution: Sea Marconi Technologies, Turin, Italy. Start date: 15/09/2019. End date: 15/12/2019 (3 months). Supported by the European Union's Horizon 2020 Research and Innovation Programme through the Marie Sklodowska-Curie Grant 823969.

Finally, this PhD thesis has been supported through the following research projects and grants.

- European Union's Horizon 2020 Research and Innovation Programme through the Marie Sklodowska-Curie Grant 823969.

- Spanish Ministry of Economy National Research Project: Improvement of Insulation Systems of Transformers through Dielectric Nanofluids, Grant DPI2015-71219-C2 1-R.

- University of Cantabria and Government of Cantabria through Ph.D. Scholarship Grant CVE-2016-6626.

5.5. FUTURE RESEARCHES

The results obtained in this thesis suggest the following future research lines:

- To conduct an experimental validation of the magnetic nature of the additional buoyancy forces here noticed. This work should be supported by Computational Fluid Dynamics models of the setup. The characterization of the magnetic field of the transformer at different load levels and of the nanoparticles and nanofluids tested would be required to carry out these models.

- To develop a study about the stability of the nanofluids, with different surfactants, to ensure their applicability. Different surfactants, concentrations and treatment conditions may be tested, trying to keep at the same time the enhanced properties of the nanofluids. Once identified the suitable surfactantion method, the suggested optimized preparation method should be tried and adjusted.

- As another step of the applicability study, to subject the stable nanofluids to thermal aging tests, in order to know the evolution of their properties under working conditions.

- To test the nanofluids in actual cooling circuits and transformers, focusing on the consequences of the presence of the nanoparticles in the hardware, i.e. abrasion or sedimentation, and their prevention by adapting their design to the application of nanofluids. These adaptations should be also tested.

BIBLIOGRAPHY

BIBLIOGRAPHY

[1] Eurostat, “Energy, transport and environment indicators 2017 edition,” 2017.

[2] E. E. Agency, “The first and last mile — the key to sustainable urban transport,” 2019.

[3] L. U. of T. and E. W. Group, “Global Energy System based on 100% Renewable Energy – Power, Heat, Transport and Desalination Sectors,” 2019.

[4] Red Eléctrica de España (REE), “Red eléctrica y la integración de renovables,” 2019.

[5] F. Scatiggio, C. Serafino, and F. Pepe, “Increased Loadability of Transformers Immersed in Natural Ester,” in *IEEE International Conference on Dielectric Liquids (ICDL)*, 2019, pp. 8–11.

[6] V. Vasconcellos *et al.*, “Increased loadability of transformers using natural ester and cellulosic materials as high temperature insulation systems,” *IEEE Electr. Insul. Mag.*, vol. 34, no. 5, pp. 8–17, 2018.

[7] J. D. Courtois, I. Bazán, A. Vera, and L. Leija, “Temperature Increase in Magnetic Nanoparticles by Magnetic Field Induction for Hyperthermia Treatment,” in *Global Medical Engineering Physics Exchanges/ Pan American Health Care Exchanges (GMEPE/PAHCE)*, 2019, pp. 1–6.

[8] M. Gökçe, A. Alemdar, and S. İşçi, “Comparison of ionic polymers in the targeted drug delivery applications as the coating materials on the Fe3O4 nanoparticles,” *Mater. Sci. Eng. C*, vol. 103, no. March, pp. 1–6, 2019.

[9] I. M. Nikbin, R. Mohebbi, S. Dezhampanah, S. Mehdipour, R. Mohammadi, and T. Nejat, “Gamma ray shielding properties of heavy-weight concrete containing Nano-TiO2,” *Radiat. Phys. Chem.*, vol. 162, no. April, pp. 157–167, 2019.

[10] N. Mamidi, M. Renato, M. Gamero, J. Villela, and A. Elías, “Development of ultra-high molecular weight polyethylene-functionalized carbon nano-onions composites for biomedical applications,” *Diam. Relat. Mater.*, vol. 97, no. March, pp. 1–8, 2019.

[11] S. Mahdi, H. Sahebi, H. Zandavar, and S. Mirsadeghi, “Fabrication of Fe3O4 nanoparticles coated by extracted shrimp peels chitosan as sustainable adsorbents for removal of chromium contaminates from wastewater : The design of experiment,” *Compos. Part B*, vol. 175, no. February, p. 107130, 2019.

[12] L. Wang, N. Liu, and Y. Zhao, “Nanoporous TiO_2 / MoO_2 / Fe_3O_4 composite as anode for high-performance lithium-ion batteries,” *Solid State Sci.*, vol. 95, no. March, pp. 1–7, 2019.

[13] M. Sheikholeslami, R. ul Haq, A. Shafee, Z. Li, Y. G. Elaraki, and I. Tlili, “Heat transfer simulation of heat storage unit with nanoparticles and fins through a heat exchanger,” *Int. J. Heat Mass Transf.*, vol. 135, pp. 470–478, 2019.

[14] K. Kadirgama *et al.*, “Thermal analysis of SUS 304 stainless steel using ethylene glycol/nanocellulose-based nanofluid coolant,” *Int. J. Adv. Manuf. Technol.*, vol. 97, no. 5–8, pp. 2061–2076, Jul. 2018.

[15] V. Segal, A. Hjortsberg, A. Rabinovich, D. Nattrass, and K. Raj, “AC (60 Hz) and impulse breakdown strength of a colloidal fluid based on transformer oil and magnetite nanoparticles,” in *IEEE International Symposium on Electrical Insulation (ISEI)*, 1998, vol. 2, pp. 619–622.

[16] S. U. S. S. Choi, J. A. Eastman, and S. U. S. S. Choi, “Enhancing thermal conductivity of fluids with nanoparticles,” in *ASME International Mechanical Engineering Congress & Exposition*, 1995, vol. 231, pp. 99–105.

[17] I. Fofana, “50 Years in the Development of Insulating Liquids,” *IEEE Electr. Insul. Mag.*, vol. 29, no. 5, pp. 13–25, 2013.

[18] W. Yu and H. Xie, “A review on nanofluids: Preparation, stability mechanisms, and applications,” *J. Nanomater.*, vol. 2012, 2012.

[19] D. Kim *et al.*, “Convective heat transfer characteristics of nanofluids under laminar and turbulent flow conditions,” *Curr. Appl. Phys.*, vol. 9, no. 2 SUPPL., pp. e119–e123, 2009.

[20] K. S. Meenakshi and E. Pradeep Jaya Sudhan, “Preparation and characterization

of titanium oxide-water based nanofluids by one step method for heat transfer applications," in *International Conference on Nanoscience, Engineering and Technology (ICONSET)*, 2011, pp. 84–87.

[21] T. H. Tsai, L. S. Kuo, P. H. Chen, D. S. Lee, and C. T. Yang, "Applications of ferro-nanofluid on a micro-transformer," *Sensors*, vol. 10, no. 9, pp. 8161–8172, Sep. 2010.

[22] I. Nkurikiyimfura, Y. Wang, Z. Pan, and D. Hu, "Enhancement of thermal conductivity of magnetic nanofluids in magnetic field," in *International Conference on Materials for Renewable Energy and Environment (ICMREE)*, 2011, vol. 2, pp. 1333–1337.

[23] Y. Lv, C. Li, Q. Sun, M. Huang, C. Li, and B. Qi, "Effect of Dispersion Method on Stability and Dielectric Strength of Transformer Oil-Based TiO_2 Nanofluids," *Nanoscale Res. Lett.*, vol. 11, no. 1, 2016.

[24] J. Liu, L. Zhou, G. Wu, Y. Zhao, P. Liu, and Q. Peng, "Dielectric frequency response of oil-paper composite insulation modified by nanoparticles," *IEEE Trans. Dielectr. Electr. Insul.*, vol. 19, no. 2, pp. 510–520, 2012.

[25] D. Maity and D. C. Agrawal, "Synthesis of iron oxide nanoparticles under oxidizing environment and their stabilization in aqueous and non-aqueous media," *J. Magn. Magn. Mater.*, vol. 308, no. 1, pp. 46–55, Jan. 2007.

[26] B. Du, J. Li, B. Wang, J. Xiang, and Z. Zhang, "Influence of Water Content on the Electrical Properties of Insulating Vegetable Oil-Based Nanofluids," in *IEEE Electrical Insulation Conference (EIC)*, 2013, no. June, pp. 49–51.

[27] J. Li, Z. Zhang, P. Zou, S. Grzybowski, and M. Zahn, "Preparation of a vegetable oil-based nanofluid and investigation of its breakdown and dielectric properties," *IEEE Electr. Insul. Mag.*, vol. 28, no. 5, pp. 43–50, 2012.

[28] B. Du, J. Li, F. Wang, W. Yao, and S. Yao, "Influence of Monodisperse Fe_3O_4 Nanoparticle Size on Electrical Properties of Vegetable Oil-Based Nanofluids," *J. Nanomater.*, vol. 2015, 2015.

[29] J. Li, B. Du, F. Wang, W. Yao, and S. Yao, “The effect of nanoparticle surfactant polarization on trapping depth of vegetable insulating oil-based nanofluids,” *Phys. Lett. Sect. A Gen. At. Solid State Phys.*, vol. 380, no. 4, pp. 604–608, Feb. 2016.

[30] D. Liu, Y. Zhou, Y. Yang, L. Zhang, and F. Jin, “Characterization of high performance AIN nanoparticle-based transformer oil nanofluids,” *IEEE Trans. Dielectr. Electr. Insul.*, vol. 23, no. 5, pp. 2757–2767, 2016.

[31] I. Nkurikiyimfura, Y. Wang, and Z. Pan, “Effect of chain-like magnetite nanoparticle aggregates on thermal conductivity of magnetic nanofluid in magnetic field,” *Exp. Therm. Fluid Sci.*, vol. 44, pp. 607–612, 2013.

[32] B. Du, J. Li, B.-M. Wang, and Z.-T. Zhang, “Preparation and breakdown strength of Fe_3O_4 nanofluid based on transformer oil,” in *IEEE International Conference on High Voltage Engineering and Application (ICHVE)*, 2012, pp. 311–313.

[33] C. Choi, H. S. Yoo, and J. M. Oh, “Preparation and heat transfer properties of nanoparticle-in-transformer oil dispersions as advanced energy-efficient coolants,” *Curr. Appl. Phys.*, vol. 8, no. 6, pp. 710–712, 2008.

[34] D. H. Fontes, G. Ribatski, and E. P. Bandarra Filho, “Experimental evaluation of thermal conductivity, viscosity and breakdown voltage AC of nanofluids of carbon nanotubes and diamond in transformer oil,” *Diam. Relat. Mater.*, vol. 58, pp. 115–121, 2015.

[35] D. Wen and Y. Ding, “Natural convective heat transfer of suspensions of titanium dioxide nanoparticles (nanofluids),” *IEEE Trans. Nanotechnol.*, vol. 5, no. 3, pp. 220–227, May 2006.

[36] E. Tombácz, D. Bica, A. Hajdú, E. Illés, A. Majzik, and L. Vékás, “Surfactant double layer stabilized magnetic nanofluids for biomedical application,” *J. Phys. Condens. Matter*, vol. 20, no. 20, May 2008.

[37] C. H. Chon, K. D. Kihm, S. P. Lee, and S. U. S. Choi, “Empirical correlation finding the role of temperature and particle size for nanofluid (Al_2O_3) thermal

conductivity enhancement," *Appl. Phys. Lett.*, vol. 87, no. 15, pp. 1–3, Oct. 2005.

[38] S. M. S. Murshed, K. C. Leong, and C. Yang, "Thermal conductivity of nanoparticle suspensions (nanofluids)," in *IEEE Conference on Emerging Technologies - Nanoelectronics (INEC)*, 2006, vol. 2006, pp. 155–158.

[39] K. G. K. Sarojini, S. V. Manoj, P. K. Singh, T. Pradeep, and S. K. Das, "Electrical conductivity of ceramic and metallic nanofluids," *Colloids Surfaces A Physicochem. Eng. Asp.*, vol. 417, pp. 39–46, 2013.

[40] H. Xie, J. Wang, T. Xi, Y. Liu, and F. Ai, "Dependence of the thermal conductivity on nanoparticle-fluid mixture on the base fluid," *J. Mater. Sci. Lett.*, vol. 21, no. 19, pp. 1469–1471, 2002.

[41] Y. Xuan and Q. Li, "Heat transfer enhancement of nanofluids," *Int. J. Heat Fluid Flow*, vol. 21, no. 1, pp. 58–64, 2000.

[42] Y. Hwang, H. S. Park, J. K. Lee, and W. H. Jung, "Thermal conductivity and lubrication characteristics of nanofluids," *Curr. Appl. Phys.*, vol. 6, no. SUPPL. 1, pp. e67–e71, 2006.

[43] C. T. Nguyen, G. Roy, C. Gauthier, and N. Galanis, "Heat transfer enhancement using Al_2O_3-water nanofluid for an electronic liquid cooling system," *Appl. Therm. Eng.*, vol. 27, no. 8–9, pp. 1501–1506, Jun. 2007.

[44] A. Nasiri, M. Shariaty-Niasar, A. Rashidi, A. Amrollahi, and R. Khodafarin, "Effect of dispersion method on thermal conductivity and stability of nanofluid," *Exp. Therm. Fluid Sci.*, vol. 35, no. 4, pp. 717–723, May 2011.

[45] J. Amici, P. Allia, P. Tiberto, and M. Sangermano, "Poly(ethylene glycol)-coated Fe_3O_4 nanoparticles by UV-thiol-ene addition of PEG dithiol on vinyl-functionalized magnetite surface," *Macromol. Chem. Phys.*, vol. 212, no. 15, pp. 1629–1635, Aug. 2011.

[46] Z. Talaei, A. M. Rashidi, A. Amrollahi, and A. R. Mahjoub, "The effect of carboxylic group concentration on the stability and thermal conductivity of carbon nanotub fluid as heat transfer media," in *International Vacuum Electron Sources*

Conference (IVESC) and NANOcarbon, 2010, pp. 435–436.

[47] T.-P. Teng, W.-P. Wang, and Y.-C. Hsu, “Fabrication and Characterization of Nanocarbon-Based Nanofluids by Using an Oxygen–Acetylene Flame Synthesis System,” *Nanoscale Res. Lett.*, vol. 11, no. 1, 2016.

[48] S. K. Das, N. Putra, P. Thiesen, and W. Roetzel, “Temperature dependence of thermal conductivity enhancement for nanofluids,” *J. Heat Transfer*, vol. 125, no. 4, pp. 567–574, Aug. 2003.

[49] M. T. Imani, P. Werle, J. F. Miethe, and N. C. Bigall, “Magnetite nanofluid as alternative for conventional insulating liquids,” in *IEEE International Conference on Dielectric Liquids (ICDL)*, 2017, pp. 1–4.

[50] Y. Lv, M. Rafiq, C. Li, and B. Shan, “Study of dielectric breakdown performance of transformer oil based magnetic nanofluids,” *Energies*, vol. 10, no. 7, 2017.

[51] A. Fallah-Shojaie, A. Tavakoli, M. Ghomashpasand, and S. Hoseinzadeh, “Experimental evaluation on the dielectric breakdown voltage of fresh and used transformer oil mixed with titanium dioxide nanoparticles in the Gilan electrical distribution company,” in *Iranian Conference on Electrical Engineering (ICEE)*, 2013.

[52] J. Miao, M. Dong, and L.-P. Shen, “A modified electrical conductivity model for insulating oil-based nanofluids,” in *IEEE International Conference on Condition Monitoring and Diagnosis (CMD)*, 2012, pp. 1126–1129.

[53] M. Chiesa and S. K. Das, “Experimental investigation of the dielectric and cooling performance of colloidal suspensions in insulating media,” *Colloids Surfaces A Physicochem. Eng. Asp.*, vol. 335, no. 1–3, pp. 88–97, Mar. 2009.

[54] A. Cavallini, R. Karthik, and F. Negri, “The effect of magnetite, graphene oxide and silicone oxide nanoparticles on dielectric withstand characteristics of mineral oil,” *IEEE Trans. Dielectr. Electr. Insul.*, vol. 22, no. 5, pp. 2592–2600, 2015.

[55] J. Ghasemi, S. Jafarmadar, and M. Nazari, “Effect of magnetic nanoparticles on the lightning impulse breakdown voltage of transformer oil,” *J. Magn. Magn.*

Mater., vol. 389, pp. 148–152, 2015.

[56] M. Hanai, S. Hosomi, H. Kojima, N. Hayakawa, and H. Okubo, "Dependence of TiO_2 and ZnO nanoparticle concentration on electrical insulation characteristics of insulating oil," in *IEEE Conference on Electrical Insulation and Dielectric Phenomena (CEIDP)*, 2013, pp. 780–783.

[57] M. Nazari, M. H. Rasoulifard, and H. Hosseini, "Dielectric breakdown strength of magnetic nanofluid based on insulation oil after impulse test," *J. Magn. Magn. Mater.*, vol. 399, pp. 1–4, 2016.

[58] S. Li, M. Karlsson, R. Liu, A. Ahniyaz, A. Fornara, and E. J. Salazar-Sandoval, "The Effect of Ceria Nanoparticles on the Breakdown Strength of Transformer Oil," in *IEEE International Conference on the Properties and Applications of Dielectric Materials (ICPADM)*, 2015, pp. 289–292.

[59] E. G. Atiya, D. E. A. Mansour, R. M. Khattab, and A. M. Azmy, "Dispersion behavior and breakdown strength of transformer oil filled with TiO_2 nanoparticles," *IEEE Trans. Dielectr. Electr. Insul.*, vol. 22, no. 5, pp. 2463–2472, Oct. 2015.

[60] H. Jin, T. Andritsch, I. A. Tsekmes, R. Kochetov, P. H. F. Morshuis, and J. J. Smit, "Properties of Mineral Oil based Silica Nanofluids," *IEEE Trans. Dielectr. Electr. Insul.*, vol. 21, no. 3, pp. 1100–1108, 2014.

[61] H. Jin, P. H. F. Morshuis, A. R. Mor, and T. Andritsch, "An investigation into the dynamics of partial discharge propagation in mineral oil based nanofluids," in *IEEE International Conference on Dielectric Liquids (ICDL)*, 2014.

[62] M. M. Emara, D. E. A. Mansour, and A. M. Azmy, "Dielectric properties of aged mineral oil filled with TiO_2 nanoparticles," in *International Conference on Electric Power and Energy Conversion Systems (EPECS)*, 2015.

[63] H. Jin, T. Andritsch, P. H. F. Morshuis, and J. J. Smit, "AC Breakdown Voltage and Viscosity of Mineral Oil based SiO_2 Nanofluids," in *IEEE Conference on Electrical Insulation and Dielectric Phenomena (CEIDP)*, 2012, pp. 902–905.

[64] D. E. A. Mansour and A. M. Elsaeed, "Heat transfer properties of transformer oil-

based nanofluids filled with Al_2O_3 nanoparticles," in *IEEE International Conference on Power and Energy (PECon)*, 2014, pp. 123–127.

[65] H. Jin, T. Andritsch, I. A. Tsekmes, R. Kochetov, P. H. F. Morshuis, and J. J. Smit, "Thermal Conductivity of Fullerene and TiO_2 Nanofluids," in *IEEE Conference on Electrical Insulation and Dielectric Phenomena (CEIDP)*, 2013, pp. 711–714.

[66] H. Jin, P. Morshuis, A. R. Mor, J. J. Smit, and T. Andritsch, "Partial Discharge Behavior of Mineral Oil based Nanofluids," *IEEE Trans. Dielectr. Electr. Insul.*, vol. 22, no. 5, pp. 2747–2753, 2015.

[67] B. X. Du and X. L. Li, "High thermal conductivity transformer oil filled with BN nanoparticles," in *IEEE International Conference on Dielectric Liquids (ICDL)*, 2014.

[68] V. Segal, A. Rabinovich, D. Nattrass, K. Raj, and A. Nunes, "Experimental study of magnetic colloidal fluids behavior in power transformers," *J. Magn. Magn. Mater.*, vol. 215, pp. 513–515, 2000.

[69] W. Sima, J. Shi, Q. Yang, S. Huang, and X. Cao, "Effects of conductivity and permittivity of nanoparticle on transformer oil insulation performance: Experiment and theory," *IEEE Trans. Dielectr. Electr. Insul.*, vol. 22, no. 1, pp. 380–390, Feb. 2015.

[70] R. Karthik, A. Cavallini, and C. G. Azcarraga, "Investigations on the effect of nanoparticles in mineral oil," in *IEEE Conference on Electrical Insulation and Dielectric Phenomena (CEIDP)*, 2014, pp. 695–698.

[71] H. Jin, T. Andritsch, P. H. F. Morshuis, and J. J. Smit, "AC breakdown voltage and viscosity of mineral oil based fullerene nanofluids," in *IEEE Conference on Electrical Insulation and Dielectric Phenomena (CEIDP)*, 2013, pp. 703–706.

[72] P. Kopčanský, L. Tomčo, K. Marton, M. Koneracká, M. Timko, and I. Potočová, "The DC dielectric breakdown strength of magnetic fluids based on transformer oil," *J. Magn. Magn. Mater.*, vol. 289, pp. 415–418, Mar. 2005.

[73] M. J. Given *et al.*, "The influence of magnetite nano particles on the behaviour of insulating oils for pulse power applications," in *IEEE Conference on Electrical*

Insulation and Dielectric Phenomena (CEIDP), 2011, pp. 40–43.

[74] Y. Lv *et al.*, "Nanoparticle Effect on Electrical Properties of Aged Mineral Oil Based Nanofluids," 2012.

[75] M. Timko *et al.*, "Magnetic fluid as cooling and insulation medium for high power transformers," in *WSEAS International Conference on Energy, Environment, Ecosystems and Sustainable Development (EEESD)*, 2010, pp. 321–326.

[76] J. C. Lee, H. S. Seo, and Y. J. Kim, "The increased dielectric breakdown voltage of transformer oil-based nanofluids by an external magnetic field," *Int. J. Therm. Sci.*, vol. 62, pp. 29–33, Dec. 2012.

[77] J. Kúdelčík, P. Bury, J. Drga, P. Kopčanský, V. Závišová, and M. Timko, "The anisotropy of transformer oil-based magnetic fluids studied by acoustic spectroscopy," in *ELEKTRO*, 2012, pp. 508–513.

[78] L. Pislaru-Danescu, A. M. Morega, G. Telipan, M. Morega, J. B. Dumitru, and V. Marinescu, "Magnetic nanofluid applications in electrical engineering," *IEEE Trans. Magn.*, vol. 49, no. 11, pp. 5489–5497, 2013.

[79] R. Liu, L. A. A. Pettersson, T. Auletta, and O. Hjortstam, "Fundamental research on the application of nano dielectrics to transformers," in *IEEE Conference on Electrical Insulation and Dielectric Phenomena (CEIDP)*, 2011, pp. 423–427.

[80] Y. Du, Y. Lv, F. Wang, X. Li, and C. Li, "Effect of TiO2 nanoparticles on the breakdown strength of transformer oil," in *IEEE International Symposium on Electrical Insulation (ISEI)*, 2010.

[81] Y. Lv, L. Wang, X. Li, Y. Du, J. Zhou, and C. Li, "Experimental investigation of breakdown strength of mineral oil-based nanofluids," in *IEEE International Conference on Dielectric Liquids (ICDL)*, 2011.

[82] Y. Lv *et al.*, "Nanoparticle effects on creeping flashover characteristics of oil/pressboard interface," *IEEE Trans. Dielectr. Electr. Insul.*, vol. 21, no. 2, pp. 556–562, 2014.

[83] Y. Zhou *et al.*, "Effect of nanoparticles on electrical characteristics of transformer

oil-based nanofluids impregnated pressboard," in *IEEE International Symposium on Electrical Insulation (ISEI)*, 2012, pp. 650–653.

[84] M. Rafiq *et al.*, "Insulating and aging properties of transformer oil-based TiO_2 nanofluids," in *IEEE Conference on Electrical Insulation and Dielectric Phenomena (CEIDP)*, 2014, pp. 457–461.

[85] Z. F. Hu *et al.*, "Thermal aging properties of transformer oil-based TiO_2 nanofluids," in *IEEE International Conference on Dielectric Liquids (ICDL)*, 2014, pp. 2–5.

[86] M. Chen, Y. Du, Y. Lv, J. Zhou, X. Li, and C. Li, "Effect of nanoparticles on the dielectric strength of aged transformer oil," in *Conference on Electrical Insulation and Dielectric Phenomena (CEIDP)*, 2011, pp. 664–667.

[87] Y. Lv *et al.*, "Nanoparticle Effect on Dielectric Breakdown Strength of Transformer Oil-Based Nanofluids," in *IEEE Conference on Electrical Insulation and Dielectric Phenomena (CEIDP)*, 2013, pp. 680–682.

[88] Y. Lv, X. Li, Y. Du, F. Wang, and C. Li, "Preparation and breakdown strength of TiO_2 fluids based on transformer oil," in *IEEE Conference on Electrical Insulation and Dielectric Phenomena (CEIDP)*, 2010, pp. 1–3.

[89] Y. Du, Y. Lv, J. Zhou, X. Li, and C. Li, "Breakdown properties of transformer oil-based TiO_2 nanofluid," in *IEEE Conference on Electrical Insulation and Dielectric Phenomena (CEIDP)*, 2010, pp. 1–4.

[90] J. Kúdelčík, P. Bury, P. Kopčanský, and M. Timko, "Dielectric breakdown in mineral oil ITO 100 based magnetic fluid," in *Physics Procedia - International Conference on Magnetic Fluids (ICMF)*, 2010, vol. 9, pp. 78–81.

[91] M. T. Imani, J. F. Miethe, P. Werle, N. C. Bigall, and H. Borsi, "Engineering of multifunctional nanofluids for insulation systems of high voltage apparatus," in *IEEE Conference on Electrical Insulation and Dielectric Phenomena (CEIDP)*, 2016, pp. 44–47.

[92] L. Pislaru-Danescu *et al.*, "Prototyping a Ferrofluid-Cooled Transformer," *IEEE*

Trans. Ind. Appl., vol. 49, no. 3, pp. 1289–1298, 2013.

[93] R. T. A. R. Prasath, R. Karthik, and M. W. Iruthayarajan, "Enhancement of critical properties of pure and aged transformer oil using nanocomposites," in *International Conference on Circuits, Power and Computing Technologies (ICCPCT)*, 2014, pp. 382–387.

[94] M. Dong, L. P. Shen, H. Wang, H. B. Wang, and J. Miao, "Investigation on the Electrical Conductivity of Transformer Oil-Based AlN Nanofluid," *J. Nanomater.*, vol. 2013, 2013.

[95] Q. Wang, M. Rafiq, Y. Lv, C. Li, and K. Yi, "Preparation of three types of transformer oil-based nanofluids and comparative study on the effect of nanoparticle concentrations on insulating property of transformer oil," *J. Nanotechnol.*, vol. 2016, 2016.

[96] D. E. A. Mansour, E. G. Atiya, R. M. Khattab, and A. M. Azmy, "Effect of titania nanoparticles on the dielectric properties of transformer oil-based nanofluids," in *IEEE Conference on Electrical Insulation and Dielectric Phenomena (CEIDP)*, 2012, pp. 295–298.

[97] R. Karthik, T. Raja, and R. Madavan, "Enhancement of Critical Characteristics of Transformer Oil Using Nanomaterials," *Arab. J. Sci. Eng.*, vol. 38, no. 10, pp. 2725–2733, 2013.

[98] M. A. Sens *et al.*, "Electromagnetic characterization of Magnetic Nanofluid," in *Conference on Precision Electromagnetic Measurements (CPEM)*, 2014, pp. 184–185.

[99] J. Zhou, Y. Du, M. Chen, C. Li, X. Li, and Y. Lv, "AC and lightning breakdown strength of transformer oil modified by semiconducting nanoparticles," in *IEEE Conference on Electrical Insulation and Dielectric Phenomena (CEIDP)*, 2011, pp. 652–654.

[100] K. Ma, Y. Lv, W. Wang, Y. Zhou, S. Zhang, and C. Li, "Influence of semiconductive nanoparticle on sulfur corrosion behaviors in oil-paper insulation," in *IEEE Conference on Electrical Insulation and Dielectric Phenomena (CEIDP)*, 2013, pp.

715–718.

[101] Y. Lv, S. Zhang, Y. Du, M. Chen, and C. Li, “Effect of oleic acid surface modification on dispersibility of TiO_2 nanoparticles in transformer oils,” *Wuji Cailiao Xuebao/Journal Inorg. Mater.*, vol. 28, no. 6, pp. 594–598, 2013.

[102] R. Cimbala, J. Király, M. German-Sobek, and M. Pavlik, “Dielectric spectroscopy of transformer oil based ferrofluid from view of i(t) characteristics at initial stage of ageing,” in *International Scientific Conference on Electric Power Engineering (EPE)*, 2014, pp. 467–472.

[103] Y. Du, Y. Lv, J. Zhou, M. Chen, X. Li, and C. Li, “Effect of ageing on insulating property of mineral Oil-based TiO_2 nanofluids,” in *IEEE International Conference on Dielectric Liquids (ICDL)*, 2011, pp. 1–4.

[104] Y. Du *et al.*, “Effect of semiconductive nanoparticles on insulating performances of transformer oil,” *IEEE Trans. Dielectr. Electr. Insul.*, vol. 19, no. 3, pp. 770–776, 2012.

[105] Y. Du *et al.*, “Effect of electron shallow trap on breakdown performance of transformer oil-based nanofluids,” *J. Appl. Phys.*, vol. 110, no. 10, Nov. 2011.

[106] Y. Du *et al.*, “Effect of water adsorption at nanoparticle-oil interface on charge transport in high humidity transformer oil-based nanofluid,” *Colloids Surfaces A Physicochem. Eng. Asp.*, vol. 415, pp. 153–158, 2012.

[107] C. Pugazhendhi Sugumaran, “Experimental evaluation on dielectric and thermal characteristics of nano filler added transformer oil,” in *IEEE International Conference on High Voltage Engineering and Application (ICHVE)*, 2012, vol. 9, pp. 207–210.

[108] J. A. Mergos, M. D. Athanassopoulou, T. G. Argyropoulos, and C. T. Dervos, “Dielectric properties of nanopowder dispersions in paraffin oil,” *IEEE Trans. Dielectr. Electr. Insul.*, vol. 19, no. 5, pp. 1502–1507, 2012.

[109] P. Dhar, A. Katiyar, L. S. Maganti, A. Pattamatta, and S. K. Das, “Superior dielectric breakdown strength of graphene and carbon nanotube infused nano-oils,” *IEEE*

Trans. Dielectr. Electr. Insul., vol. 23, no. 2, pp. 943–956, 2016.

[110] M. Bakrutheen, R. Karthik, and R. Madavan, "Investigation of Critical Parameters of Insulating Mineral Oil Using Semiconductive Nanoparticles," in *International Conference on Circuits, Power and Computing Technologies (ICCPCT)*, 2013, pp. 294–299.

[111] J.-C. Lee, W.-H. Lee, S.-H. Lee, and S. Lee, "Positive and negative effects of dielectric breakdown in transformer oil based magnetic fluids," *Mater. Res. Bull.*, vol. 47, no. 10, pp. 2984–2987, 2012.

[112] F. D. Stoian *et al.*, "Characteristic properties of a magnetic nanofluid used as cooling and insulating medium in a power transformer," in *International Symposium on Advanced Topics in Electrical Engineering (ATEE)*, 2013, pp. 23–26.

[113] S. R. Chitra and S. Sendhilnathan, "Experimental Investigations on Dielectric Fluids Behavior in High-Power Transformers," *Int. J. Appl. Ceram. Technol.*, vol. 13, no. 6, pp. 1096–1103, 2016.

[114] J. Taha-Tijerina *et al.*, "Electrically insulating thermal nano-oils using 2D fillers," *ACS Nano*, vol. 6, no. 2, pp. 1214–1220, 2012.

[115] B. X. Du, X. L. Li, and J. Li, "Thermal conductivity and dielectric characteristics of transformer oil filled with bn and Fe_3O_4 nanoparticles," *IEEE Trans. Dielectr. Electr. Insul.*, vol. 22, no. 5, pp. 2530–2536, Oct. 2015.

[116] Irwanto, C. G. Azcarraga, Suwarno, A. Cavallini, and F. Negri, "Ferrofluid effect in mineral oil: PDIV, streamer, and breakdown voltage," in *IEEE International Conference on High Voltage Engineering and Application (ICHVE)*, 2014, pp. 3–6.

[117] M. Rafiq, C. Li, I. Khan, H. Zhifeng, Y. Lv, and K. Yi, "Preparation and Breakdown Properties of Mineral Oil Based Alumina Nanofluids," in *International Conference on Emerging Technologies (ICET)*, 2015, pp. 1–3.

[118] M. Rafiq, C. Li, Ge, Y. Lv, and K. Yi, "Effect of Fe_3O_4 nanoparticle concentrations on dielectric property of transformer oil," in *IEEE International Conference on High Voltage Engineering and Application (ICHVE)*, 2016, pp. 1–4.

[119] L. Pislaru-Danescu, A. Morega, G. Telipan, and V. Stoica, “Nanoparticles of ferrofluid Fe_3O_4 synthetised by coprecipitation method used in microactuation process,” *Optoelectron. Adv. Mater. - Rapid Commun.*, vol. 4, no. 8, pp. 1182–1186, 2010.

[120] A. M. Morega, M. Morega, L. Pislaru-Danescu, V. Stoica, F. Nouras, and F. D. Stoian, “A novel, ferrofluid-cooled transformer. electromagnetic field and heat transfer by numerical simulation,” in *International Conference on Optimization of Electrical and Electronic Equipment (OPTIM)*, 2010, pp. 140–146.

[121] M. Rafiq, D. Khan, and M. Ali, “Dielectric Properties of Transformer Oil based Silica Nanofluids,” in *Power Generation System and Renewable Energy Technologies (PGSRET)*, 2015, pp. 1–3.

[122] S. Aberoumand, A. Jafarimoghaddam, M. Moravej, H. Aberoumand, and K. Javaherdeh, “Experimental study on the rheological behavior of silver-heat transfer oil nanofluid and suggesting two empirical based correlations for thermal conductivity and viscosity of oil based nanofluids,” *Appl. Therm. Eng.*, vol. 101, pp. 362–372, 2016.

[123] K. Parekh and R. V. Upadhyay, “Characterization of transformer oil based magnetic fluid,” *Indian J. Eng. Mater. Sci.*, vol. 11, no. 4, pp. 262–266, 2004.

[124] E. Ettefaghi, H. Ahmadi, A. Rashidi, A. Nouralishahi, and S. S. Mohtasebi, “Preparation and thermal properties of oil-based nanofluid from multi-walled carbon nanotubes and engine oil as nano-lubricant,” *Int. Commun. Heat Mass Transf.*, vol. 46, pp. 142–147, Aug. 2013.

[125] R. Patel, K. Parekh, R. V. Upadhyay, and R. V. Mehta, “Rheology of transformer oil based ferrofluids,” *Indian J. Eng. Mater. Sci.*, vol. 11, no. 4, pp. 301–304, 2004.

[126] P. Krishna Kumar, S. Senthil Kumar, and M. Ravindran, “Investigation on mixed insulating fluids with nano fluids and antioxidants,” in *International Conference on Advances in Electrical Engineering (ICAEE)*, 2014, pp. 1–4.

[127] V. A. Primo, D. Pérez-Rosa, B. García, and J. C. Cabanelas, “Evaluation of the

Stability of Dielectric Nanofluids for Use in Transformers under Real Operating Conditions," *Nanomaterials*, vol. 9, no. 2, p. 143, 2019.

[128] L. Tomčo *et al.*, "The DC and AC insulating properties of magnetic fluids based on transformer oil," in *Physica Status Solidi C: Conferences*, 2006, vol. 3, no. 1, pp. 195–198.

[129] Z. Zhang, J. Li, P. Zou, and S. Grzybowski, "Electrical properties of nano-modified insulating vegetable oil," in *IEEE Conference on Electrical Insulation and Dielectric Phenomena (CEIDP)*, 2010.

[130] G. D. Peppas, V. P. Charalampakos, E. C. Pyrgioti, M. G. Danikas, A. Bakandritsos, and I. F. Gonos, "Statistical investigation of AC breakdown voltage of nanofluids compared with mineral and natural ester oil," *IET Sci. Meas. Technol.*, vol. 10, no. 6, pp. 644–652, 2016.

[131] Y. Zhong *et al.*, "Insulating Properties and Charge Characteristics of Natural Ester Fluid Modified by TiO_2 Semiconductive Nanoparticles," *IEEE Trans. Dielectr. Electr. Insul.*, vol. 20, no. 1, p. 135, 2013.

[132] J. Li, R. Liao, and L. Yang, "Investigation of natural ester based liquid dielectrics and nanofluids," in *IEEE International Conference on High Voltage Engineering and Application (ICHVE)*, 2012, pp. 16–21.

[133] W. R. Viali *et al.*, "Investigation of the molecular surface coating on the stability of insulating magnetic oils," *J. Phys. Chem. C*, vol. 114, no. 1, pp. 179–188, Jan. 2010.

[134] G. D. Peppas *et al.*, "Ultrastable Natural Ester-Based Nanofluids for High Voltage Insulation Applications," *ACS Appl. Mater. Interfaces*, vol. 8, no. 38, pp. 25202–25209, 2016.

[135] W. Li, C. Zou, and X. Li, "Thermo-physical properties of waste cooking oil-based nanofluids," *Appl. Therm. Eng.*, vol. 112, pp. 784–792, 2017.

[136] S. Witharana and J. A. Weliwita, "Suspended nanoparticles as a way to improve thermal energy transfer efficiency," in *IEEE International Conference on*

Information and Automation for Sustainability (ICIAFS), 2012, pp. 308–311.

[137] C. Tangthieng, B. A. Finlayson, J. Maulbetsch, and T. Cader, "Heat transfer enhancement in ferrofluids subjected to steady magnetic fields," *J. Magn. Magn. Mater.*, vol. 201, no. 1–3, pp. 252–255, 1999.

[138] B. Yang and Z. H. Han, "Temperature-dependent thermal conductivity of nanorod-based nanofluids," *Appl. Phys. Lett.*, vol. 89, no. 8, 2006.

[139] G. Qiu, Q. Wang, C. Wang, W. Lau, and Y. Guo, "Polystyrene/Fe_3O_4 magnetic emulsion and nanocomposite prepared by ultrasonically initiated miniemulsion polymerization," *Ultrason. Sonochem.*, vol. 14, no. 1, pp. 55–61, 2007.

[140] I. Gil, "Brettis." [Online]. Available: https://www.brettis.com/Tutorial/08Transformadores.pdf. [Accessed 5 April 2018].

[141] "ISO." [Online]. Available: https://www.iso.org/obp/ui/#iso:std:iso:ts:80004:-2:ed-1:v1:en. [Accessed 7 April 2018].

[142] S. Jovanović, M. Spreitzer, M. Tramšek, Z. Trontelj, and D. Suvorov, "Effect of oleic acid concentration on the physicochemical properties of cobalt ferrite nanoparticles," *J. Phys. Chem. C*, vol. 118, no. 25, pp. 13844–13856, Jun. 2014.

[143] T. S. Ramu, B. K. Keshavan, and K. N. Balasubramanya Murthy, "Application of a class of nano fluids to improve the loadability of power transformers," in *IEEE International Conference on Properties and Applications of Dielectric Materials (ICPADM)*, 2012, pp. 1–6.

[144] L. Zhang, R. He, and H. C. Gu, "Oleic acid coating on the monodisperse magnetite nanoparticles," *Appl. Surf. Sci.*, vol. 253, no. 5, pp. 2611–2617, Dec. 2006.

[145] Y. Lv, Y. Zhou, C. Li, Q. Wang, and B. Qi, "Recent progress in nanofluids based on transformer oil: Preparation and electrical insulation properties," *IEEE Electr. Insul. Mag.*, vol. 30, no. 5, pp. 23–32, 2014.

[146] M. Khalil, J. Yu, N. Liu, and R. L. Lee, "Non-aqueous modification of synthesized hematite nanoparticles with oleic acid," *Colloids Surfaces A Physicochem. Eng.*

Asp., vol. 453, no. 1, pp. 7–12, Jul. 2014.

[147] L. Vékás, D. Bica, and O. Marinica, “Magnetic nanofluids stabilized with various chain length surfactants,” *Rom. Reports Phys.*, vol. 58, no. 3, pp. 257–267, 2006.

[148] A. B. Bourlinos, A. Bakandritsos, V. Georgakilas, and D. Petridis, “Surface modification of ultrafine magnetic iron oxide particles,” *Chem. Mater.*, vol. 14, no. 8, pp. 3226–3228, Aug. 2002.

[149] K. Do Kim, S. S. Kim, Y.-H. Choa, and H. T. Kim, “Formation and Surface Modification of Fe3O4 Nanoparticles by Co-precipitation and Sol-gel Method,” *J. Ind. Eng. Chem*, vol. 13, no. 7, pp. 1137–1141, 2007.

[150] R. Hong, T. Pan, J. Qian, and H. Li, “Synthesis and surface modification of ZnO nanoparticles,” *Chem. Eng. J.*, vol. 119, no. 2–3, pp. 71–81, Jun. 2006.

[151] M. Yamaura, R. L. Camilo, L. C. Sampaio, M. A. Macêdo, M. Nakamura, and H. E. Toma, “Preparation and characterization of (3-aminopropyl)triethoxysilane-coated magnetite nanoparticles,” *J. Magn. Magn. Mater.*, vol. 279, no. 2–3, pp. 210–217, Aug. 2004.

[152] G. A. Van Ewijk, G. J. Vroege, and A. P. Philipse, “Convenient preparation methods for magnetic colloids,” *J. Magn. Magn. Mater.*, vol. 201, no. 1–3, pp. 31–33, 1999.

[153] A. Józefczak, “Study of low concentrated ionic ferrrofluid stability in magnetic field by ultrasound spectroscopy,” *J. Magn. Magn. Mater.*, vol. 321, no. 14, pp. 2225–2231, 2009.

[154] D. Li, “Preparation and characterization of lipophilic copper nanoparticle,” in *International Conference on Remote Sensing, Environment and Transportation Engineering (RSETE)*, 2011, pp. 6166–6169.

[155] W. Zhou, Z. Zhou, L. Zhang, L. Guo, Y. Du, and Y. Lv, “Seed-mediated synthesis and characterization of Ni flower-like nanomaterials,” *J. Nanosci. Nanotechnol.*, vol. 10, no. 8, pp. 5004–5007, Aug. 2010.

[156] J. Zhou, B. Song, G. Zhao, and G. Han, “Effects of acid on the microstructures and properties of three-dimensional TiO_2 hierarchical structures by solvothermal

method," *Nanoscale Res. Lett.*, vol. 7, pp. 1–10, 2012.

[157] X. Liu, Z. Ma, J. Xing, and H. Liu, "Preparation and characterization of amino-silane modified superparamagnetic silica nanospheres," *J. Magn. Magn. Mater.*, vol. 270, no. 1–2, pp. 1–6, Mar. 2004.

[158] M. Masteri-Farahani, M. Bahmanyar, and M. Mohammadikish, "Organic-inorganic hybrid nanomaterials prepared from 4-formyl benzo-12-crown-4-ether and silica coated magnetite nanoparticles," *J. Nanostructures*, vol. 1, pp. 191–197, 2012.

[159] M. Koneracká *et al.*, "Immobilization of proteins and enzymes to fine magnetic particles," *J. Magn. Magn. Mater.*, vol. 201, pp. 427–430, 1999.

[160] B. Jia and L. Gao, "Fabrication of 'tadpole'-like magnetite/multiwalled carbon nanotube heterojunctions and their self-assembly under external magnetic field," *J. Phys. Chem. B*, vol. 111, no. 19, pp. 5337–5343, May 2007.

[161] J. H. Lienhard, *A heat transfer textbook.* Prentice-Hall Inc, 1981.

[162] P. Keblinski, S. R. Phillpot, S. U. S. Choi, and J. A. Eastman, "Mechanisms of heat flow in suspensions of nano-sized particles (nanofluids)," *Int. J. Heat Mass Transf.*, vol. 45, no. 4, pp. 855–863, 2001.

[163] J. G. Hwang, M. Zahn, F. M. O'Sullivan, L. A. A. Pettersson, O. Hjortstam, and R. Liu, "Effects of nanoparticle charging on streamer development in transformer oil-based nanofluids," *J. Appl. Phys.*, vol. 107, no. 1, 2010.

[164] J. G. Hwang, F. O'Sullivan, M. Zahn, O. Hjortstam, L. A. A. Pettersson, and R. Liu, "Modeling of streamer propagation in transformer oil-based nanofluids," in *IEEE Conference on Electrical Insulation and Dielectric Phenomena (CEIDP)*, 2008, pp. 361–366.

[165] H. Jin, P. H. F. Morshuis, J. J. Smit, and T. Andritsch, "The effect of surface treatment of silica nanoparticles on the breakdown strength of mineral oil," in *IEEE International Conference on Dielectric Liquids (ICDL)*, 2014, pp. 1–4.

[166] V. S. Mendelev and A. O. Ivanov, "Ferrofluid aggregation in chains under the

influence of a magnetic field," *Phys. Rev. E - Stat. Nonlinear, Soft Matter Phys.*, vol. 70, no. 5 1, pp. 51502–51510, 2004.

[167] D. Thapa, V. R. Palkar, M. B. Kurup, and S. K. Malik, "Properties of magnetite nanoparticles synthesized through a novel chemical route," *Mater. Lett.*, vol. 58, no. 21, pp. 2692–2694, 2004.

[168] V. Segal and K. Raj, "An investigation of power transformer cooling with magnetic fluids," *Indian J. Eng. Mater. Sci.*, vol. 5, pp. 416–422, 1998.

[169] R. Liao *et al.*, "Quantitative analysis of insulation condition of oil-paper insulation based on frequency domain spectroscopy," *IEEE Trans. Dielectr. Electr. Insul.*, vol. 22, no. 1, pp. 322–334, 2015.

[170] M.-L. Coulibaly, C. Perrier, M. Marugan, and A. Beroual, "Aging behavior of cellulosic materials in presence of mineral oil and ester liquids under various conditions," *IEEE Trans. Dielectr. Electr. Insul.*, vol. 20, no. 6, pp. 1971–1976, 2013.

[171] N. Lelekakis, W. Guo, D. Martin, J. Wijaya, and D. Susa, "A field study of aging in paper-oil insulation systems," *IEEE Electr. Insul. Mag.*, vol. 28, no. 1, pp. 12–19, 2012.

[172] S. Chaudhari, S. Patil, R. Zambare, S. Chakraborty, IEEE Staff, and IEEE Staff, "Exploration on use of ferrofluid in power transformers," in *IEEE International Conference on Properties and Applications of Dielectric Materials (ICPADM)*, 2012, pp. 1–4.

[173] IEC, *IEC 62770:2018. Fluids for electrotechnical applications - Unused natural esters for transformers and similar electrical equipment.* 2013.

[174] IEC, "IEC 60156:2018 Insulating liquids – Determination of the breakdown voltage at power frequency – Test method," *61010-1 © Iec:2001*, vol. 2006. p. 41, 2018.

[175] IEC, "IEC 60247:2004. Insulating liquids - Measurement of relative permittivity, dielectric dissipation factor (tan d) and d.c. resistivity." .

[176] IEC, "IEC 60814:1997. Insulating Liquids - Oil-impregnated Paper and Pressboard - Determination of Water by Automatic Coulometric Karl Fischer Titration." p. 43,

1997.

[177] Metrohm, “899 Coulometer Manual.” 2015.

[178] J. Patel, K. Parekh, and R. V. Upadhyay, “Prevention of hot spot temperature in a distribution transformer using magnetic fluid as a coolant,” *Int. J. Therm. Sci.*, vol. 103, pp. 35–40, 2016.

[179] A. Ortiz, F. Delgado, F. Ortiz, I. Fernández, and A. Santisteban, “The aging impact on the cooling capacity of a natural ester used in power transformers,” *Appl. Therm. Eng.*, vol. 144, no. April, pp. 797–803, 2018.

[180] S. I. S. Enanv, H. Medical, S. Ab, and S. Bertling, *IEC 60076-2 Power Transformer-Part 2_Temperature rise for liquid-immersed transformers*, vol. 2004. 2010.